



Theses and Dissertations

2013-06-11

Accuracy of a Simplified Analysis Model for Modern Skyscrapers

Jacob Scott Lee

Brigham Young University - Provo

Follow this and additional works at: <https://scholarsarchive.byu.edu/etd>



Part of the [Civil and Environmental Engineering Commons](#)

BYU ScholarsArchive Citation

Lee, Jacob Scott, "Accuracy of a Simplified Analysis Model for Modern Skyscrapers" (2013). *Theses and Dissertations*. 4055.

<https://scholarsarchive.byu.edu/etd/4055>

This Thesis is brought to you for free and open access by BYU ScholarsArchive. It has been accepted for inclusion in Theses and Dissertations by an authorized administrator of BYU ScholarsArchive. For more information, please contact scholarsarchive@byu.edu, ellen_amatangelo@byu.edu.

Accuracy of a Simplified Analysis Model
for Modern Skyscrapers

Jacob S. Lee

A thesis submitted to the faculty of
Brigham Young University
in partial fulfillment of the requirements for the degree of
Master of Science

Richard J. Balling, Chair
Paul W. Richards
Fernando S. Fonseca

Department of Civil and Environmental Engineering
Brigham Young University

June 2013

Copyright © 2013 Jacob S. Lee

All Rights Reserved

ABSTRACT

Accuracy of a Simplified Analysis Model for Modern Skyscrapers

Jacob S. Lee

Department of Civil and Environmental Engineering, BYU
Master of Science

A new simplified skyscraper analysis model (SSAM) was developed and implemented in a spreadsheet to be used for preliminary skyscraper design and teaching purposes. The SSAM predicts linear and nonlinear response to gravity, wind, and seismic loading of "modern" skyscrapers which involve a core, megacolumns, outrigger trusses, belt trusses, and diagonals. The SSAM may be classified as a discrete method that constructs a reduced system stiffness matrix involving selected degrees of freedom (DOF's). The steps in the SSAM consist of: 1) determination of megacolumn areas, 2) construction of stiffness matrix, 3) calculation of lateral forces and displacements, and 4) calculation of stresses. Seven configurations of a generic skyscraper were used to compare the accuracy of the SSAM against a space frame finite element model. The SSAM was able to predict the existence of points of contraflexure in the deflected shape which are known to exist in modern skyscrapers. The accuracy of the SSAM was found to be very good for displacements (translations and rotations), and reasonably good for stress in configurations that exclude diagonals. The speed of execution, data preparation, data extraction, and optimization were found to be much faster with the SSAM than with general space frame finite element programs.

Keywords: Jacob S. Lee, skyscraper, structural analysis, optimization, preliminary design

ACKNOWLEDGEMENTS

I wish to express my sincere appreciation and thanks to my advisor, Dr. Richard J. Balling, for his help and dedication that went into our research. I am grateful for his motivation and encouragement in stretching my mind in ways I never thought possible. I was blessed with the opportunity he gave me to explore an area of structural engineering that inspires me and share that experience alongside him. I am indeed indebted to him for making it possible to travel to China to study the skyscrapers there and collaborate with the engineers behind their designs as part of his Megastructures class. That unforgettable experience has given me a wider perspective of what structural engineering has to offer and excites me about my future career aspirations in engineering. I would also like to thank my committee members, Dr. Paul W. Richards and Dr. Fernando S. Fonseca, who have truly been inspirational professors to me in my academic life at BYU.

I would like to thank my family and friends who have supported me throughout this endeavor and my graduate degree, and who have instilled in me the values of one who strives to emulate the pure love of Christ. I would also like to thank my fellow colleagues for their hard work and insight during this project.

TABLE OF CONTENTS

LIST OF TABLES	vii
LIST OF FIGURES	x
1 Introduction.....	1
2 Literature review.....	13
2.1 Continuum Methods for Low/Medium-Rise Buildings.....	13
2.2 Continuum Method for Framed Tubes	16
2.3 Inherent Problems with Continuum Methods.....	17
2.4 Discrete Outrigger Methods.....	20
2.5 Discrete Substructuring Methods.....	22
3 Simplified Skyscraper Analysis Model	24
3.1 Determination of Megacolumn Areas.....	24
3.2 Construction of the Stiffness Matrix.....	27
3.3 Calculation of Lateral Forces/Displacements	39
3.4 Calculation of Stresses.....	44
3.5 Rapid Trial-and-Error Optimization	52
4 Space frame model.....	54
4.1 Nodes	54
4.2 Members	55
4.3 Supports	58
4.4 Loads.....	59
4.5 Output	59
5 Results	60
5.1 Configuration #1 – core+megacolumns.....	61

5.2	Configuration #2 – core+megacolumns+outriggers	65
5.3	Configuration #3 – core+megacolumns+belts.....	68
5.4	Configuration #4 – core+megacolumns+diagonals	72
5.5	Configuration #5 – core+megacolumns+outriggers+belts	76
5.6	Configuration #6 – core+megacolumns+outriggers+belts+diagonals.....	81
5.7	Configuration #7 – core+megacolumns+outrigger at one level only	85
6	Conclusions.....	89
	REFERENCES	91
	APPENDIX A. SSAM Excel Spreadsheet (Configuration #6).....	95

LIST OF TABLES

Table 3-1: Stiffness matrix - contribution of the core and megacolumns.....	29
Table 3-2: Stiffness matrix - contribution of outriggers	32
Table 3-3: Stiffness matrix - contribution of the belt trusses.....	35
Table 3-4: Stiffness matrix - contribution of diagonals	37
Table 5-1: Configuration #1 - design variables and calculated megacolumn areas	61
Table 5-2: Configuration #1 - lateral core translation (m).....	62
Table 5-3: Configuration #1 - core rotation (rad).....	62
Table 5-4: Configuration #1 - vertical megacolumn translation minus vertical core translation.....	63
Table 5-5: Configuration #1 - core stress (KPa).....	63
Table 5-6: Configuration #1 - megacolumn stress (KPa).....	64
Table 5-7: Configuration #2 - design variables and calculated megacolumn areas	65
Table 5-8: Configuration #2 - lateral core translation (m).....	65
Table 5-9: Configuration #2 - core rotation (rad).....	65
Table 5-10: Configuration #2 - vertical megacolumn translation minus vertical core translation.....	66
Table 5-11: Configuration #2 - core stress (KPa).....	66
Table 5-12: Configuration #2 - megacolumn stress (KPa).....	67
Table 5-13: Configuration #2 - outrigger stress under lateral load only (KPa).....	67
Table 5-14: Configuration #3 – design variables and calculated megacolumn areas.....	68
Table 5-15: Configuration #3 - lateral core translation (m).....	69
Table 5-16: Configuration #3 - core rotation (rad).....	69
Table 5-17: Configuration #3 - vertical megacolumn translation minus vertical core translation.....	70
Table 5-18: Configuration #3 - core stress (KPa).....	70

Table 5-19: Configuration #3 - megacolumn stress (KPa)	71
Table 5-20: Configuration #3 - belt truss stress under lateral load only (KPa)	71
Table 5-21: Configuration #4 – design variables and calculated megacolumn areas	72
Table 5-22: Configuration #4 - lateral core translation (m).....	73
Table 5-23: Configuration #4 - core rotation (rad)	73
Table 5-24: Configuration #4 - vertical megacolumn translation minus core vertical translation.....	73
Table 5-25: Configuration #4 - core stress (KPa).....	74
Table 5-26: Configuration #4 - megacolumn stress (KPa)	74
Table 5-27: Configuration #4 - diagonal stress (KPa)	75
Table 5-28: Configuration #5 – design variables and calculated megacolumn areas	76
Table 5-29 Configuration #5: - lateral core translation (m).....	77
Table 5-30: Configuration #5 - core rotation (rad)	77
Table 5-31: Configuration #5 - vertical megacolumn translation minus core vertical translation.....	78
Table 5-32: Configuration #5 - core stress (KPa).....	78
Table 5-33: Configuration #5 - megacolumn stress (KPa).....	79
Table 5-34: Configuration #5 - outrigger stress under lateral load only (KPa)	79
Table 5-35: Configuration #5 - belt truss stress under lateral load only (KPa)	80
Table 5-36: Configuration #6 – design variables and calculated megacolumn areas	81
Table 5-37: Configuration #6 - lateral core translation (m).....	81
Table 5-38: Configuration #6 - core rotation (rad)	81
Table 5-39: Configuration #6 - vertical megacolumn translation minus vertical core translation.....	82
Table 5-40: Configuration #6 - core stress (KPa).....	82
Table 5-41: Configuration #6 - megacolumn stress (KPa)	83

Table 5-42: Configuration #6 - outrigger stress under lateral load only (KPa)	83
Table 5-43: Configuration #6 - belt truss stress under lateral load only (KPa)	84
Table 5-44: Configuration #6 - diagonal stress (KPa)	84
Table 5-45: Configuration #7 - design variables and calculated megacolumn areas	85
Table 5-46: Configuration #7 - lateral core translation (m).....	86
Table 5-47: Configuration #7 - core rotation (rad)	86
Table 5-48: Configuration #7 - vertical megacolumn translation minus vertical core translation.....	87

LIST OF FIGURES

Figure 1-1: Jin Mao Tower – Shanghai, China.....	2
Figure 1-2: Jin Mao Tower - structural system elevation view (Choi et al. 2012).....	3
Figure 1-3: Jin Mao Tower - typical framing plan (Choi et al. 2012)	3
Figure 1-4: Two International Finance Centre (IFC2) - Hong Kong, China	4
Figure 1-5: IFC2 - typical floor plan.....	5
Figure 1-6: IFC2 - typical layout of outrigger and belt trusses (Emporis.com)	5
Figure 1-7: Shanghai Tower	6
Figure 1-8: Shanghai Tower - isometric of core, megacolumns, outrigger, and belt trusses	7
Figure 1-9: Guangzhou International Finance Center	8
Figure 1-10: Shanghai World Financial Center (WFC).....	9
Figure 1-11: Shanghai WFC structural system - core, megacolumns, outrigger truss, belt truss, and megadiagonal (Katz et al. 2008).....	9
Figure 1-12: Shanghai WFC structural system elevation views (http://www4.kke.co.jp)	10
Figure 1-13: Generic skyscraper elevation and plan views	11
Figure 1-14: Generic skyscraper - outrigger truss, belt truss, and diagonal systems.....	12
Figure 2-1: One Liberty Place deflected shape.....	17
Figure 2-2: Contraflexure in core created by cap truss (Taranath 2005).....	19
Figure 2-3: Behavior of system with outrigger located at $z = L$ (Taranath 2005).....	19
Figure 2-4: Behavior of system with outrigger located at $z = 0.75L$ (Taranath 2005).....	19
Figure 2-5: Behavior of system with outrigger located at $z = 0.5L$ (Taranath 2005).....	20
Figure 2-6: Behavior of system with outrigger located at $z = 0.25L$ (Taranath 2005).....	20
Figure 3-1: Displaced core with location of DOF's	28
Figure 3-2: Typical outrigger truss subject to unit load.....	30

Figure 3-3: Two-member outrigger truss subject to unit load	31
Figure 3-4: Unit upward vertical displacement (top) and unit clockwise core rotation (bottom)	33
Figure 3-5: Eight-member belt truss subject to unit load	33
Figure 3-6: Belt truss in generic skyscraper subject to unit load	34
Figure 3-7: Unit displacement at megacolumns A (top) and D (middle), and a unit core rotation (bottom).....	36
Figure 3-8: Diagonal in generic skyscraper subject to unit load	37
Figure 3-9: Unit vertical displacements at megacolumns A (left), D (middle), and E (right).....	38
Figure 3-10: Interval with a wind/seismic force at a particular story k	41
Figure 3-11: Interval and a P-delta moment at a particular story k	44
Figure 3-12: Typical outrigger member subject to unit load	47
Figure 3-13: Two-member outrigger truss subject to unit load	47
Figure 3-14: Eight-member belt truss subject to unit load	49
Figure 3-15: Belt truss in generic skyscraper subject to unit load	49
Figure 3-16: Diagonal in generic skyscraper subject to unit load	51
Figure 4-1: Space frame model – all members without floors.....	57
Figure 4-2: Space frame model – single floor configurations between intervals and at intervals	58
Figure 5-1: Configuration #1 - lateral displacement and interstory drift.....	64
Figure 5-2: Configuration #2 - lateral displacement and interstory drift.....	68
Figure 5-3: Configuration #3 - lateral displacement and interstory drift.....	72
Figure 5-4: Configuration #4 - lateral displacement and interstory drift.....	76
Figure 5-5: Configuration #5 - lateral displacement and interstory drift.....	80
Figure 5-6: Configuration #6 - lateral displacement and interstory drift.....	85
Figure 5-7: Configuration #7 - lateral displacement and interstory drift.....	88

1 INTRODUCTION

A new simplified skyscraper analysis model (SSAM) is described herein. The model can be implemented on a spreadsheet. The accuracy of the SSAM has been compared to results from sophisticated space frame and finite element analysis models. Those results will be presented and discussed in this thesis. The SSAM is intended to be used in the preliminary design phase of skyscrapers where a fast, reasonably-accurate model is needed in design iterations. The model can also be used in an educational setting where senior/graduate students are introduced to the behavior and design of skyscrapers.

The SSAM predicts the linear and nonlinear response of "modern" skyscrapers subject to gravity, wind, and seismic loads. Modern skyscrapers are defined herein to be third generation skyscrapers. First generation skyscrapers such as the Empire State Building in New York City consisted of steel braced and unbraced frames. Such skyscrapers had many interior columns obstructing the space. Fazlur Khan is regarded as the father of second generation skyscrapers characterized as framed tubes or tube-in-tube skyscrapers such as the former World Trade Center in New York City. These skyscrapers possess an interior core tube that encloses elevator shafts, and a perimeter tube with many columns. There are no columns in between the core tube and perimeter tube, thus providing unobstructed space. By moving the columns to the perimeter, a system with maximum moment of inertia is created to resist lateral loads. The third generation of skyscrapers coalesces perimeter columns into a few megacolumns to provide an unobstructed view to the outside. Such megacolumns are usually composite members made from steel

sections encased in high-stiffness, high-strength concrete. To provide the necessary moment of inertia to resist lateral loads, the megacolumns and core are periodically connected with outrigger trusses, belt trusses, and diagonals. The SSAM is used to analyze core-megacolumn-outrigger-belt-diagonal systems. Some examples of core-megacolumn-outrigger-belt-diagonal skyscrapers will now be given.

The 88-story Jin Mao Tower (see Figure 1-1), completed in 1999 in Shanghai, China, consists of an octagonal concrete core and eight composite steel/concrete megacolumns. Steel outrigger trusses connect the core and megacolumns at stories 25, 54, and 86 (see Figure 1-2 and Figure 1-3). A belt truss is located at the top of the tower, which is typically called a cap truss.



Figure 1-1: Jin Mao Tower – Shanghai, China
© SOM

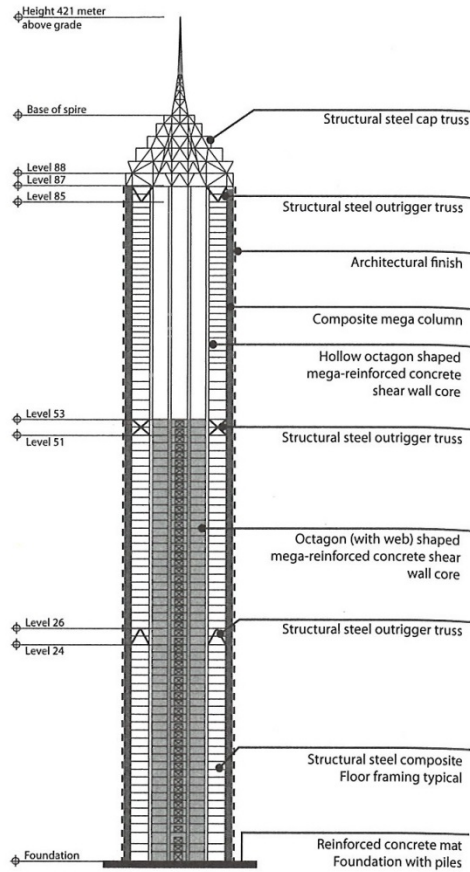


Figure 1-2: Jin Mao Tower - structural system elevation view (Choi et al. 2012)

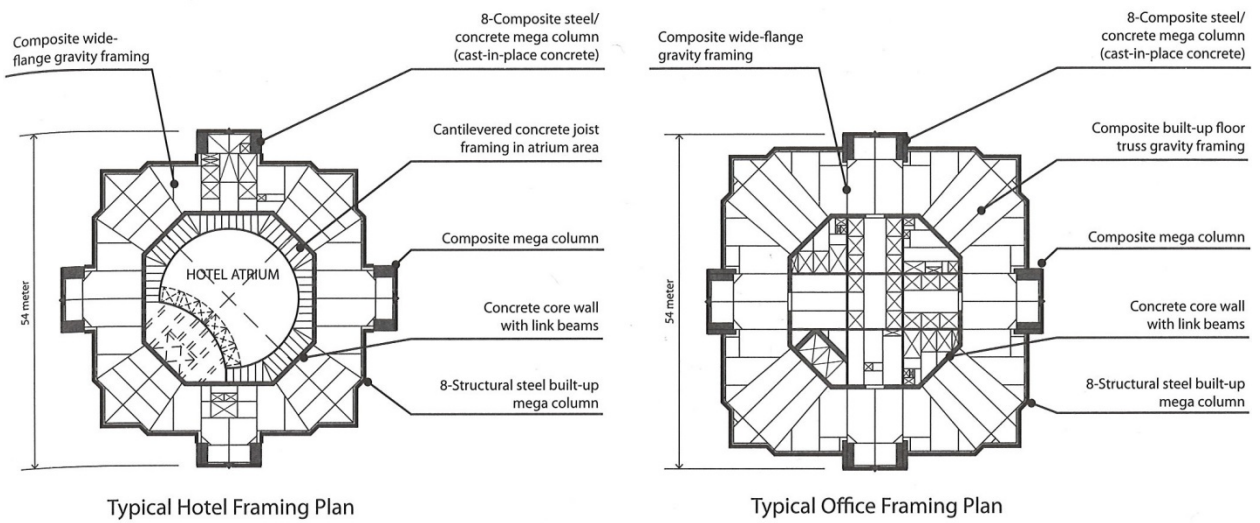


Figure 1-3: Jin Mao Tower - typical framing plan (Choi et al. 2012)

Hong Kong's 2 International Finance Centre is an excellent example of a core-mega column-outrigger-belt system (see Figure 1-4). This 88-story skyscraper completed in 2004 has a core with eight megacolumns shown in red in Figure 1-5. Outrigger and belt trusses are located at stories 33, 55, and 67. The 24m spacing between megacolumns provides unobstructed view to the outside for offices on the perimeter. A typical outrigger-belt truss configuration is shown in Figure 1-6. Belt trusses transfer loads from secondary corner columns to the megacolumns (Choi et al. 2012).



Figure 1-4: Two International Finance Centre (IFC2) - Hong Kong, China
© Antony Wood/CTBUH

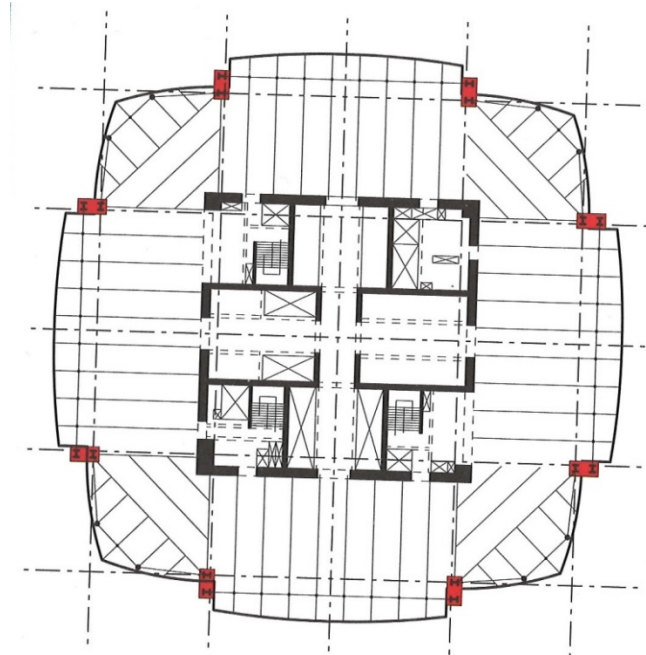


Figure 1-5: IFC2 - typical floor plan
©Arup



Figure 1-6: IFC2 - typical layout of outrigger and belt trusses (Emporis.com)

The Shanghai Tower is a 126-story 632m tall skyscraper scheduled for completion in 2014 (see Figure 1-7). Even though the exterior facade has a twisting irregular shape that significantly reduces wind load, the core is square and the composite megacolumns are arranged in a regular circular pattern whose diameter decreases with height (see Figure 1-8). The outrigger trusses and circular belt trusses occur at nine levels separated by 12 to 15 stories (Mass et al. 2010). Radial trusses extend outward from the megacolumns to support the irregular twisting facade. The space between the perimeter megacolumns and the exterior facade will be used as atria open to the public.



Figure 1-7: Shanghai Tower
© Gensler

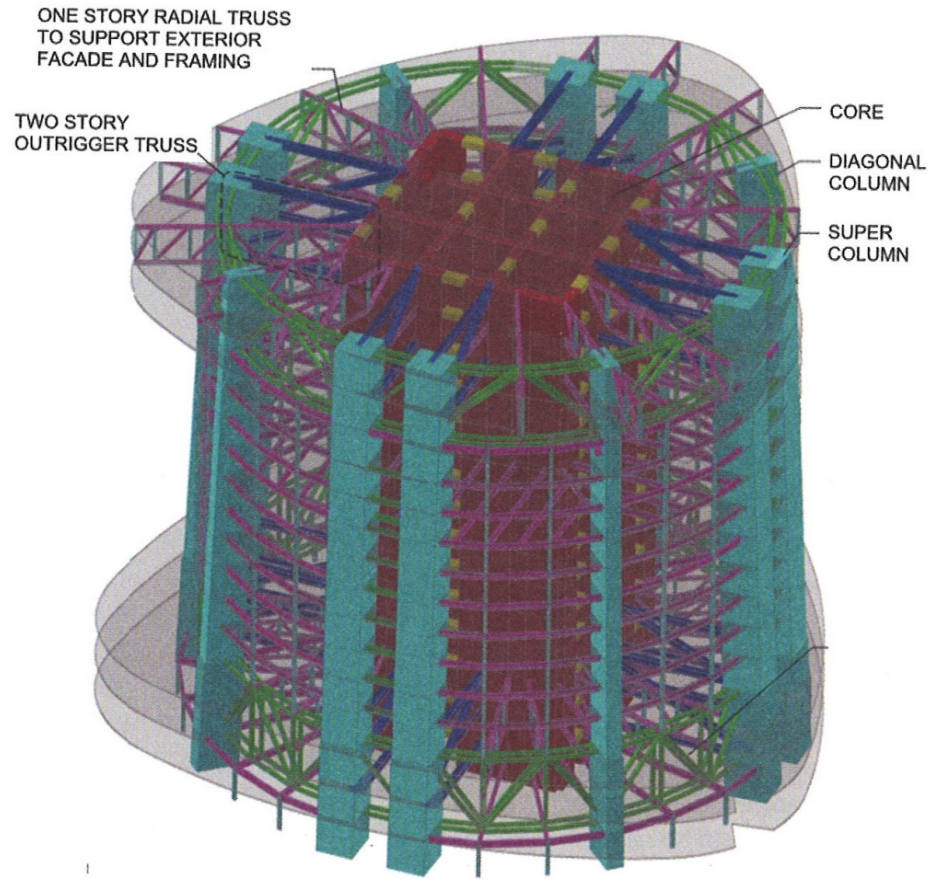


Figure 1-8: Shanghai Tower - isometric of core, megacolumns, outrigger, and belt trusses
 © Thornton Tomasetti

The Guangzhou International Finance Center is a 440m high skyscraper with 73 stories of office space and 30 stories of hotel space (see Figure 1-9). The structure consists of a central core and perimeter diagonals arranged in what is known as a diagrid system. There are no vertical megacolumns, outriggers, or belt trusses in the diagrid system. The diagonals are concrete-filled steel tubes.



Figure 1-9: Guangzhou International Finance Center
© Christian Richters

The Shanghai World Financial Center includes core, megacolumns, outrigger trusses, belt trusses, and megadiagonals (see Figures 1-10, 1-11, and 1-12). This mixed lateral load-resisting system was motivated by the need to reduce weight in the structure (Katz et al. 2008). Note that two of the megacolumns split part way up so that there are four megacolumns at the base and six megacolumns after the split.



Figure 1-10: Shanghai World Financial Center (WFC)
© Kohn Pederson Fox Associates/CTBUH

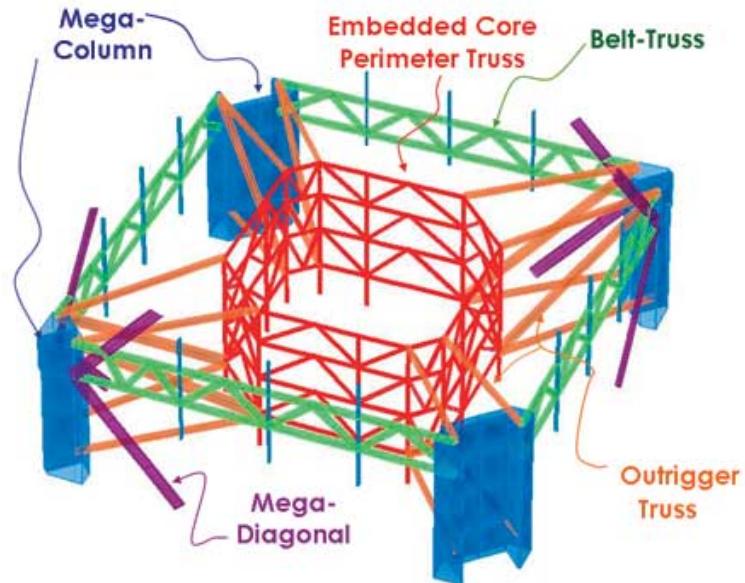


Figure 1-11: Shanghai WFC structural system - core, megacolumns, outrigger truss, belt truss, and megadiagonal (Katz et al. 2008)

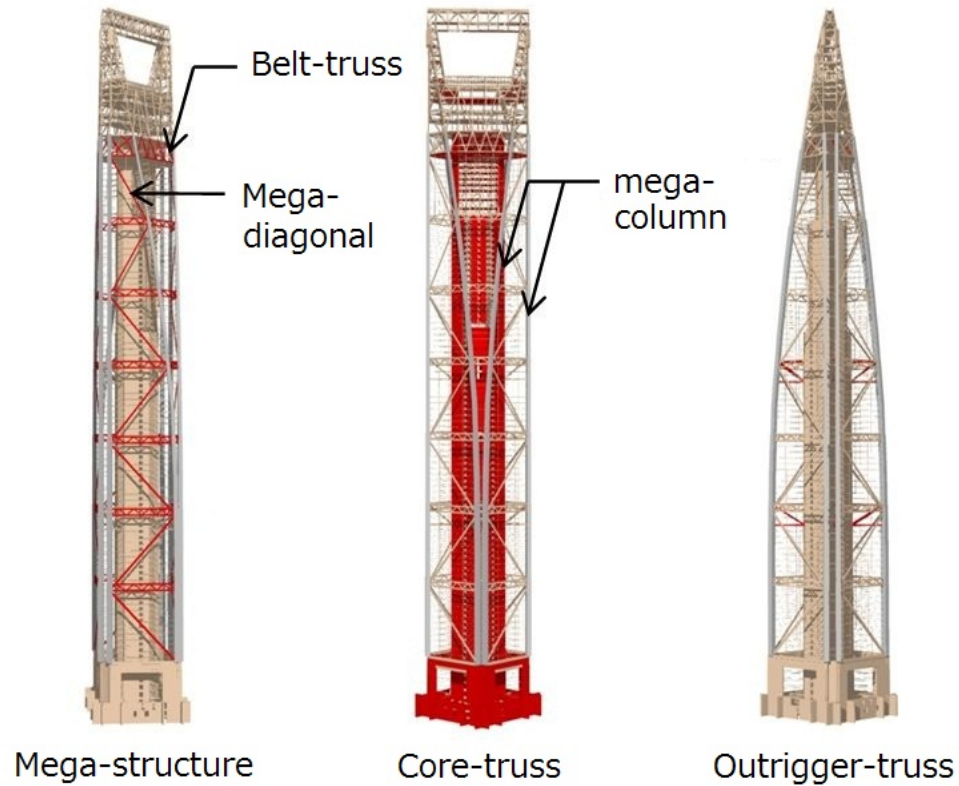


Figure 1-12: Shanghai WFC structural system elevation views (<http://www4.kke.co.jp>)

The generic skyscraper in Figures 1-13 and 1-14 will be used throughout this thesis for analysis comparison. The concrete core is shown in yellow, the 16 concrete megacolumns are shown in red, the two-member steel outrigger trusses are shown in green, the 8-member steel belt trusses are shown in blue, and the steel diagonals are shown in black. Multiple configurations of this generic skyscraper will be considered in the thesis:

- 1) core+megacolumns
- 2) core+megacolumns+outriggers
- 3) core+megacolumns+belts
- 4) core+megacolumns+diagonals
- 5) core+megacolumns+outriggers+belts
- 6) core+megacolumns+outriggers+belts+diagonals

The remainder of the thesis is divided into five chapters. Chapter 2 reviews the literature on related approximate analysis methods. Chapter 3 describes the SSAM. Chapter 4 describes the sophisticated linear space frame and nonlinear ADINA models. Chapter 5 presents results from the SSAM, the space frame model, and the ADINA model for the six configurations of the generic skyscraper. Chapter 6 submits conclusions based on the results. The appendix includes a copy of the spreadsheet implementation of the SSAM for the generic skyscraper.

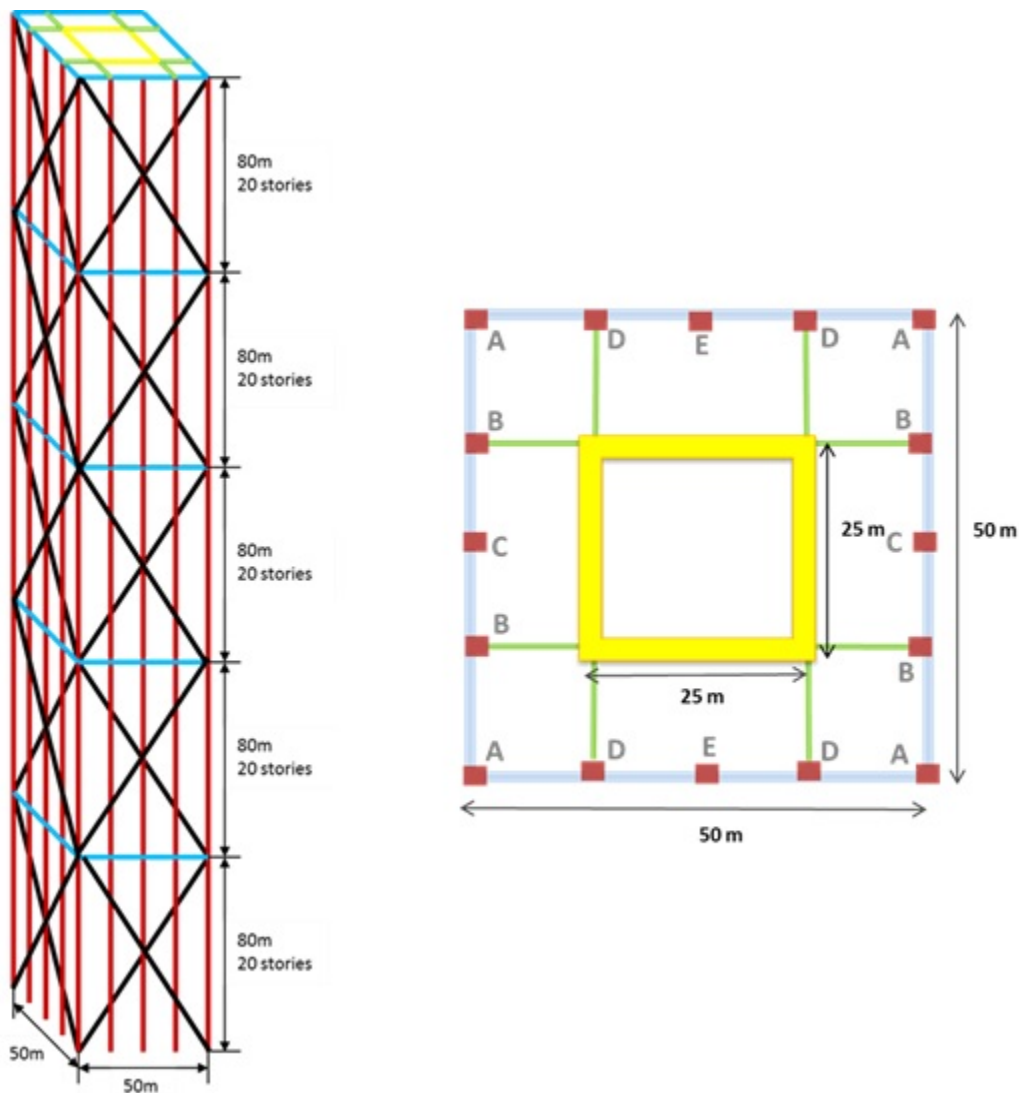


Figure 1-13: Generic skyscraper elevation and plan views

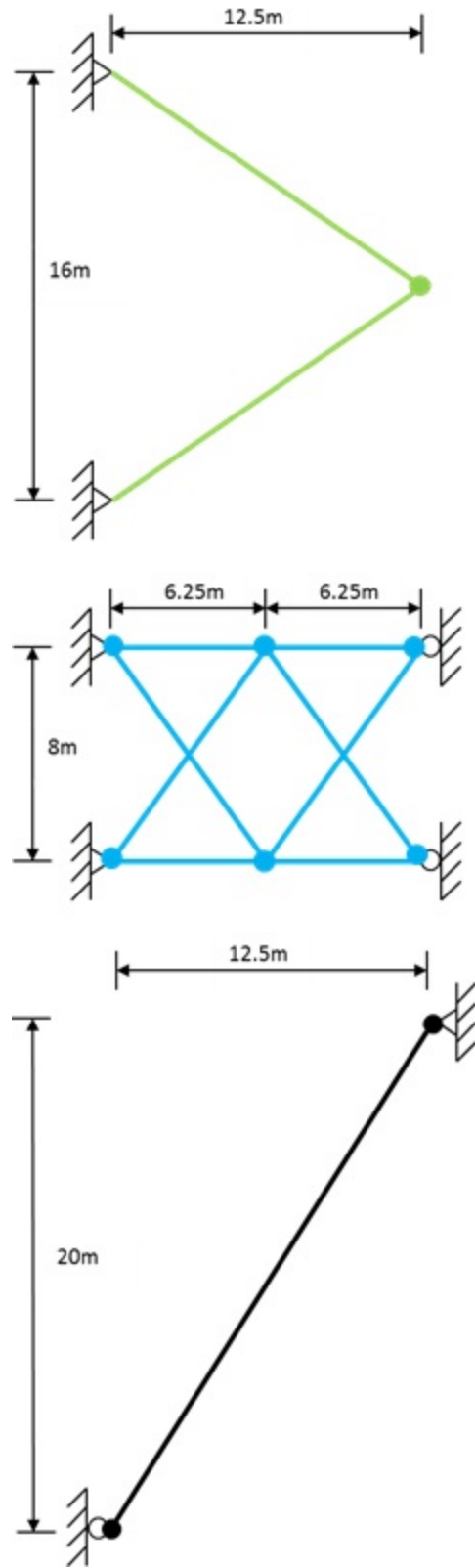


Figure 1-14: Generic skyscraper - outrigger truss, belt truss, and diagonal systems

2 LITERATURE REVIEW

The literature on approximate analysis methods for tall buildings can be subdivided into continuum methods and discrete methods. Continuum methods model tall buildings as vertical cantilevers, and approximate displacements as continuous functions of vertical position using flexure/shear beam theory. Discrete methods construct stiffness or flexibility matrices for the system. The finite element method is an example of a discrete method. Some of the approximate discrete methods surveyed enforce compatibility conditions at the discrete locations of outrigger and belt trusses. Other approximate discrete methods construct reduced system stiffness matrices through the use of substructuring or super-elements. The SSAM is a discrete method that constructs a reduced system stiffness matrix.

2.1 Continuum Methods for Low/Medium-Rise Buildings

Bozdogan and Ozturk (2009) proposed an approximate method based on the continuum method idealizing low-rise wall-frame and tube-in-tube structures of 11 stories and 15 stories, respectively, as sandwich beams. Their sandwich beam consists of two vertical Timoshenko cantilever beams attached by horizontal connecting beams in parallel. One beam consists of the sum of the flexural and shear rigidities of shear walls and columns. The second beam consists of the sum of shear rigidities of frames and connecting beams. By solving a set of differential equations for the shear force equilibrium in both beams, continuous equations for displacement

and rotation with respect to vertical position are obtained. Bozdogan (2009) also applied this method to dynamic analyses on the same example wall-frame structure.

Potzta and Kollar (2003) discussed the development of replacement beams as sandwich beams in simplifying the analysis of low-rise buildings with combinations of shear walls, coupled shear walls, frames, and trusses. Again, the sandwich beam applies the continuum method by representing the system as a Timoshenko beam that is supported laterally by a beam with bending stiffness. Each lateral load-resisting system is replaced by a continuous cantilever beam with connecting beams between them. The strain energy of the sandwich beam is presented as the strain energies of a Timoshenko beam and of a beam with bending deformation only. An example 7-story building with two coupled shear walls and a frame is used to demonstrate this method. This same procedure is used by Kaviani et al. (2008) who extends the method to structures of variable cross-section.

An approximate hand calculated method for asymmetric wall-frame structures was proposed by Rutenberg and Heidebrecht (1975). Lateral loads from wind or earthquakes produce both lateral deflections and twisting in asymmetric configurations. The flexural walls and frames are modeled as vertical flexural and shear cantilevers where torsional behavior is treated in addition. Coupled torsion-bending differential equations governing the static equilibrium of the structure are solved to obtain continuous functions for story displacements and rotations with height. Their method is applied to a 16-story wall-frame structure.

A new concept to increase the lateral stiffness of wall-frame tall building structures by stiffening a story of the frame system was proposed by Nollet and Smith (1997). The wall-frame structure is modeled using the continuum theory by representing the system as two cantilever beams in parallel by connecting beams. The shear wall, with a modified flexural rigidity, is

connected to and constrained to have the same deflected shape as the frame by axially rigid connecting links. The rigid links that provide horizontal rigidity represent a continuum between the wall and frame. A continuous displacement function with respect to height was then obtained by modifying and solving the differential equation for bending moment of a cantilever with the added stiffness parameter. An example 20-story wall-frame structure with shear walls and four moment resisting frames was analyzed to verify the method.

Abergel and Smith (1983) developed an approximate method of analysis for non-twisting medium-rise structures composed of shear walls, cores, and identical coupled walls. An alternative to previous approximations is made based on the differential equations of deflection of a cantilever beam. By replacing the coupled wall with a comparable structure where the connecting beams are treated as a continuous medium with equivalent bending and shear properties, a differential equation relating the horizontal loading is derived. The differential equation relating horizontal loading was developed from two previously derived equations for shear walls. A 20-story building with four coupled walls, two shear walls, and a core is used as an example.

Heidebrecht and Smith (1973) present a simple hand method for the static and dynamic analysis of uniform low to medium-rise structures consisting of interacting shear walls and frames. The mathematical model consists of a combination of flexural and shear vertical cantilever beams deforming either in shear or bending and is very similar to other methods where the governing differential equations for flexural and shear beams subject to lateral load are solved. Differently from other approximations, their method has application to nonuniform shear wall-frame structures. The method is applied to a 12-story wall-frame building. Similarly, Hoenderkamp et al. (1984) and Toutanji (1997) use variations of this method by modeling

medium-rise buildings with coupled walls and shear walls with frames as flexural and shear vertical cantilevers.

2.2 Continuum Method for Framed Tubes

Kwan (1994) developed a simple hand calculation method for the analysis of framed tube structures accounting for shear lag effects. This method assumes that framed tube structures can primarily behave like cantilevered box beams. The framed tube structure is modeled as two web panels and two flange panels. It is assumed that there is uniform stiffness throughout the structure and the differential equation of moment equilibrium in a cantilever beam was solved to obtain continuous functions of displacement and rotation with respect to height. Two examples of a 40-story high-rise and a 15-story low-rise composed of framed tubes are presented. Rahgozar and Sharifi (2009) applied a variation of Kwan's (1994) method on 30, 40, and 50-story framed tube buildings with shear cores and belt trusses.

Takabatake (2012) refers to the one-dimensional rod theory as a method in the preliminary design stage that is most suitable when replacing a high rise structure as a continuous member. This extended rod theory includes the Timoshenko beam theory effects along with longitudinal deformation and shear-lag effects by replacing the structure with an equivalent stiffness distribution. The theory is extended to two-dimensional extended rod theory by considering structural components with different stiffness and mass distributions that are continuously connected. They are modeled as several parallel beams. Governing equations are solved for shear and flexure in a cantilever beam where a continuous displacement function is obtained that satisfies continuity conditions between the parallel beams. A 30-story framed tube is used as an example. Kobayashi et al. (1995) applied Takabatake's (2012) method to a 30-story tube-in-tube example building.

2.3 Inherent Problems with Continuum Methods

Note that none of the continuum models surveyed thus far have been applied to buildings with outriggers. This is because continuum models based on cantilever beam theory cannot reproduce the points of contraflexure exhibited in the deflected shapes of tall buildings with outriggers as shown in Figure 2-1 taken from Choi et al. (2012). The bending moment in a cantilever beam loaded laterally in one direction does not change sign, and therefore, points of contraflexure do not exist. Many studies have recognized the possibility that points of contraflexure exist in tall buildings with outriggers.

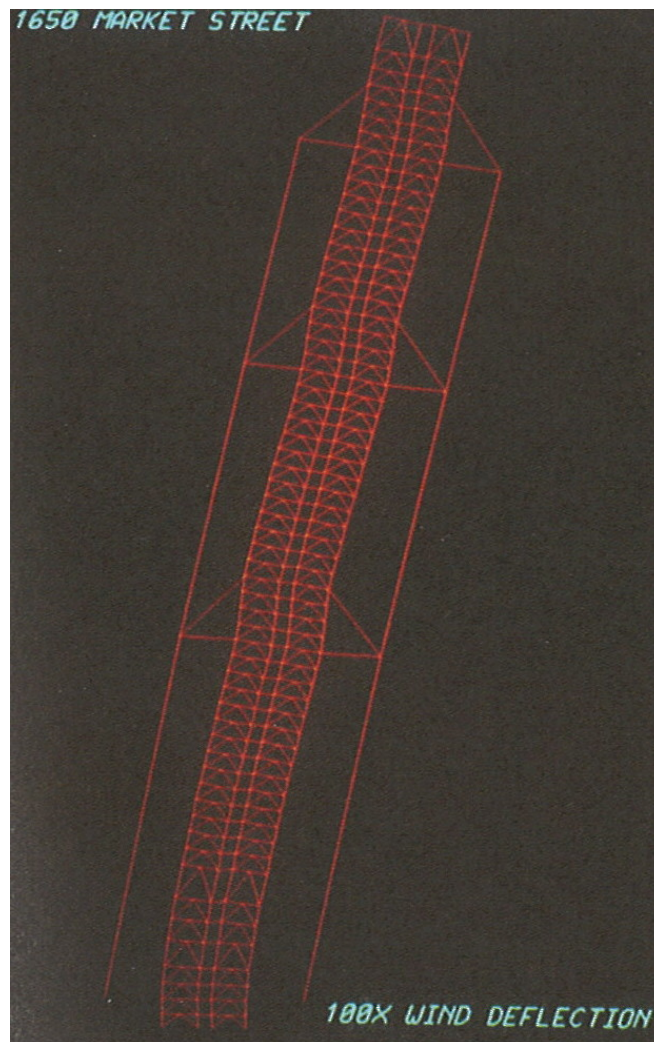


Figure 2-1: One Liberty Place deflected shape
© Thornton Tomasetti

Choi et al. (2012) explain the outrigger-core coupling as follows: "When laterally loaded the outriggers resist core rotation by using perimeter columns to push and pull in opposition, introducing a change in slope of the vertical deflection curve, a portion of the core overturning moment is transferred to the outriggers and, in turn, tension in windward columns and compression in leeward columns... Analysis and design of a complete core-and-outrigger system is not that simple: distribution of forces between the core and the outrigger system depends on the relative stiffness of each element. One cannot arbitrarily assign overturning forces to the core and the outrigger columns. However, it is certain that bringing perimeter structural elements together with the core as one lateral load resisting system will reduce core overturning moment." Kowalczyk et al. (1995) explain the function of outriggers with the following: "...outriggers serve to reduce the overturning moment in the core that would otherwise act as a pure cantilever, and to transfer the reduced moment to columns outside the core by way of a tension-compression couple, which takes advantage of the increased moment arm between these columns." Stafford Smith and Coull (1991) state that, "the outrigger-braced structure, with at most four outriggers, is not strictly amenable to a continuum analysis and has to be considered in its discrete arrangement."

Figure 2-2 through Figure 2-6 were taken from a study by (Taranath 2005) about the relationship between outrigger location and the existence of points of contraflexure. In Figure 2-4, the tie-down action of the cap truss generates a restoring couple at the building top, resulting in a point of contraflexure in its deflection curve. Figure 2-3, Figure 2-4, Figure 2-5, and Figure 2-6 show deflected shape and bending moment diagrams for different vertical locations of a single outrigger truss.

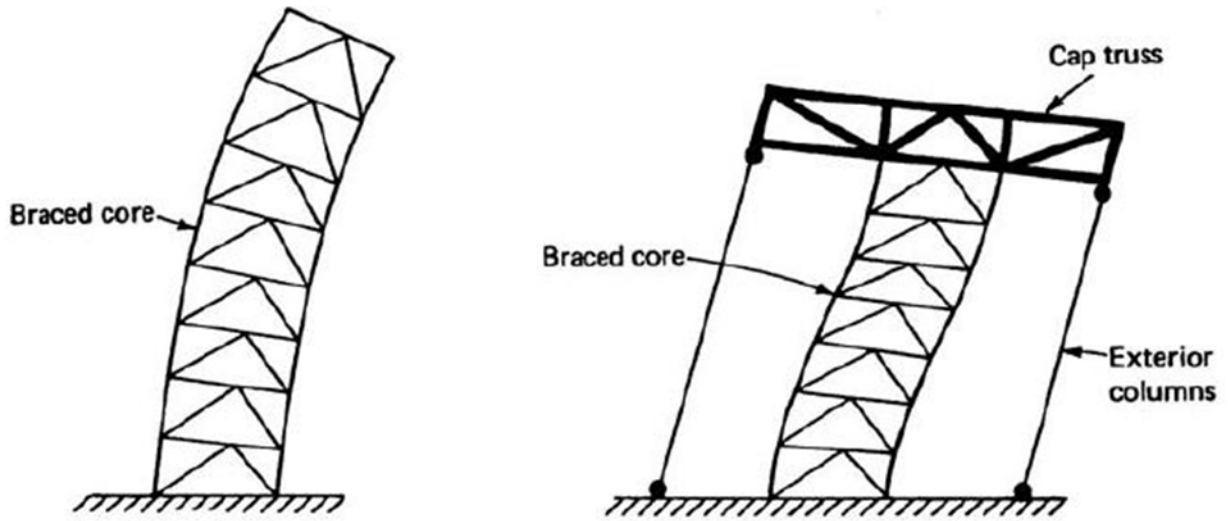


Figure 2-2: Contraflexure in core created by cap truss (Taranath 2005)

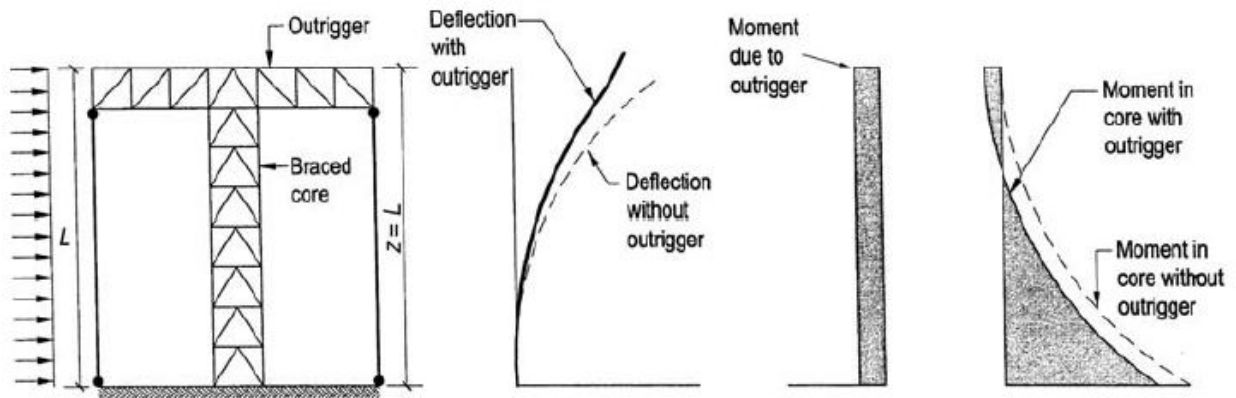


Figure 2-3: Behavior of system with outrigger located at $z = L$ (Taranath 2005)

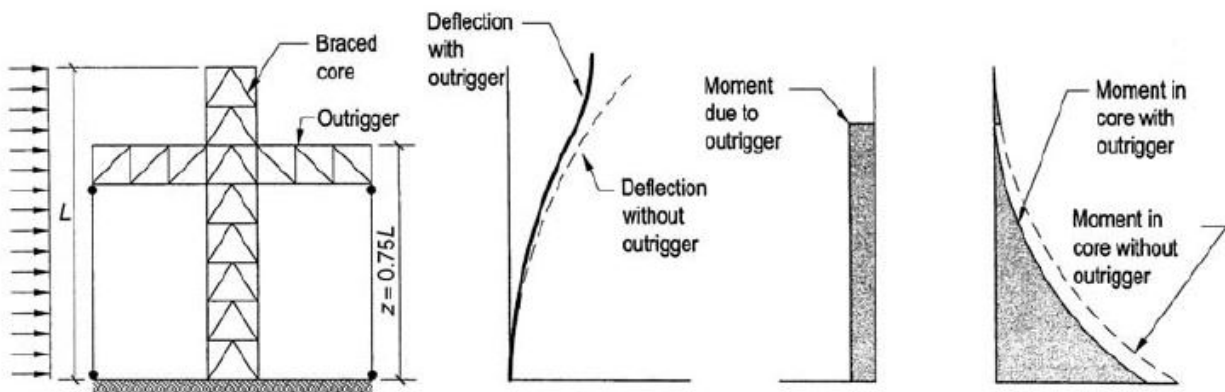


Figure 2-4: Behavior of system with outrigger located at $z = 0.75L$ (Taranath 2005)

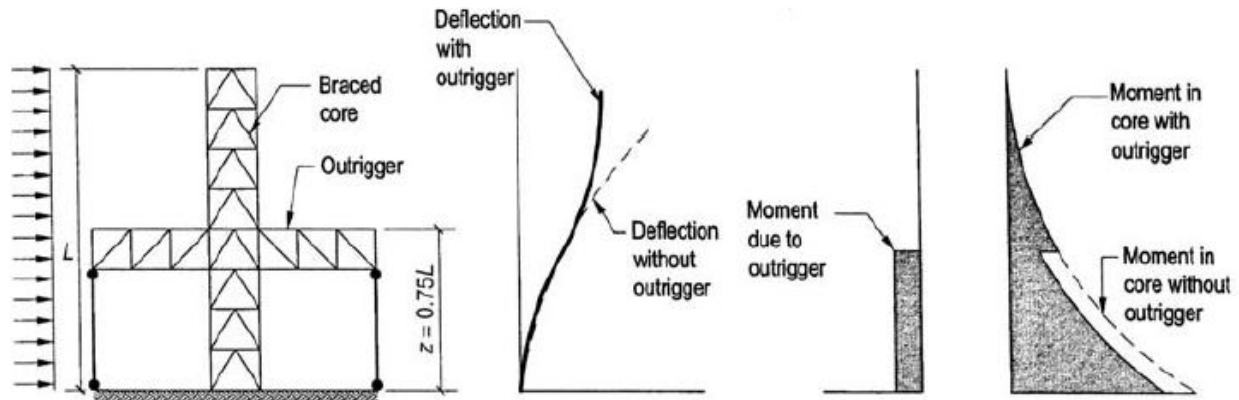


Figure 2-5: Behavior of system with outrigger located at $z = 0.75L$ (Taranath 2005)

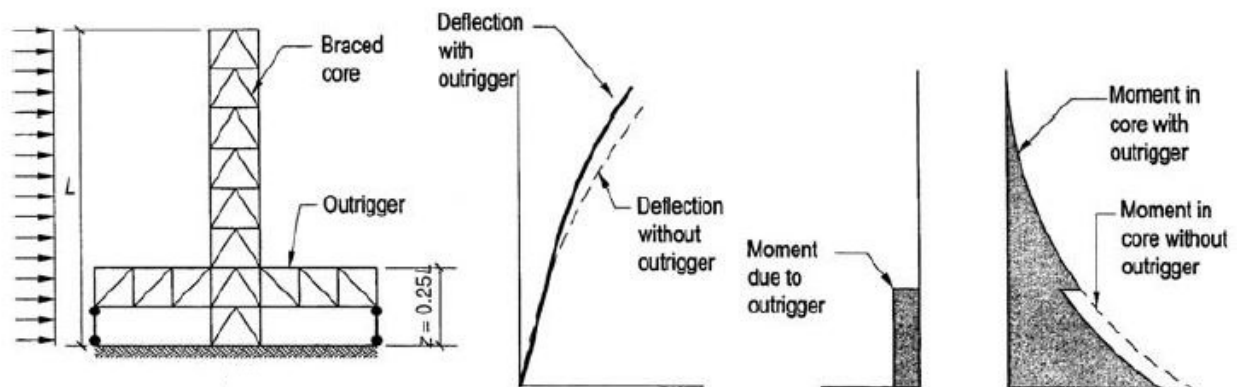


Figure 2-6: Behavior of system with outrigger located at $z = 0.25L$ (Taranath 2005)

2.4 Discrete Outrigger Methods

Hoenderkamp and Bakker (2003) wrote about analyzing high-rise braced frames with outriggers. Three stiffness parameters are considered which represent the frame wall, outriggers and columns at the single story where the outrigger is present. Two degrees of freedom for the braced frame are taken as a rotation and a translation about the vertical axis. The rotation equation assumes the rotation of a free cantilever with respect to height subject to a uniformly distributed load. A third degree of freedom comes from the rotation of the outrigger that produces a restraining moment in the frame. The total rotation of the braced frame at the outrigger level becomes a product of the cantilever rotation reduced by the moment rotation

created by the outriggers. The horizontal deflection at the top of the structure is then determined by a compatibility equation for the rotation at the interface of the braced frame and outrigger. The method was tested on three braced-frame-outrigger high-rise buildings of 57.5m, 72m, and 93.6m in height. Hoenderkamp (2008) applies the method to high-rises with outriggers at two levels, and Hoenderkamp (2004) applies the method to high-rises with outriggers and flexible foundations.

Taranath (2005) conceptualizes outriggers as restraining springs located on the cantilever. The ratio of the outrigger moment to the outrigger stiffness is equated to the rotation of a uniformly loaded cantilever beam with constant stiffness. The resulting deflection is obtained by superposing the deflection of the cantilever and the moment induced by the spring. Rahgozar et al. (2010) apply a similar method to 45-story and 55-story buildings composed of framed tube, shear core, belt truss, and an outrigger where the belt truss, outrigger, and shear core are considered as a bending spring with constant rotational stiffness acting as a concentrated moment where the belt truss and outrigger are located.

Stafford Smith and Coull (1991) created compatibility equations for each outrigger level to equate the rotation of the core to the rotation of the outrigger. The rotation of the core is expressed in terms of its bending deformation and that of the outrigger in terms of the axial deformations of the columns and the bending of the outrigger. The top drift of the structure may then be determined from the resulting bending moment diagram for the core by using the moment-area method. Furthermore, this same method of analysis can be applied to structures with more than two outriggers by expressing them as restraining moments in the equation of horizontal deflection for a cantilever beam. These multiple restraining moments can be expressed in matrix form for simultaneous solution of multiple equations. This method of

compatibility was published earlier by Smith and Salim (1981) which was then improved upon by Stafford Smith and Coull (1991).

Wu and Li (2003) take this compatibility approach as well for multi-outrigger-braced tall buildings with an additional application to their dynamic characteristics. Rutenberg (1987) made a parametric study for this method investigating the effect of outrigger location, ratio of perimeter column to core stiffness, and stiffness variation along the height on the horizontal displacement at roof level.

2.5 Discrete Substructuring Methods

Lin et al. (1994) presented an approximate approach called the finite story method (FSM) to analyze the displacement and natural frequencies of tall framed tube buildings. The method reduces the system stiffness matrix to involve horizontal displacements and rotations about the vertical axis. It is based on the displacements of two-story substructures to approximate shear, bending, and torsion components of global deformations. A 30-story framed tube building is used as an example.

De Llera and Chopra (1995) developed a new simplified model for analysis and design of multistory buildings. The model is based on a single super-element per building story that is capable of representing the elastic and inelastic properties of the story. This is done by matching the stiffness matrices and ultimate yield surface of the story with that of the element. The analysis consists of multistory buildings with rigid diaphragms where the masses are lumped together and where lateral resistance is provided by resisting planes in both horizontal directions composed of elasto-plastic elements. A single fictitious structural super-element per story has three degrees of freedom, two horizontal translations and the rotation of the floor connected by

the element, where a reduced stiffness matrix is created. This method was applied to a small building with 4 stories.

3 SIMPLIFIED SKYSCRAPER ANALYSIS MODEL

The steps of the simplified skyscraper analysis model (SSAM) consist of: 1) determination of megacolumn areas, 2) construction of stiffness matrix, 3) calculation of lateral forces and displacements, and 4) calculation of stresses. The SSAM was implemented on a spreadsheet. The spreadsheet can be used for rapid trial-and-error optimization of the skyscraper. Such usage will be addressed at the end of this chapter.

3.1 Determination of Megacolumn Areas

The SSAM subdivides the skyscraper vertically into **intervals**. Outrigger and belt trusses are located at interval boundaries. It will be assumed that the cross-sectional areas of the core, megacolumns, and diagonals remain constant in each interval. It will also be assumed that the cross-sectional areas of composite steel/concrete cores and megacolumns are the cross-sectional areas of the transformed all-concrete sections where steel area has been multiplied by the ratio of steel elastic modulus to concrete elastic modulus. Define the following terms:

- n_i = number of stories in interval i (20 for generic skyscraper)
- h_i = vertical height of interval i (80m for generic skyscraper)
- A_i^{core} = cross-sectional area of the core in interval i
- $A_i^{\text{col}j}$ = cross-sectional area of megacolumn j in interval i
- $A_i^{\text{diag}j}$ = cross-sectional area of diagonal j in interval i
- V_i^{diag} = volume of all diagonal members in interval i
- S_i^{diag} = sine of angle from horizontal for diagonals in interval i
- L_i^{diag} = length of diagonals in interval i

k_i^{diag} = vertical stiffness of all diagonals in interval i
 F_i^{core} = axial force in core at base of interval i excluding interval i self weight
 F_i^{colj} = axial force in megacolumn j at base of interval i excluding interval i self weight
 γ = concrete unit weight (core and megacolumns)
 ε_i = axial strain at bottom of interval i
 E = concrete modulus of elasticity (core and megacolumns)
 E^s = steel modulus of elasticity (diagonals, outriggers, belts)
 A_T^{core} = core tributary area
 A_T^{colj} = tributary area for megacolumn j
 P_T^{colj} = tributary perimeter for megacolumn j
 L^{dead} = floor dead load per area
 L^{live} = floor live load per area
 L^{clad} = cladding load per area
 T_i^{core} = outrigger truss weight in interval i supported by the core
 T_i^{colj} = outrigger-belt-diagonal truss weight in interval i supported by megacolumn j

Assume that intervals are numbered with $i=1$ being the top interval and increasing downward. Assume that $h_0 = A_0^{\text{core}} = A_0^{\text{colj}} = 0$ in the following formulas. Assume that the weight of any pinnacle or cap on top of the skyscraper is distributed appropriately among the core and megacolumns to get values for F_0^{core} and F_0^{colj} . The core and megacolumn axial forces excluding interval self weight are calculated from Equations 3-1 and 3-2:

$$F_i^{\text{core}} = F_{i-1}^{\text{core}} + \gamma h_{i-1} A_{i-1}^{\text{core}} + n_i A_T^{\text{core}} (L^{\text{dead}} + L^{\text{live}}) + T_i^{\text{core}} \quad (3-1)$$

$$F_i^{\text{colj}} = F_{i-1}^{\text{colj}} + \gamma h_{i-1} A_{i-1}^{\text{colj}} + n_i A_T^{\text{colj}} (L^{\text{dead}} + L^{\text{live}}) + h_i P_T^{\text{colj}} L^{\text{clad}} + T_i^{\text{colj}} \quad (3-2)$$

Given the cross-sectional area of the core, the cross-sectional areas of the megacolumns are determined from the principle that **the axial strain in the megacolumns must be the same as the axial strain in the core under gravity loads** in order to prevent unacceptably large differential vertical displacements from accumulating in the upper floors of the skyscraper. If there are no diagonals, then at the base of interval i, the axial strain in the core is equated to the axial strain in each megacolumn j in Equation 3-3,

$$\varepsilon_i = \frac{F_i^{\text{core}} + \gamma h_i A_i^{\text{core}}}{EA_i^{\text{core}}} = \frac{F_i^{\text{colj}} + \gamma h_i A_i^{\text{colj}}}{EA_i^{\text{colj}}} \quad (3-3)$$

This can be solved for the area of megacolumn j in interval i in Equation 3-4:

$$A_i^{\text{colj}} = A_i^{\text{core}} \frac{F_i^{\text{colj}}}{F_i^{\text{core}}} \quad (3-4)$$

The above formula must be modified if diagonals are present because diagonals contribute to the support of gravity loads. The vertical stiffness of all diagonals in interval i is calculated in Equation 3-5:

$$k_i^{\text{diag}} = \frac{E^s \left(\sum_j A_i^{\text{diagj}} \right) (S_i^{\text{diag}})^2}{L_i^{\text{diag}}} = \frac{E^s \left(\sum_j A_i^{\text{diagj}} \right) (S_i^{\text{diag}})^3}{h_i} \quad (3-5)$$

The sum of diagonal areas in interval i can be calculated from the volume of diagonal members in interval i from Equation 3-6:

$$\sum_j A_i^{\text{diagj}} = V_i^{\text{diag}} \frac{S_i^{\text{diag}}}{h_i} \quad (3-6)$$

At the base of interval i, the axial strain in the core is equated to the axial strain in all the megacolumns and diagonals together by Equation 3-7:

$$\varepsilon_i = \frac{F_i^{\text{core}} + \gamma h_i A_i^{\text{core}}}{EA_i^{\text{core}}} = \frac{\left(\sum_j F_i^{\text{colj}} \right) + \gamma h_i \left(\sum_j A_i^{\text{colj}} \right)}{E \left(\sum_j A_i^{\text{colj}} \right) + E^s \left(\sum_j A_i^{\text{diagj}} \right) (S_i^{\text{diag}})^3} \quad (3-7)$$

This can be solved for the sum of megacolumn areas in interval i in Equation 3-8:

$$\begin{aligned}\sum_j A_i^{\text{colj}} &= A_i^{\text{core}} \frac{\sum_j F_i^{\text{colj}}}{F_i^{\text{core}}} - \left(\sum_j A_i^{\text{diagj}} \right) (S_i^{\text{diag}})^3 \frac{E^s}{E} \left(1 + \frac{\gamma h_i A_i^{\text{core}}}{F_i^{\text{core}}} \right) \\ &= A_i^{\text{core}} \frac{\sum_j F_i^{\text{colj}}}{F_i^{\text{core}}} - \frac{V_i^{\text{diag}}}{h_i} (S_i^{\text{diag}})^4 \frac{E^s}{E} \left(1 + \frac{\gamma h_i A_i^{\text{core}}}{F_i^{\text{core}}} \right)\end{aligned}\quad (3-8)$$

The area of megacolumn j in interval i is solved for in Equation 3-9:

$$\begin{aligned}A_i^{\text{colj}} &= \frac{F_i^{\text{colj}}}{\sum_j F_i^{\text{colj}}} \sum_j A_i^{\text{colj}} \\ &= A_i^{\text{core}} \frac{F_i^{\text{colj}}}{F_i^{\text{core}}} - \frac{V_i^{\text{diag}}}{h_i} (S_i^{\text{diag}})^4 \frac{F_i^{\text{colj}}}{\sum_j F_i^{\text{colj}}} \frac{E^s}{E} \left(1 + \frac{\gamma h_i A_i^{\text{core}}}{F_i^{\text{core}}} \right)\end{aligned}\quad (3-9)$$

The above formula is used in the spreadsheet. Note that if the area of the diagonals is big enough, the megacolumn areas may drop to zero resulting in a diagrid skyscraper.

3.2 Construction of the Stiffness Matrix

Lateral load analysis in the SSAM is performed by constructing a stiffness matrix in the spreadsheet for the skyscraper. The degrees of freedom (DOF's) consist of the horizontal displacement of the core at the top of each interval, the rotation of the core at the top of each interval, and the vertical displacements of each of the megacolumns at the top of each interval. Figure 3-1 below shows a laterally displaced core (thick line), a single megacolumn B (thin line), and outrigger trusses at the top of each interval (dotted lines). The dashed lines show the undisplaced position of the structure. The DOF's are identified in Figure 3-1 where subscripts correspond to story numbers. Symmetry is exploited if possible. The generic skyscraper is doubly symmetric so that only one quarter of the skyscraper is included in the model. The model consists of one-fourth of the core, one-half of megacolumns C and E, and a full portion of

megacolumns A, B, and D. Assume that the lateral load is perpendicular to the wall containing megacolumns A, B, and C. Since the vertical displacement in megacolumn E is zero under lateral loading, only the vertical displacements for megacolumns A, B, C, and D will be counted as DOF's. Thus, there are 6 DOF's at the top of each interval for a total of 30 DOF's.

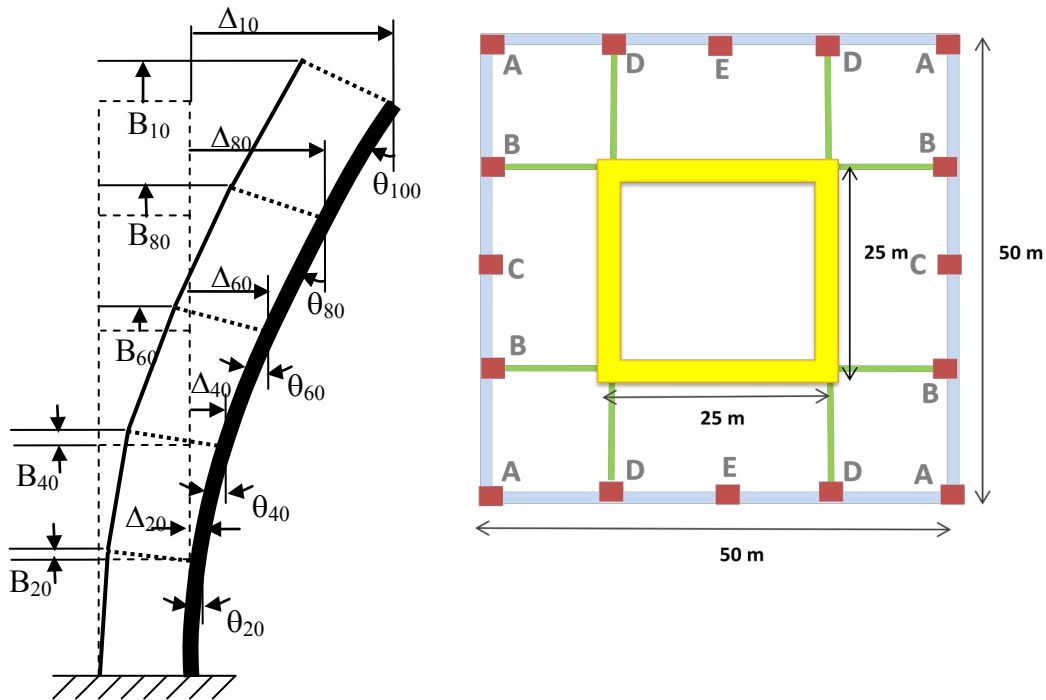


Figure 3-1: Displaced core with location of DOF's

The moment of inertia of the core must be calculated for each interval. This is done by dividing the core into thin rectangles where it is assumed that all rectangles have the same thickness in Equation 3-10:

I_i^{core} = moment of inertia of the core in interval i

t_i = core wall thickness in interval i

d_i^j = length of rectangle j in interval i

y_i^j = distance from centroid of rectangle j to neutral axis in interval i

α_i^j = angle from neutral axis to axis parallel to length of rectangle j in interval i

$$I_i^{\text{core}} = t_i \sum_j \left(d_i^j (y_i^j)^2 + \frac{(d_i^j)^3 (\sin \alpha_i^j)^2}{12} \right) \quad (3-10)$$

The local moments of inertia of the megacolumns are much less than the core moment of inertia, and may be calculated from the megacolumn areas in Equation 3-11:

$$\begin{aligned}
 I_i^{\text{colj}} &= \text{local moment of inertia of megacolumn j in interval i} \\
 A_i^{\text{colj}} &= \text{cross-sectional area of megacolumn j in interval i} \\
 \eta &= 12 \text{ for solid square and } 4\pi \text{ for solid circle} \\
 I_i^{\text{colj}} &= \frac{(A_i^{\text{colj}})^2}{\eta} \tag{3-11}
 \end{aligned}$$

For the generic skyscraper, the contribution of the core and megacolumns to the first 12 rows and columns of the stiffness matrix is shown in Table 3-1 with Equations 3-12 to 3-20:

$$I_i = \frac{I_i^{\text{core}}}{4} + I_i^{\text{colA}} + I_i^{\text{colB}} + \frac{I_i^{\text{colC}}}{2} + I_i^{\text{colD}} + \frac{I_i^{\text{colE}}}{2} \tag{3-12}$$

$$k_i^{\text{cor1}} = \frac{12EI_i}{h_i^3} \quad k_i^{\text{cor2}} = \frac{6EI_i}{h_i^2} \quad k_i^{\text{cor3}} = \frac{4EI_i}{h_i} \quad k_i^{\text{cor4}} = \frac{2EI_i}{h_i} \tag{3-13, 3-14, 3-15, 3-16}$$

$$k_i^{\text{colA}} = \frac{EA_i^{\text{colA}}}{h_i} \quad k_i^{\text{colB}} = \frac{EA_i^{\text{colB}}}{h_i} \quad k_i^{\text{colC}} = \frac{EA_i^{\text{colC}}}{2h_i} \quad k_i^{\text{colD}} = \frac{EA_i^{\text{colD}}}{h_i} \tag{3-17, 3-18, 3-19, 3-20}$$

Table 3-1: Stiffness matrix - contribution of the core and megacolumns

	Δ_{100}	θ_{100}	A_{100}	B_{100}	C_{100}	D_{100}	Δ_{80}	θ_{80}	A_{80}	B_{80}	C_{80}	D_{80}
Δ_{100}	k_1^{cor1}	$-k_1^{\text{cor2}}$					$-k_1^{\text{cor1}}$	$-k_1^{\text{cor2}}$				
θ_{100}	$-k_1^{\text{cor2}}$	k_1^{cor3}					k_1^{cor2}	k_1^{cor4}				
A_{100}			k_1^{colA}						$-k_1^{\text{colA}}$			
B_{100}				k_1^{colB}						$-k_1^{\text{colB}}$		
C_{100}					k_1^{colC}						$-k_1^{\text{colC}}$	
D_{100}						k_1^{colD}						$-k_1^{\text{colD}}$
Δ_{80}	$-k_1^{\text{cor1}}$	k_1^{cor2}					k_1^{cor1} $+k_2^{\text{cor1}}$	k_1^{cor2} $-k_2^{\text{cor2}}$				
θ_{80}	$-k_1^{\text{cor2}}$	k_1^{cor4}					k_1^{cor2} $-k_2^{\text{cor2}}$	k_1^{cor3} $+k_2^{\text{cor3}}$				
A_{80}			$-k_1^{\text{colA}}$						k_1^{colA} $+k_2^{\text{colA}}$			
B_{80}				$-k_1^{\text{colB}}$						k_1^{colB} $+k_2^{\text{colB}}$		
C_{80}					$-k_1^{\text{colC}}$						k_1^{colC} $+k_2^{\text{colC}}$	
D_{80}						$-k_1^{\text{colD}}$						k_1^{colD} $+k_2^{\text{colD}}$

The shear stiffness of a typical outrigger truss as shown in Figure 3-2 is the reciprocal of the vertical tip displacement due to a unit load.

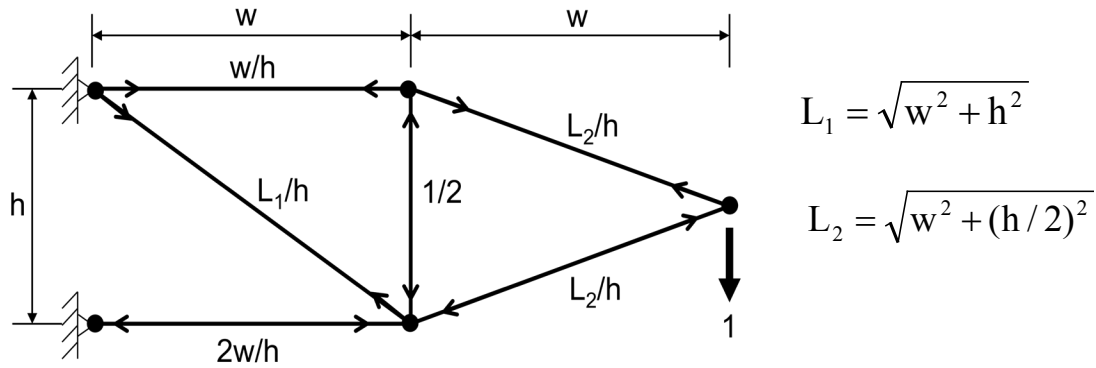


Figure 3-2: Typical outrigger truss subject to unit load

Assume that the cross-sectional area of each member of the outrigger truss is proportional to the magnitude of the axial force F indicated in the figure above as in Equation 3-21. Let C be the constant of proportionality:

$$A = C|F| \quad (3-21)$$

The total volume of N outrigger trusses at the top of an interval is calculated in Equation 3-22:

$$V = N \sum AL = NC \sum |F|L \quad (3-22)$$

The stiffness of any outrigger truss is the reciprocal of the tip displacement as determined by the principle of virtual forces in Equation 3-23:

$$k^{\text{out}} = \frac{1}{\sum \frac{F^2 L}{EA}} = \frac{CE}{\sum |F|L} = \frac{EV}{N(\sum |F|L)^2} \quad (3-23)$$

For the outrigger truss in Figure 3-2 its stiffness is calculated from Equations 3-24 and 3-25:

$$\sum |F|L = \frac{w^2}{h} + \frac{2w^2}{h} + \frac{L_1^2}{h} + \frac{2L_2^2}{h} + \frac{h}{2} = \frac{6w^2 + 2h^2}{h} \quad (3-24)$$

$$k^{\text{out}} = \frac{Eh^2V}{N(6w^2 + 2h^2)^2} \quad (3-25)$$

The shear stiffness of each of the 8 two-member outrigger trusses per interval in the generic skyscraper is shown in Figure 3-3 and calculated in Equation 3-26:

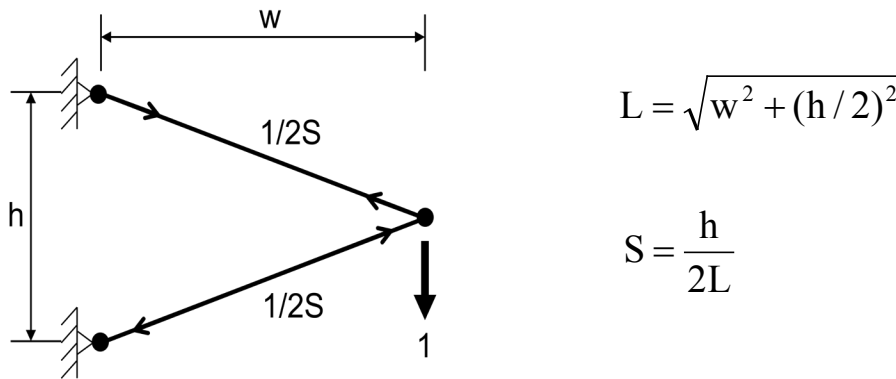


Figure 3-3: Two-member outrigger truss subject to unit load

k_i^{out} = shear stiffness of an outrigger truss at top of interval i

V_i^{out} = volume of all outrigger trusses at top of interval i

S_i^{out} = sine of angle from horizontal of members of outrigger truss at top of interval i

h_i^{out} = height of outrigger truss at top of interval i (16m for generic skyscraper)

E^s = steel modulus of elasticity

$$k_i^{\text{out}} = \frac{EV}{N(\sum |F|L)^2} = \frac{EV}{8\left(2\left(\frac{1}{2S}\right)\left(\frac{h}{2S}\right)\right)^2} = \frac{E^s (S_i^{\text{out}})^4 V_i^{\text{out}}}{2(h_i^{\text{out}})^2} \quad (3-26)$$

For the generic skyscraper, the contribution of the outriggers to the first 12 rows and columns of the stiffness matrix is shown in Table 3-2. Since there are no outriggers at story 100 in the generic skyscraper, $k_1^{\text{out}} = 0$, but it is retained in the table to illustrate the pattern.

Table 3-2: Stiffness matrix - contribution of outriggers

	Δ_{100}	θ_{100}	A_{100}	B_{100}	C_{100}	D_{100}	Δ_{80}	θ_{80}	A_{80}	B_{80}	C_{80}	D_{80}
Δ_{100}												
θ_{100}		$12.5^2 k_1^{out}$ $+25^2 k_1^{out}$		$-25 k_1^{out}$		$-12.5 k_1^{out}$						
A_{100}												
B_{100}		$-25 k_1^{out}$		k_1^{out}								
C_{100}												
D_{100}		$-12.5 k_1^{out}$				k_1^{out}						
Δ_{80}												
θ_{80}								$12.5^2 k_2^{out}$ $+25^2 k_2^{out}$		$-25 k_2^{out}$		$-12.5 k_2^{out}$
A_{80}												
B_{80}								$-25 k_2^{out}$		k_2^{out}		
C_{80}												
D_{80}								$-12.5 k_2^{out}$				k_2^{out}

Note that there is coupling between the vertical displacements of megacolumns B and D and the rotation of the core. To understand this coupling, Figure 3-4 shows the left half of the core in solid black and a two-member outrigger truss extending from the core to megacolumn B. The top part of the figure shows a unit upward vertical displacement at megacolumn B and the bottom part of the figure shows a unit clockwise core rotation.

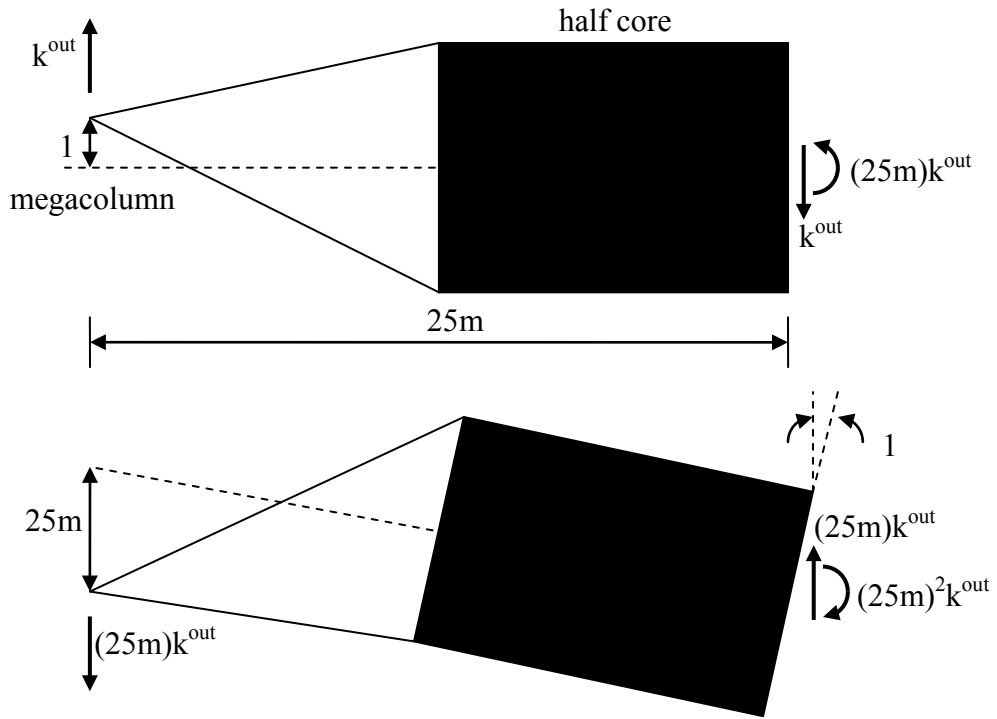


Figure 3-4: Unit upward vertical displacement (top) and unit clockwise core rotation (bottom)

The shear stiffness of each of the 16 eight-member belt trusses per interval in the generic skyscraper is shown in Figure 3-5 and calculated in Equation 3-27:

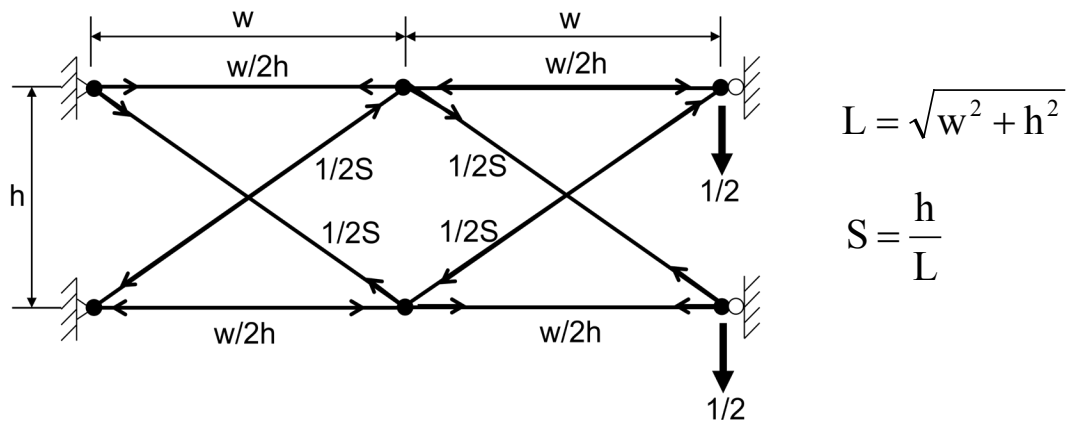


Figure 3-5: Eight-member belt truss subject to unit load

k_i^{belt} = shear stiffness of a belt truss at top of interval i
 V_i^{belt} = volume of all belt trusses at top of interval i
 S_i^{belt} = sine of angle from horizontal of members of belt truss at top of interval i
 h_i^{belt} = height of belt truss at top of interval i (8m for generic skyscraper)
 E^s = steel modulus of elasticity

$$k_i^{\text{belt}} = \frac{EV}{N(\sum |F|L)^2} = \frac{EV}{16\left(\frac{4w^2}{2h} + \frac{4L}{2S}\right)^2} = \frac{E^s (S_i^{\text{belt}})^4 V_i^{\text{belt}}}{64(h_i^{\text{belt}})^2 (2 - (S_i^{\text{belt}})^2)^2} \quad (3-27)$$

If it is assumed that the horizontal members of the belt truss consist of infinitely stiff floor diaphragms, then the shear stiffness of each of the belt trusses in the generic skyscraper is increased as shown in Figure 3-6 and calculated in Equation 3-28:

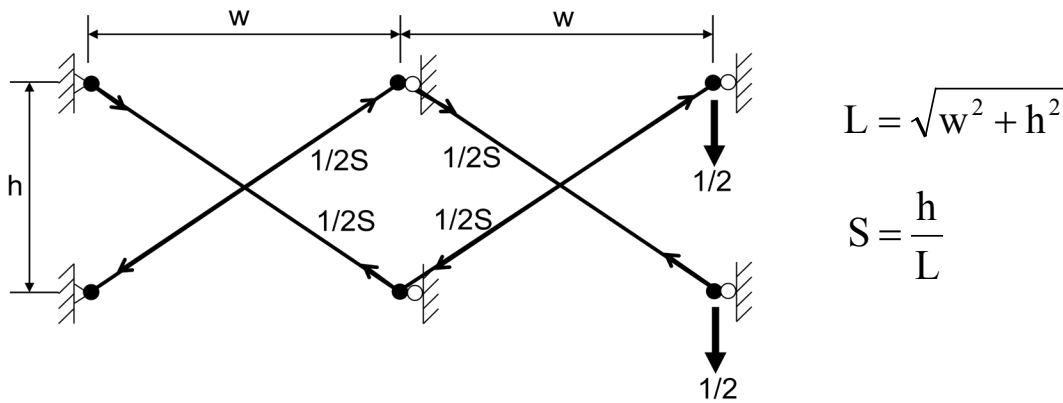


Figure 3-6: Belt truss in generic skyscraper subject to unit load

$$k_i^{\text{belt}} = \frac{EV}{N(\sum |F|L)^2} = \frac{EV}{16\left(4\left(\frac{1}{2S}\right)\left(\frac{h}{S}\right)\right)^2} = \frac{E^s (S_i^{\text{belt}})^4 V_i^{\text{belt}}}{64(h_i^{\text{belt}})^2} \quad (3-28)$$

For the generic skyscraper, the contribution of the belts to the first 12 rows and columns of the stiffness matrix is shown in Table 3-3. Since there are no belts at story 100 in the generic skyscraper, $k_1^{\text{belt}} = 0$, but it is retained in the table to illustrate the pattern.

Table 3-3: Stiffness matrix - contribution of the belt trusses

	Δ_{100}	θ_{100}	A_{100}	B_{100}	C_{100}	D_{100}	Δ_{80}	θ_{80}	A_{80}	B_{80}	C_{80}	D_{80}
Δ_{100}												
θ_{100}		$2(12.5^2)k_1^{belt}$	$-12.5k_1^{belt}$									
A_{100}		$-12.5k_1^{belt}$	$2k_1^{belt}$	$-k_1^{belt}$		$-k_1^{belt}$						
B_{100}			$-k_1^{belt}$	$2k_1^{belt}$	$-k_1^{belt}$							
C_{100}				$-k_1^{belt}$	k_1^{belt}							
D_{100}			$-k_1^{belt}$			$2k_1^{belt}$						
Δ_{80}												
θ_{80}								$2(12.5^2)k_2^{belt}$	$-12.5k_2^{belt}$			
A_{80}								$-12.5k_2^{belt}$	$2k_2^{belt}$	$-k_2^{belt}$		$-k_2^{belt}$
B_{80}									$-k_2^{belt}$	$2k_2^{belt}$	$-k_2^{belt}$	
C_{80}										$-k_2^{belt}$	k_2^{belt}	
D_{80}									$-k_2^{belt}$			$2k_2^{belt}$

Note that there is coupling between the vertical displacement of megacolumn A and the rotation of the core. To understand this coupling, Figure 3-7 shows belt trusses spanning between megacolumn A on the left, megacolumn D in the middle, and megacolumn E on the right. The top part of the figure shows a unit vertical displacement at megacolumn A, the middle part of the figure shows a unit vertical displacement at megacolumn D, and the bottom part of the figure shows a unit core rotation. It is assumed that the rotation of all megacolumns is the same as the rotation of the core because the core and megacolumns are connected with axially rigid floor diaphragms at every story.

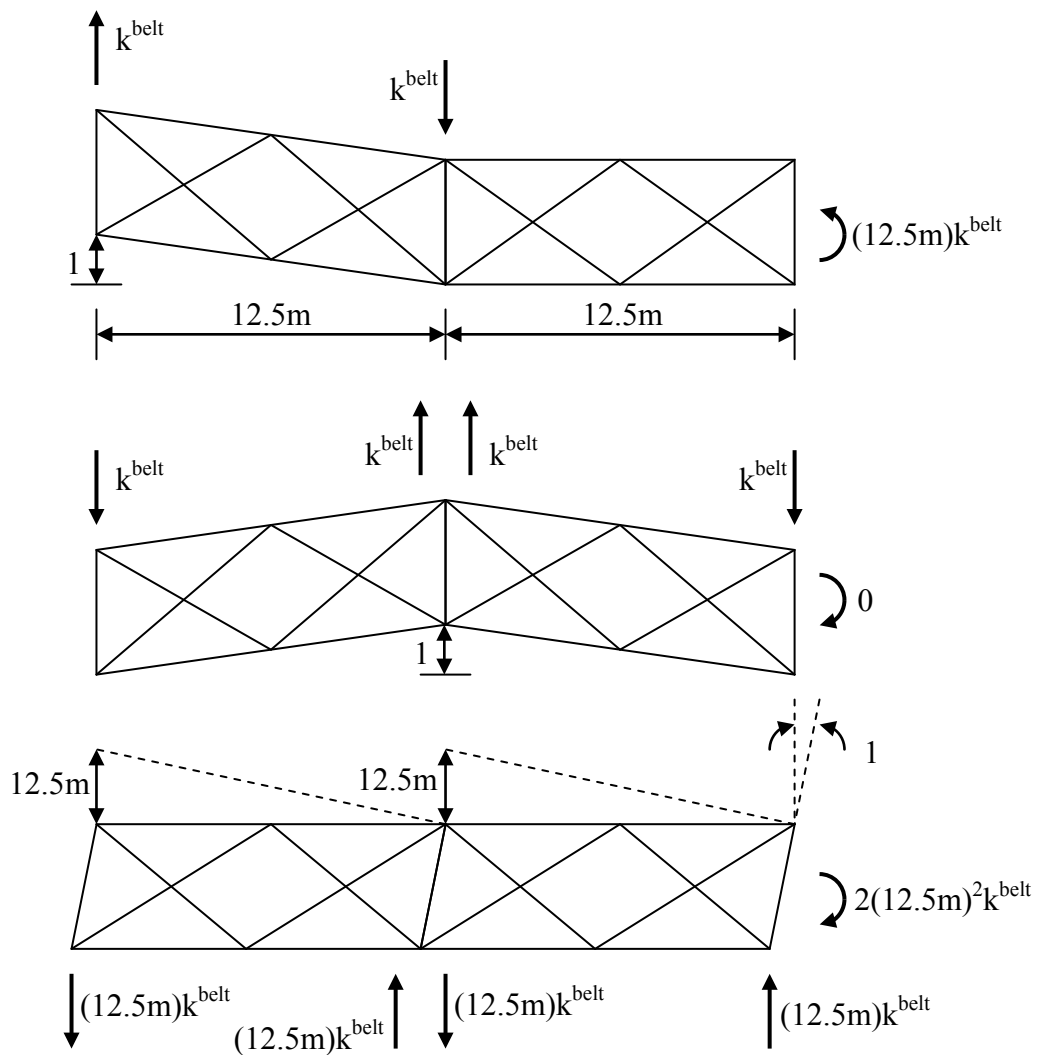
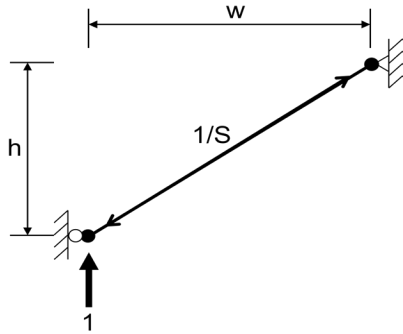


Figure 3-7: Unit displacement at megacolumns A (top) and D (middle), and a unit core rotation (bottom)

The vertical stiffness of each of the 32 diagonals per interval in the generic skyscraper is given in Figure 3-8 and calculated in Equation 3-29:



$$L = \sqrt{w^2 + h^2}$$

$$S = \frac{h}{L}$$

Figure 3-8: Diagonal in generic skyscraper subject to unit load

k_i^{diag} = vertical stiffness of a diagonal member in interval i

V_i^{diag} = volume of all diagonal members in interval i

S_i^{diag} = sine of angle from horizontal for diagonals in interval i

h_i^{diag} = height of diagonal between adjacent megacolumns (20m for generic skyscraper)

E^s = steel modulus of elasticity

$$k_i^{diag} = \frac{EV}{N(\sum |F|L)^2} = \frac{EV}{32\left(\left(\frac{1}{S}\right)\left(\frac{h}{S}\right)\right)^2} = \frac{E^s(S_i^{diag})^4 V_i^{diag}}{32(h_i^{diag})^2} \quad (3-29)$$

For the generic skyscraper, the contribution of the diagonals to the first 12 rows and columns of the stiffness matrix is shown in Table 3-4.

Table 3-4: Stiffness matrix - contribution of diagonals

	Δ_{100}	θ_{100}	A_{100}	B_{100}	C_{100}	D_{100}	Δ_{80}	θ_{80}	A_{80}	B_{80}	C_{80}	D_{80}
Δ_{100}	$4k_1^{diag}/6.4^2$		$-k_1^{diag}/6.4$				$-4k_1^{diag}/6.4^2$		$-k_1^{diag}/6.4$			
θ_{100}												
A_{100}	$-k_1^{diag}/6.4$		$2k_1^{diag}$	$-k_1^{diag}$		$-k_1^{diag}$	$k_1^{diag}/6.4$					
B_{100}			$-k_1^{diag}$	$2k_1^{diag}$	$-k_1^{diag}$							
C_{100}				$-k_1^{diag}$	k_1^{diag}							
D_{100}			$-k_1^{diag}$			$2k_1^{diag}$						
Δ_{80}	$-4k_1^{diag}/6.4^2$		$k_1^{diag}/6.4$				$4k_1^{diag}/6.4^2$ $+4k_2^{diag}/6.4^2$		$k_1^{diag}/6.4$ $-k_2^{diag}/6.4$			
θ_{80}												
A_{80}	$-k_1^{diag}/6.4$						$k_1^{diag}/6.4$ $-k_2^{diag}/6.4$		$2k_1^{diag}$ $+2k_2^{diag}$	$-k_1^{diag}$ $-k_2^{diag}$		$-k_1^{diag}$ $-k_2^{diag}$
B_{80}									$-k_1^{diag}$ $-k_2^{diag}$	$2k_1^{diag}$ $+2k_2^{diag}$	$-k_1^{diag}$ $-k_2^{diag}$	
C_{80}										$-k_1^{diag}$ $-k_2^{diag}$	k_1^{diag} $+k_2^{diag}$	
D_{80}									$-k_1^{diag}$ $-k_2^{diag}$			$2k_1^{diag}$ $+2k_2^{diag}$

Note that there is coupling between the vertical displacement of megacolumn A and the horizontal displacement of the core. To understand this coupling, Figure 3-9 shows diagonals and megacolumns A, D, and E in the top two intervals. The left part of the figure shows a unit vertical displacement at megacolumn A at the top of interval 2 (bottom of interval 1), the middle part of the figure shows a unit vertical displacement at megacolumn D at the top of interval 2, and the right part of the figure shows a unit horizontal displacement at the top of interval 2. It is assumed that the horizontal displacement of all megacolumns is the same as the horizontal displacement of the core because the core and megacolumns are connected with axially rigid floor diaphragms at every story.

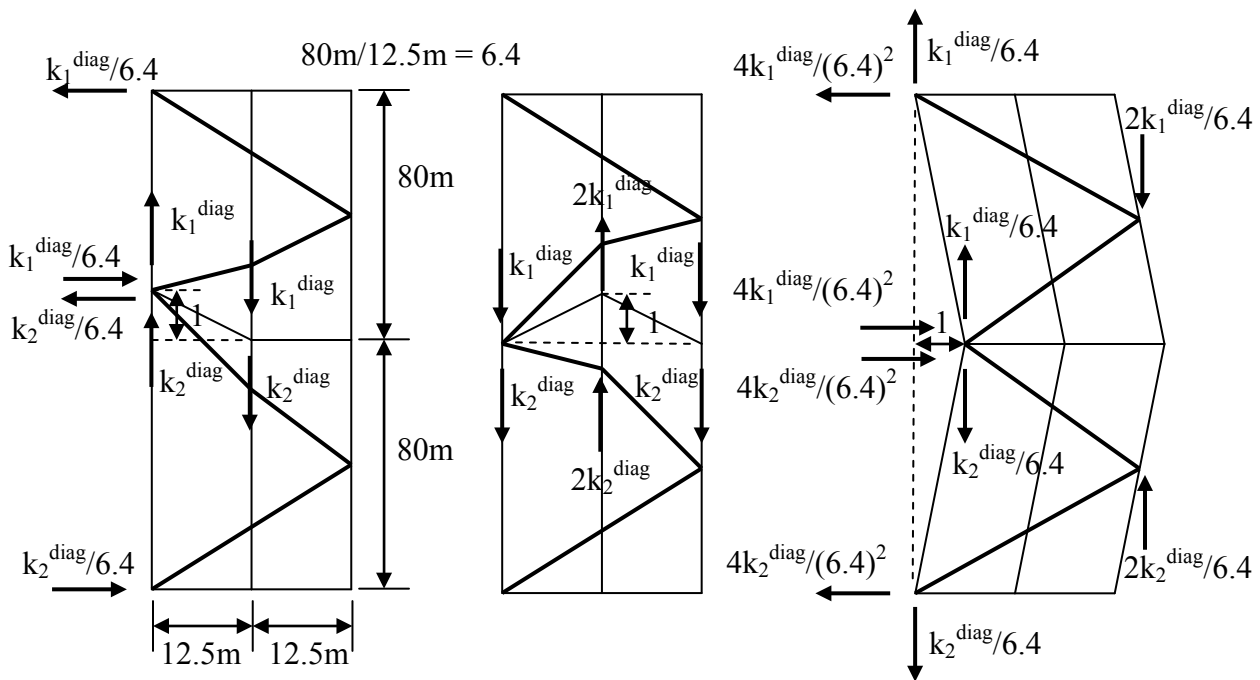


Figure 3-9: Unit vertical displacements at megacolumns A (left), D (middle), and E (right)

3.3 Calculation of Lateral Forces/Displacements

The lateral force vectors have zero values for the DOF's corresponding to vertical displacements in the megacolumns at the top of each interval. To get the values for the DOF's corresponding to the horizontal displacements and rotations in the core at the top of each interval, the lateral forces for wind and seismic loading are determined at every story and then aggregated over the intervals. The spreadsheet includes a sheet with a row for each story in the building starting at the bottom and increasing upward (100 stories for the generic skyscraper).

For the lateral wind pressure, a formula such as Equation (3-30 taken from ASCE 7-05 could be used:

P_k^{wind} = wind pressure at story k in psf
 v = design wind speed in miles per hour (123mph for the generic skyscraper)
 H_k = height of story k above the ground
 H_g = reference height parameter reflecting exposure (274m for the generic skyscraper)
 α = another parameter reflecting the exposure (9.5 for the generic skyscraper)

$$P_k^{wind} = 0.00256 \left(2.01 \left(\frac{H_k}{H_g} \right)^{2/\alpha} \right) v^2 \quad (3-30)$$

After getting the wind pressure at each story and converting it to the appropriate units, the wind force at each story is obtained from Equation 3-31:

F_k^{wind} = lateral wind force at story k
 s_k = story height for story k (4m for the generic skyscraper)
 w_k = building width at story k (50m for the generic skyscraper)

$$F_k^{wind} = P_k^{wind} s_k w_k \quad (3-31)$$

For lateral seismic forces, the dead weight of each story must be obtained from Equation 3-32:

W_k = weight of story k (excluding live load)
 A_k = floor area of story k
 P_k = building perimeter at story k
 s_k = story height for story k (4m for the generic skyscraper)
 L^{dead} = floor dead load per area
 L^{clad} = cladding load per area
 γ = concrete unit weight
 $A_k^{\text{core-col}}$ = cross-sectional area of core and all megacolumns at story k
 γ^s = steel unit weight
 $V_k^{\text{out-belt-diag}}$ = volume of all outriggers, belts, and diagonals at story k

$$W_k = A_k L^{\text{dead}} + s_k P_k L^{\text{clad}} + \gamma s_k A_k^{\text{core-col}} + \gamma^s V_k^{\text{out-belt-diag}} \quad (3-32)$$

The seismic force at each story is obtained with a formula such as Equation 3-33 taken from ASCE 7-05:

F_k^{seismic} = lateral seismic force at story k
 H_k = height of story k above the ground
 S_a = spectral acceleration in g (0.2 for generic skyscraper)
 R = ductility factor (3 for generic skyscraper)
 β = seismic exponent (2 for generic skyscraper)

$$F_k^{\text{seismic}} = \frac{W_k (H_k)^\beta}{\sum_k (W_k (H_k)^\beta)} \frac{S_a}{R} \sum_k W_k \quad (3-33)$$

The wind and seismic forces at each story must be aggregated over intervals to get the forces and moments at the DOF's corresponding to the horizontal displacements and rotations in the core at the top of each interval. Figure 3-10 shows a particular interval of height h_i and a wind or seismic lateral force F_k at a particular story k. In the generic skyscraper there are 20 stories in each interval. Formulas for the fixed end force and moment support reactions at the top and bottom of the interval are given in the figure. In the spreadsheet, these formulas are evaluated for every lateral force in every interval. The negative of these support reactions are the

equivalent forces and moments applied at the DOF's. The rightward force at a particular DOF corresponding to a core horizontal displacement is equal to the sum of F_k^{bot} for all lateral forces in the interval above the DOF plus the sum of F_k^{top} for all lateral forces in the interval below the DOF. The clockwise moment at a particular DOF corresponding to a core rotation is equal to the sum of M_k^{bot} for all lateral forces in the interval above the DOF minus the sum of M_k^{top} for all lateral forces in the interval below the DOF.

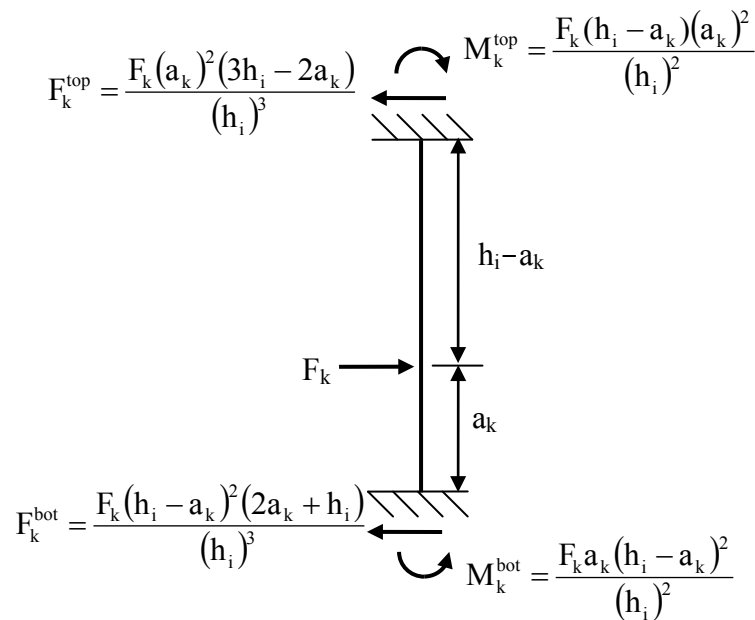


Figure 3-10: Interval with a wind/seismic force at a particular story k

The stiffness matrix is inverted and multiplied by the lateral force vector for wind loading to get the core horizontal displacements, the core rotations, and the megacolumn vertical displacements at the top of each interval. The inverted stiffness matrix is multiplied by the lateral force vector for seismic loading to get these same displacements for seismic loading. The principle of superposition is used to get the lateral displacement at a particular story within an interval. Superposition begins with a cubic polynomial for the displacement due to displacements and rotations at the top and bottom of the interval, and then adds the

displacements of the fixed-fixed beam in Figure 3-11 due to all of the point loads F_k in the interval and calculated in Equation 3-34:

- Δ_k = lateral displacement at story k
- h_i = height of interval i
- a_k = height from bottom of interval i to story k
- Δ_i = core lateral displacement at top of interval i
- Δ_{i+1} = core lateral displacement at bottom of interval i
- θ_i = core rotation at top of interval i
- θ_{i+1} = core rotation at bottom of interval i
- F_m^{bot} = fixed end force at bottom of interval due to point force m
- F_m^{top} = fixed end force at top of interval due to point force m
- M_m^{bot} = fixed end moment at bottom of interval due to point force m
- M_m^{top} = fixed end moment at top of interval due to point force m
- E = concrete modulus of elasticity (core and megacolumns)
- I_i = moment of inertia of core and local moment of inertia of megacolumns

$$\Delta_k = \left(\frac{2(\Delta_{i+1} - \Delta_i)}{h_i^3} + \frac{\theta_i + \theta_{i+1}}{h_i^2} \right) a_k^3 + \left(\frac{3(\Delta_i - \Delta_{i+1})}{h_i^2} - \frac{\theta_i + 2\theta_{i+1}}{h_i} \right) a_k^2 + \theta_{i+1} a_k + \Delta_{i+1} \quad (3-34)$$

$$- \left(\frac{a_k^3 \sum_{m>k} F_m^{bot}}{6} - \frac{a_k^2 \sum_{m>k} M_m^{bot}}{2} + \frac{(h_i - a_k)^3 \sum_{m \leq k} F_m^{top}}{6} - \frac{(h_i - a_k)^2 \sum_{m \leq k} M_m^{top}}{2} \right) \left(\frac{1}{EI_i} \right)$$

Interstory drifts can be calculated and compared to allowable values (e.g. 1/360 for wind and 1/50 for seismic) in Equation 3-35:

- D_k = interstory drift at story k
- Δ_k = lateral displacement at story k
- s_k = story height for story k (4m for the generic skyscraper)

$$D_k = \frac{|\Delta_k - \Delta_{k-1}|}{s_k} \quad (3-35)$$

As the skyscraper displaces laterally under wind and seismic loads, the weight of the structure creates an additional overturning moment equal to the weight times the lateral

displacement. This moment, called the $P\Delta$ effect, increases the lateral displacement, and thus, nonlinear iteration is necessary to converge to the final equilibrium position when the $P\Delta$ moments no longer change:

$$\begin{aligned}
 W_k &= \text{weight of story } k \text{ (including live load)} \\
 F_k &= F_{k+1} + W_k = \text{total axial force at story } k \\
 \Delta_k &= \text{lateral displacement at story } k \\
 M_k &= F_k(\Delta_k - \Delta_{k-1}) \text{ moment at story } k \text{ due to } P\Delta \text{ effect}
 \end{aligned}$$

The moments at each story must be aggregated over intervals to get the forces and moments at the DOF's corresponding to the horizontal displacements and rotations in the core at the top of each interval. Figure 3-11 shows a particular interval of height h_i and a $P\Delta$ moment M_k at a particular story k . Formulas for the fixed end force and moment support reactions at the top and bottom of the interval are given in the figure. In the spreadsheet, these formulas are evaluated for every $P\Delta$ moment in every interval. The negative of these support reactions are the equivalent forces and moments applied at the DOF's. The rightward force at a particular DOF corresponding to a core horizontal displacement is equal to the sum of F_k^{bot} for all lateral forces in the interval above the DOF plus the sum of F_k^{top} for all lateral forces in the interval below the DOF. The clockwise moment at a particular DOF corresponding to a core rotation is equal to the sum of M_k^{bot} for all lateral forces in the interval above the DOF minus the sum of M_k^{top} for all lateral forces in the interval below the DOF.

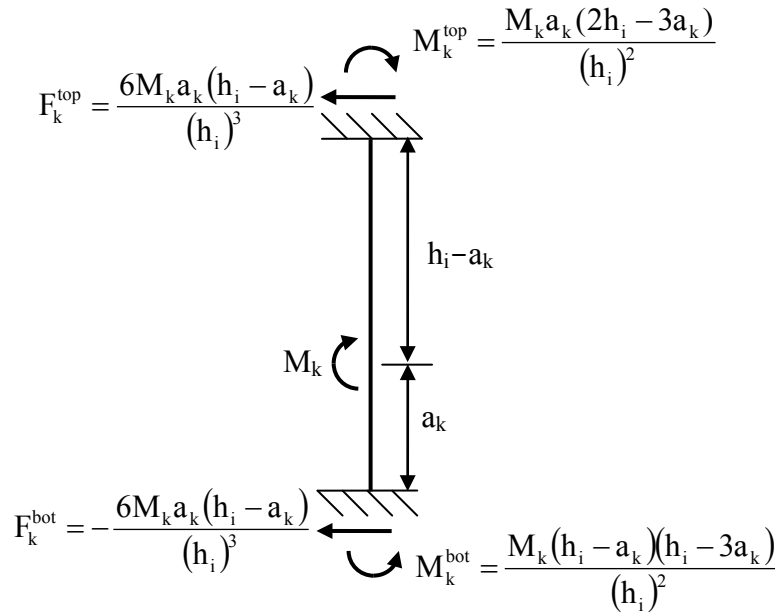


Figure 3-11: Interval and a P-delta moment at a particular story k

Nonlinear iteration is accomplished in the spreadsheet by creating two columns for the $P\Delta$ lateral force vector -- a starting column and an ending column. The starting column is initialized to zero and is added to the wind lateral force vector. The ending column calculates the new $P\Delta$ lateral force vector by the procedure described above. The values from the ending column are repeatedly pasted into the starting column until the two columns are the same. Starting and ending columns for the $P\Delta$ lateral force vector are likewise created for seismic loading.

3.4 Calculation of Stresses

Gravity load stresses are greatest at the bottom of each interval for the core, megacolumns, and diagonals. The gravity load stress is the same for the core and the megacolumns since megacolumn areas were determined earlier by equating their gravity load

strains to that of the core (see Equations 3-36 and 3-37). The gravity load stress in diagonals is also determined by equating the respective gravity load strain to that of the core in Equation 3-38. The gravity load stress in interior diagonal members is decreased by a fraction of the relative increment in axial force for the interval in Equation 3-39:

- $\sigma_i^{\text{core_grav}}$ = gravity load stress in core at bottom of interval i
- $\sigma_i^{\text{colj_grav}}$ = gravity load stress in megacolumn j at bottom of interval i
- $\sigma_i^{\text{outB_grav}}$ = gravity load stress in outrigger B at top of interval i
- $\sigma_i^{\text{outD_grav}}$ = gravity load stress in outrigger D at top of interval i
- $\sigma_i^{\text{diagAB_grav}}$ = gravity load stress in bottom diagonal AB in interval i
- $\sigma_i^{\text{diagAD_grav}}$ = gravity load stress in bottom diagonal AD in interval i
- $\sigma_i^{\text{diagBC_grav}}$ = gravity load stress in bottom diagonal BC in interval i
- $\sigma_i^{\text{diagDE_grav}}$ = gravity load stress in bottom diagonal DE in interval i
- h_i = vertical height of interval i (80m for generic skyscraper)
- A_i^{core} = cross-sectional area of the core in interval i
- F_i^{core} = axial force in core at base of interval i excluding interval i self weight
- γ = concrete unit weight (core and megacolumns)
- E = concrete modulus of elasticity
- E^s = steel modulus of elasticity
- S_i^{out} = sine of angle from horizontal of members of outrigger truss at top of interval i
- S_i^{diag} = sine of angle from horizontal for diagonals in interval i

$$\sigma_i^{\text{core_grav}} = \frac{F_i^{\text{core}}}{A_i^{\text{core}}} + \gamma h_i \quad (3-36)$$

$$\sigma_i^{\text{colj_grav}} = \sigma_i^{\text{core_grav}} \quad (3-37)$$

$$\sigma_i^{\text{diagAB_grav}} = \sigma_i^{\text{diagAD_grav}} = \frac{E^s (S_i^{\text{diag}})^2 \sigma_i^{\text{core_grav}}}{E} \quad (3-38)$$

$$\sigma_i^{\text{diagBC_grav}} = \sigma_i^{\text{diagDE_grav}} = \frac{E^s (S_i^{\text{diag}})^2 \sigma_i^{\text{core_grav}}}{E} \left(1 - .25 \frac{F_i^{\text{core}} - F_{i-1}^{\text{core}}}{F_i^{\text{core}}} \right) \quad (3-39)$$

The lateral load stress in the core and megacolumns at the bottom of each interval is equal to the modulus of elasticity times axial strain plus the modulus of elasticity times flexural curvature times distance from local neutral axis to outermost fiber in Equations 3-40 and 3-41.

The flexural curvature is the same for core and megacolumns and is obtained by differentiating

the lateral displacement formulas twice and evaluating at $a_k = 0$ (bottom of the interval). Under lateral loading, the axial strain is zero in the core. The megacolumn axial strain is equal to the difference between vertical displacements in the megacolumn at the top and bottom of the interval divided by the interval height:

- $\sigma_i^{\text{core_lat}}$ = lateral load stress in core at bottom of interval i
- $\sigma_i^{\text{colj_lat}}$ = lateral load stress in megacolumn j at bottom of interval i
- h_i = height of interval i
- E = concrete modulus of elasticity (core and megacolumns)
- I_i = moment of inertia of core and local moment of inertia of megacolumns
- c_i^{core} = distance to outermost fiber in core in interval i (12.5m for generic skyscraper)
- c_i^{colj} = distance to outermost fiber in megacolumn j in interval i
- A_i^{colj} = cross-sectional area of megacolumn j in interval i
- $\mu = 4$ for solid square and π for solid circle
- Δ_i = core lateral displacement at top of interval i
- Δ_{i+1} = core lateral displacement at bottom of interval i
- θ_i = core rotation at top of interval i
- θ_{i+1} = core rotation at bottom of interval i
- Δ_i^{colj} = vertical displacement in megacolumn j at top of interval i
- $\Delta_{i+1}^{\text{colj}}$ = vertical displacement in megacolumn j at bottom of interval i
- M_m^{bot} = moment at bottom of interval due to lateral force at story m within interval i

$$\sigma_i^{\text{core_lat}} = E c_i^{\text{core}} \left(\frac{6(\Delta_i - \Delta_{i+1})}{h_i^2} - \frac{2\theta_i + 4\theta_{i+1}}{h_i} \right) + \frac{c_i^{\text{core}} \sum_m M_m^{\text{bot}}}{I_i} \quad (3-40)$$

$$\sigma_i^{\text{colj_lat}} = \frac{E(\Delta_i^{\text{colj}} - \Delta_{i+1}^{\text{colj}})}{h_i} + \sigma_i^{\text{core_lat}} \frac{c_i^{\text{colj}}}{c_i^{\text{core}}} \quad c_i^{\text{colj}} = \sqrt{\frac{A_i^{\text{colj}}}{\mu}} \quad (3-41)$$

For the typical outrigger truss in Figure 3-12, recall the formulas developed earlier when the stiffness of this truss was considered:

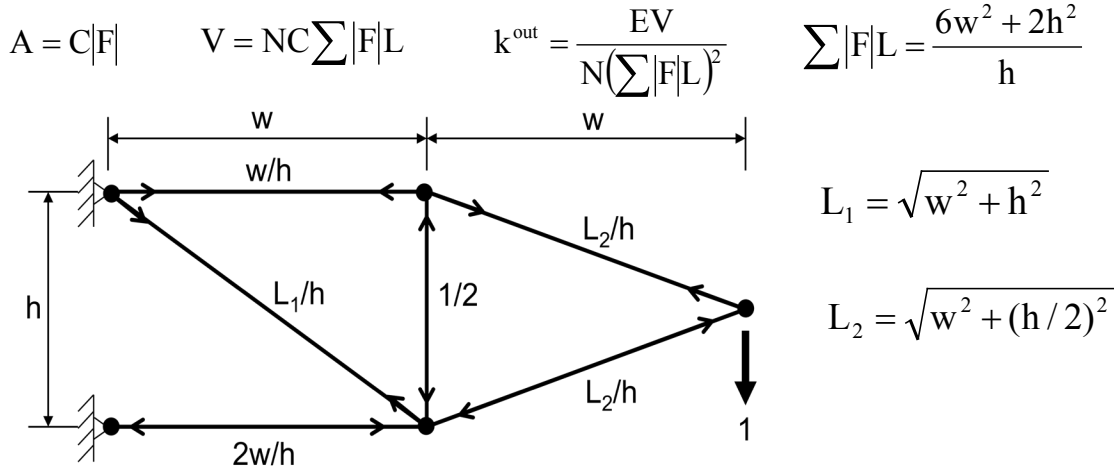


Figure 3-12: Typical outrigger member subject to unit load

To get the lateral load stress for the members of this outrigger truss, the axial forces due to a unit load must be multiplied by the stiffness k^{out} times the shear displacement Δ^{out} . These axial forces must then be divided by the cross-sectional area to get stress as in Equation 3-42:

$$\sigma^{out_lat} = \frac{|F|}{A} k^{out} \Delta^{out} = \frac{E}{\sum |F|L} \Delta^{out} = \frac{Eh}{6w^2 + 2h^2} \Delta^{out} \quad (3-42)$$

The lateral load stress in the members of each of the 8 two-member outrigger trusses per interval in the generic skyscraper is shown in Figure 3-13 and calculated in Equation 3-43:

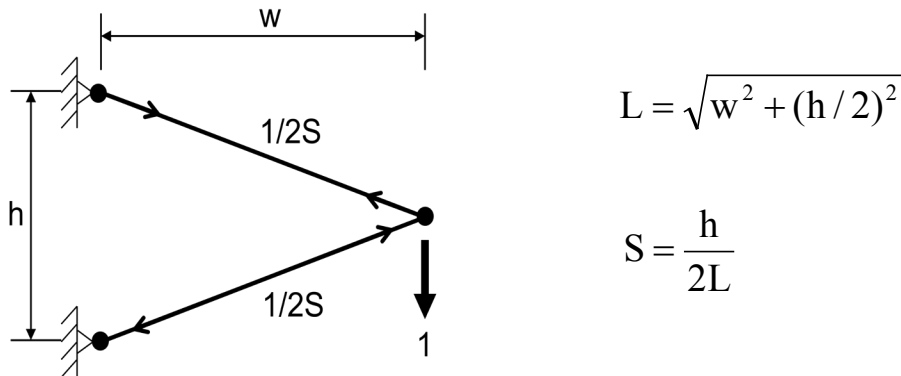


Figure 3-13: Two-member outrigger truss subject to unit load

$\sigma_i^{\text{out_lat}}$ = lateral load stress in outrigger at top of interval i
 Δ_i^{out} = shear displacement in outrigger at top of interval i
 S_i^{out} = sine of angle from horizontal of members of outrigger truss at top of interval i
 h_i^{out} = height of outrigger truss at top of interval i (16m for generic skyscraper)
 E^s = steel modulus of elasticity

$$\sigma_i^{\text{out_lat}} = \frac{E}{\sum |F|L} \Delta_i^{\text{out}} = \frac{E}{2 \left(\frac{1}{2S} \right) \left(\frac{h}{2S} \right)} \Delta_i^{\text{out}} = \frac{2E^s (S_i^{\text{out}})^2}{h_i^{\text{out}}} \Delta_i^{\text{out}} \quad (3-43)$$

The shear displacement in each outrigger is the difference between megacolumn vertical displacement and the product of core rotation and distance from core centerline to megacolumn as calculated in Equations 3-44 and 3-45. The shear displacement is greater for the upper member of the outrigger than for the lower member. The core rotation at the top of the upper member must be appropriately interpolated from the core rotation at the top of the interval and the core rotation at the top interval above:

Δ_i^{outB} = shear displacement in outrigger B at top of interval i
 Δ_i^{outD} = shear displacement in outrigger D at top of interval i
 θ_i = core rotation at top of interval i
 θ_{i-1} = core rotation at top of interval i-1
 Δ_i^{colB} = vertical displacement in megacolumn B at top of interval i
 Δ_i^{colD} = vertical displacement in megacolumn D at top of interval i

$$\Delta_i^{\text{outB}} = \left| 25m(\theta_i) - \Delta_i^{\text{colB}} \right| \quad (3-44)$$

$$\Delta_i^{\text{outD}} = \left| 12.5m(\theta_i) - \Delta_i^{\text{colD}} \right| \quad (3-45)$$

The lateral load stress in the members of each of the 16 eight-member belt trusses per interval in the generic skyscraper is shown in Figure 3-14 and calculated in Equation 3-46:

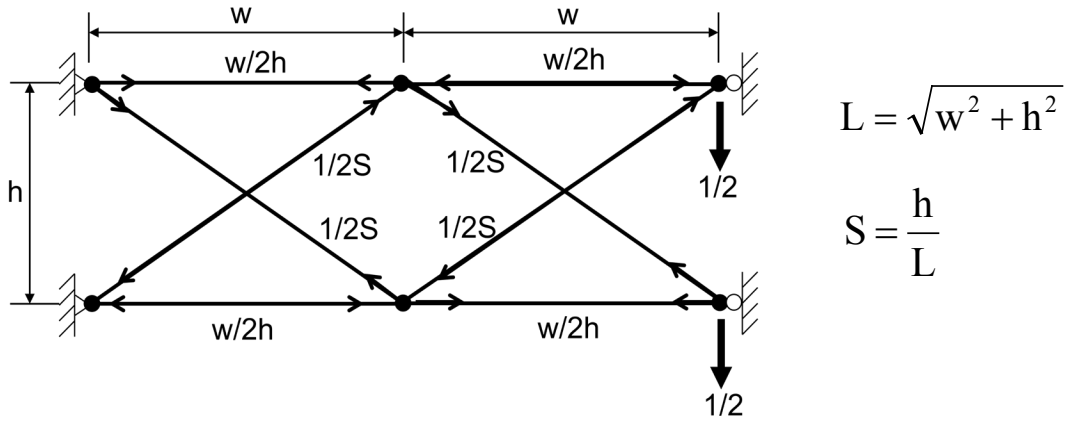


Figure 3-14: Eight-member belt truss subject to unit load

- σ_i^{belt} = lateral load stress in belt truss at top of interval i
- Δ_i^{belt} = shear displacement in belt truss at top of interval i
- S_i^{belt} = sine of angle from horizontal of members of belt truss at top of interval i
- h_i^{belt} = height of belt truss at top of interval i (8m for generic skyscraper)
- E^s = steel modulus of elasticity

$$\sigma_i^{\text{belt_lat}} = \frac{E}{\sum |F|L} \Delta_i^{\text{belt}} = \frac{E}{\frac{4w^2}{2h} + \frac{4L}{2S}} \Delta_i^{\text{belt}} = \frac{E^s (S_i^{\text{belt}})^2}{2h_i^{\text{belt}} (2 - (S_i^{\text{belt}})^2)} \Delta_i^{\text{belt}} \quad (3-46)$$

If it is assumed that the horizontal members of the belt truss consist of infinitely stiff floor diaphragms, then the lateral load stress in the members of each of the belt trusses in the generic skyscraper is increased in Figure 3-15 and calculated in Equation 3-47:

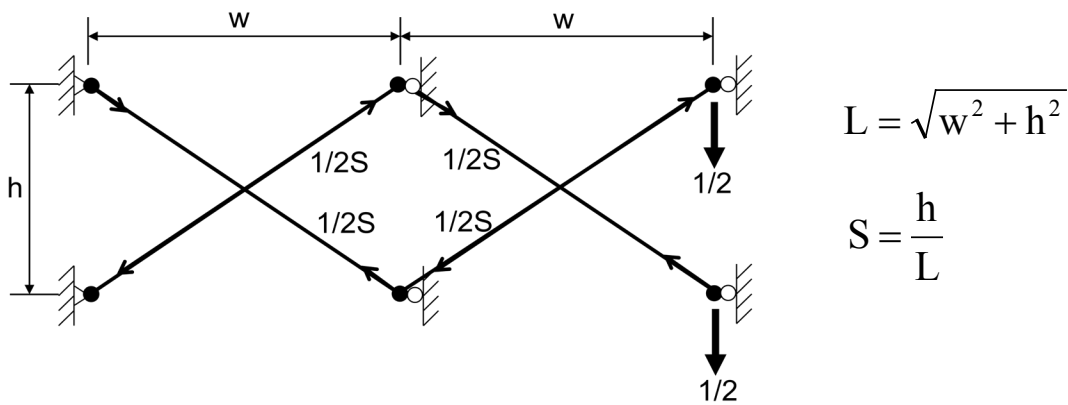


Figure 3-15: Belt truss in generic skyscraper subject to unit load

$$\sigma_i^{\text{belt_lat}} = \frac{E}{\sum |F|L} \Delta^{\text{belt}} = \frac{E}{4 \left(\frac{1}{2S} \right) \left(\frac{h}{S} \right)} \Delta^{\text{belt}} = \frac{E^s (S_i^{\text{belt}})^2}{2h_i^{\text{belt}}} \Delta_i^{\text{belt}} \quad (3-47)$$

The shear displacement in belts AB and BC is the difference between the two ends of the belt of the megacolumn vertical displacements as calculated in Equations 3-48 and 3-49. The shear displacement in belt DE is the difference between megacolumn D vertical displacement and the product of core rotation and distance from core centerline to megacolumn D as calculated in Equation 3-50. The shear displacement in belt AD is the difference between the two ends of the belt of the difference between megacolumn vertical displacement and the product of core rotation and distance from core centerline to megacolumn as calculated in Equation 3-51:

- Δ_i^{beltAB} = shear displacement in belt AB at top of interval i
- Δ_i^{beltBC} = shear displacement in belt BC at top of interval i
- Δ_i^{beltAD} = shear displacement in belt AD at top of interval i
- Δ_i^{beltDE} = shear displacement in belt DE at top of interval i
- Δ_i^{colA} = vertical displacement in megacolumn A at top of interval i
- Δ_i^{colB} = vertical displacement in megacolumn B at top of interval i
- Δ_i^{colC} = vertical displacement in megacolumn C at top of interval i
- Δ_i^{colD} = vertical displacement in megacolumn D at top of interval i
- θ_i = core rotation at top of interval i

$$\Delta_i^{\text{beltAB}} = \left| \Delta_i^{\text{colA}} - \Delta_i^{\text{colB}} \right| \quad \Delta_i^{\text{beltBC}} = \left| \Delta_i^{\text{colB}} - \Delta_i^{\text{colC}} \right| \quad (3-48, 3-49)$$

$$\Delta_i^{\text{beltAD}} = \left| 25m(\theta_i) - \Delta_i^{\text{colA}} - 12.5m(\theta_i) + \Delta_i^{\text{colD}} \right| \quad \Delta_i^{\text{beltDE}} = \left| 12.5m(\theta_i) - \Delta_i^{\text{colD}} \right| \quad (3-50, 3-51)$$

The lateral load stress in each of the 32 diagonals per interval in the generic skyscraper is shown in Figure 3-16 and calculated in Equation 3-52:

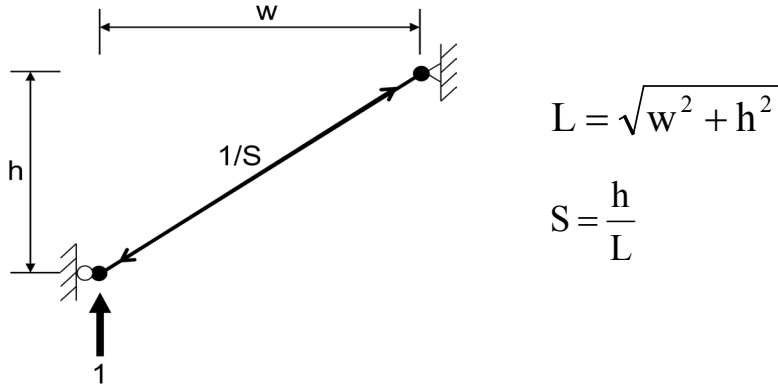


Figure 3-16: Diagonal in generic skyscraper subject to unit load

$\sigma_i^{\text{diag_lat}}$ = lateral load stress in a diagonal member in interval i
 Δ_i^{diag} = vertical displacement in diagonal members in interval i
 S_i^{diag} = sine of angle from horizontal for diagonals in interval i
 h_i^{diag} = height of diagonal between adjacent megacolumns (20m for generic skyscraper)
 E^s = steel modulus of elasticity

$$\sigma_i^{\text{diag_lat}} = \frac{E}{\sum |F|L} \Delta^{\text{diag}} = \frac{E}{\left(\frac{1}{S}\right)\left(\frac{h}{S}\right)} \Delta^{\text{diag}} = \frac{E^s (S_i^{\text{diag}})^2}{h_i^{\text{diag}}} \Delta^{\text{diag}} \quad (3-52)$$

The vertical displacement in diagonals AB and BC is the difference between the two ends of the diagonal of the megacolumn vertical displacements as calculated in Equations 3-53 and 3-54. The vertical displacement in diagonal DE is the difference between megacolumn D vertical displacement and the product of lateral drift and distance from core centerline to megacolumn D as calculated in Equation 3-56. The vertical displacement in diagonal AD is the difference between the two ends of the diagonal of the difference between megacolumn vertical displacement and the product of lateral drift and distance from core centerline to megacolumn as calculated in Equation 3-55. In these formulas, megacolumn vertical displacements must be appropriately interpolated between the top and bottom of the interval to get values at the ends of the diagonal:

Δ_i^{diagAB} = stress in bottom diagonal AB in interval i
 Δ_i^{diagAD} = stress in bottom diagonal AD in interval i
 Δ_i^{diagBC} = stress in bottom diagonal BC in interval i
 Δ_i^{diagDE} = stress in bottom diagonal DE in interval i
 Δ_i^{colA} = vertical displacement in megacolumn A at top of interval i
 Δ_i^{colB} = vertical displacement in megacolumn B at top of interval i
 Δ_i^{colC} = vertical displacement in megacolumn C at top of interval i
 Δ_i^{colD} = vertical displacement in megacolumn D at top of interval i
 $\Delta_{i+1}^{\text{colA}}$ = vertical displacement in megacolumn A at bottom of interval i
 $\Delta_{i+1}^{\text{colB}}$ = vertical displacement in megacolumn B at bottom of interval i
 $\Delta_{i+1}^{\text{colC}}$ = vertical displacement in megacolumn C at bottom of interval i
 $\Delta_{i+1}^{\text{colD}}$ = vertical displacement in megacolumn D at bottom of interval i
 D_i^{diagAD} = lateral drift at the center of diagonal AD in interval i
 D_i^{diagDE} = lateral drift at the center of diagonal DE in interval i

$$\Delta_i^{\text{diagAB}} = \left| \Delta_{i+1}^{\text{colA}} - .75\Delta_{i+1}^{\text{colB}} - .25\Delta_i^{\text{colB}} \right| \quad (3-53)$$

$$\Delta_i^{\text{diagBC}} = \left| .75\Delta_{i+1}^{\text{colB}} + .25\Delta_i^{\text{colB}} - .5\Delta_{i+1}^{\text{colC}} - .5\Delta_i^{\text{colC}} \right| \quad (3-54)$$

$$\Delta_i^{\text{diagAD}} = \left| D_i^{\text{diagAD}} (25\text{m} - 12.5\text{m}) - \Delta_{i+1}^{\text{colA}} + .75\Delta_{i+1}^{\text{colD}} + .25\Delta_i^{\text{colD}} \right| \quad (3-55)$$

$$\Delta_i^{\text{diagDE}} = \left| D_i^{\text{diagDE}} (12.5\text{m}) - .75\Delta_{i+1}^{\text{colD}} - .25\Delta_i^{\text{colD}} \right| \quad (3-56)$$

3.5 Rapid Trial-and-Error Optimization

Now that the description of the SSAM is complete, the spreadsheet can be used to optimize the skyscraper design. The design variables are the core thickness at each interval, the outrigger truss volume at each interval, the belt truss volume at each interval, and the diagonal volume at each interval. The objective is the minimization of structural cost which is the total volume of concrete in the core and megacolumns multiplied by the specified concrete cost per unit volume plus the total volume of steel in the outrigger trusses, belt trusses, and diagonals

multiplied by the specified steel cost per unit volume. The constraints to be satisfied include lateral drift in every story under wind loading, lateral drift in every story under seismic loading, stress in every member under combined gravity and wind loading, and stress in every member under combined gravity and seismic loading. For each of these types of constraints, the spreadsheet calculates a constraint ratio of actual value to allowable value. For example, the constraint ratio for wind lateral drift is equal to the maximum drift over the 100 stories divided by the specified allowable such as $1/360$ or $1/400$. The constraint ratio for wind+gravity belt stress is equal to the maximum wind+gravity stress over all belt truss members in all intervals divided by the allowable stress for steel. Design constraints are satisfied when the constraint ratios are less than or equal to one. The design variables, design objective, and design constraints are located together on the spreadsheet to facilitate rapid trial-and-error optimization. This process was carried out for all six configurations of the generic skyscraper.

4 SPACE FRAME MODEL

A 3D, skeletal, linear, static, small-displacement, space frame model was developed to compare the accuracy of the SSAM. The space frame model was executed on a program written by Balling (1991) as well as on the commercial program, ADINA. Both programs gave the same results for linear analysis. The ADINA program was also executed to get nonlinear (large-displacement) results for one configuration of the space frame model. The space frame model will be described in five sections: nodes, members, supports, loads, and output.

4.1 Nodes

There were a total of 1877 nodes in the space frame model. The y-axis was taken as the vertical axis of the building located in the center of the core. There were 101 "core-center" nodes with $x=z=0$ equally spaced every 4m in the y-direction corresponding to the 100 stories of the generic skyscraper. Likewise, there were 101 "megacolumn" nodes for each of the 16 megacolumns. For a particular megacolumn, the x and z-coordinates were constant and depended on the location of the megacolumn in the plan, and the y-coordinates were equally spaced every 4m. Four "core-corner" nodes were located at each of stories 18, 22, 38, 42, 58, 62, 78, and 82 with horizontal coordinates $x=\pm 12.5\text{m}$ and $z=\pm 12.5\text{m}$. Outrigger members connected core-corner nodes with megacolumn nodes. Sixteen "belt" nodes were located midway between

megacolumn nodes at each of levels 19, 21, 39, 41, 59, 61, 79, and 81. Belt truss members connected belt nodes to megacolumn nodes.

4.2 Members

There were a total of 5668 members in the space frame model (see Figure 4-1), including 100 core members (yellow), 1600 megacolumn members (red), 64 outrigger members (green), 256 belt truss members (light blue), 160 diagonal members (black), 32 rigid link members (dark blue), and 3456 floor members (not shown in Figure 4-1, but shown in Figure 4-2). Shear deformation was neglected in all members, and the Poisson's ratio was assumed to be 0.25.

Core members connect core-center nodes, and megacolumn members connect megacolumn nodes. Core and megacolumn members possess axial, flexural, and torsional stiffness. The modulus of elasticity and cross-sectional areas were set equal to the values used in the SSAM. Both the strong and weak core moments of inertia were set equal to the values used in the SSAM. The torsion constant was arbitrarily set to 1000m^4 , and it was verified that this did not impact the results because of the symmetry of the structure and loading, and the axial rigidity of the floor diaphragms. Both ends of core and megacolumn members were connected rigidly.

Outrigger, belt truss, and diagonal members were modeled as truss members that only possess axial stiffness. The outrigger members connect between core-corner nodes and adjacent megacolumn nodes. The belt truss members connect between megacolumn nodes and belt nodes. The diagonal members connect between megacolumn nodes. Since these members possess axial stiffness only, their moments of inertia and torsion constants were set to zero, and both ends were hinge-connected. The modulus of elasticity was set equal to the value used in the SSAM. The cross-sectional areas were calculated by dividing the volumes used in the SSAM by the number of members and member length.

Rigid link members connect core-center nodes located at the intersection of intervals to core-corner nodes. They model the finite size of the core. Rigid link members possess infinite axial, flexural, and torsional stiffness. Infinite stiffness was obtained by setting the modulus of elasticity to 10^{12} KPa. The moments of inertia and torsion constant were arbitrarily set to 1000m^4 . Both ends of the rigid link members were connected rigidly.

Floor members extend radially from core-center nodes to megacolumn and belt nodes in the same horizontal plane. Additional floor members connect circumferentially between megacolumn and belt nodes in the same horizontal plane (see Figure 4-2). These members model the axially rigid floor diaphragms. They were modeled as truss members where their moments of inertia and torsion constants were set to zero, and both ends were hinge-connected. Axial rigidity was obtained by setting the modulus of elasticity to 10^{12} KPa. The cross-sectional areas were arbitrarily set to 1000m^2 . Choi et al. (2012) mentioned that if a belt truss is used, a stiff floor diaphragm is required at the top and bottom chord of each belt truss in order to transfer the core bending moment, in the form of floor shear and axial forces, to the belt wall and eventually to the columns. Also, improperly modeled diaphragms will result in misleading behaviors and load paths, and incorrect member design forces.

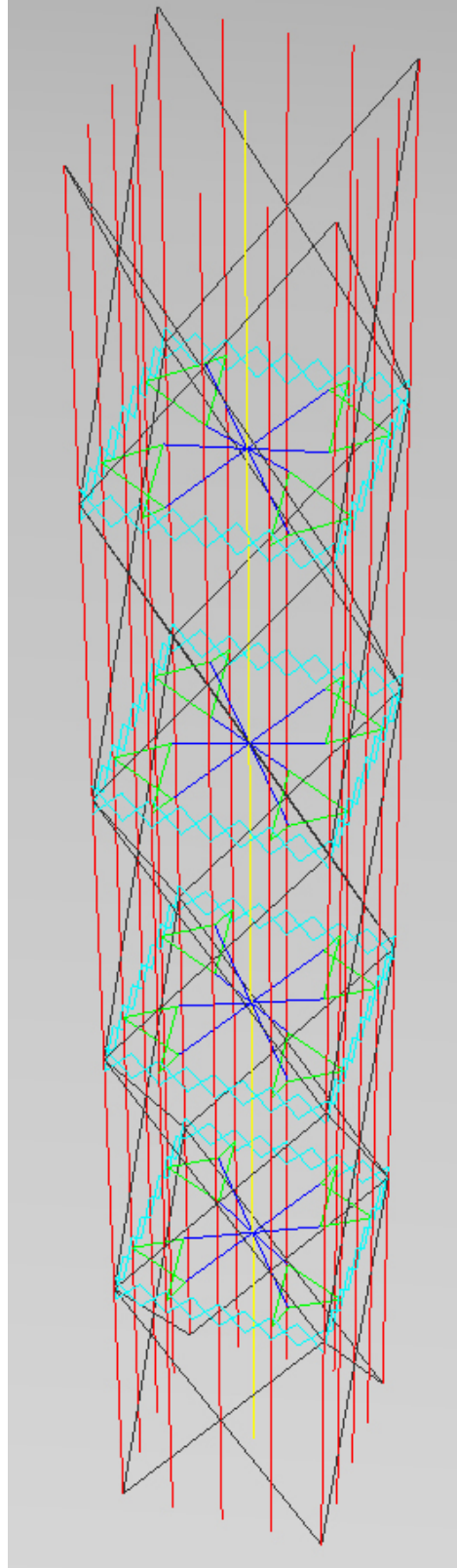


Figure 4-1: Space frame model – all members without floors

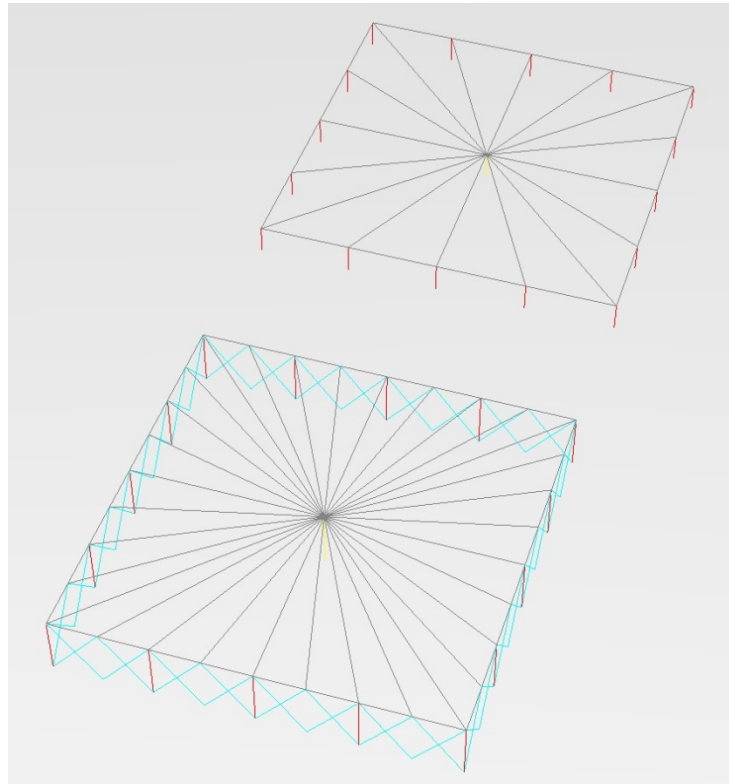


Figure 4-2: Space frame model – single floor configurations between intervals and at intervals

4.3 Supports

Supports restrained some of the DOF's. Each of the 1877 nodes in the space frame model had six displacement DOF's: three translations (Δ_x , Δ_y , and Δ_z) and three rotations (θ_x , θ_y , and θ_z). A total of 486 restraints were needed in this model. The core-center node and the sixteen megacolumn nodes at the base of the structure were fixed-supported to create $6 \times 17 = 102$ restraints. The rotational DOF's of the 128 belt nodes had to be supported for stability since the belt members were hinge-connected. This created $3 \times 128 = 384$ restraints. The number of unrestrained DOF's in the space frame model was $6 \times 1877 - 486 = 10,776$. Note that this is far greater than the 30 DOF's of the SSAM.

4.4 Loads

Both point loads and distributed loads were included in this model. A downward point load was applied at each of the core-center and megacolumn nodes representing the external dead, live, and cladding loads (1700 point loads). Horizontal point loads in the positive x direction were applied to each core-center node representing the lateral loads (100 point loads). Downward distributed loads were applied to core, megacolumn, outrigger, belt truss, and diagonal members representing member self-weight (2180 distributed loads). The magnitudes for all of these loads were obtained from the SSAM.

4.5 Output

Output from the space frame program consisted of nodal displacements and member end forces. These output files were imported into a macro-enabled Excel spreadsheet. The macro in the spreadsheet extracted appropriate data and calculated the following for comparison with the results from the SSAM:

core lateral translations

core rotations

core stresses

megacolumn stresses

outrigger stresses

belt truss stresses

diagonal stresses

5 RESULTS

Results from the SSAM and the space frame model (Sframe) are compared in the following tables for the six configurations of the generic skyscraper. For each configuration, the first table gives values of the design variables and calculated megacolumn areas for each interval. In the remaining tables for each configuration, the term "ratio" is the ratio of the SSAM value over the Sframe value. The "max error" given as a percentage below each table is equal to 100 times the maximum absolute value of the ratio minus one. The values in all tables are for linear analysis only with the exception of Table 5-2 and Table 5-3 (Configuration #1) where values are given for both linear and nonlinear analysis. All tables give results for combined gravity and lateral loading with the exception of tables for outrigger and belt stresses where the results are for lateral loading only.

It was observed in the space frame model, for configurations involving belt trusses, that the stress in the megacolumn located inside belt trusses was much greater than the stress in the megacolumn located outside belt trusses. It was assumed that the megacolumn cross-sectional area for an interval refers to the megacolumn outside belt trusses. The Sframe megacolumn stress reported in the following tables is the value for the member just above the belt truss at the bottom of the interval.

The lateral displacement and interstory drift are also plotted after the comparison tables for each configuration. Recall that interstory drift is defined as the difference in lateral displacement

between the top and bottom of the story divided by the story height. Since rotation is the derivative of lateral displacement, interstory drift is effectively a finite difference approximation of rotation. The interstory drift that is plotted in the figures that follow has been normalized by the allowable value so that when the normalized value is less than one, the drift constraint is satisfied. Points of contraflexure are also indicated on the plots. They are located at points where the drift is vertical because that is the point where the rotation changes from increasing to decreasing with height. Points of contraflexure also correspond to points where curvature changes in the plot of lateral displacement. However, the curvature changes are too subtle to observe in the lateral displacement plots for the six configurations. A seventh configuration was added with outriggers located only at interval 2. Here the points of contraflexure are observable in both the plot of drift and the plot of lateral displacement.

5.1 Configuration #1 – core+megacolumns

Table 5-1: Configuration #1 - design variables and calculated megacolumn areas

Interval	Core t (m)	Outrig V (m ³)	Belt V (m ³)	Diag V (m ³)	Megacolumn A Area (m ²)	Megacolumns B/D Area (m ²)	Megacolumns C/E Area (m ²)
1	0.5	0	0	0	1.7318	3.1207	3.1207
2	0.9	0	0	0	3.1172	5.6172	5.6172
3	1.4	0	0	0	4.8490	8.7379	8.7379
4	1.8	0	0	0	6.2344	11.2344	11.2344
5	2.3	0	0	0	7.9662	14.3551	14.3551

Table 5-2: Configuration #1 - lateral core translation (m)

Top of Interval	Linear SSAM	Linear Sframe	Linear Ratio	Nonlinear SSAM	Nonlinear Sframe	Nonlinear Ratio
1	0.693991	0.693624	1.0005	0.749785	0.748866	1.0012
2	0.491343	0.49108	1.0005	0.530263	0.529674	1.0011
3	0.302933	0.302771	1.0005	0.326322	0.326006	1.0010
4	0.146485	0.146407	1.0005	0.157324	0.157196	1.0008
5	0.039743	0.039722	1.0005	0.042491	0.042464	1.0006

max linear error = 0.05 max nonlinear error = 0.12

Table 5-3: Configuration #1 - core rotation (rad)

Top of Interval	Linear SSAM	Linear Sframe	Linear Ratio	Nonlinear SSAM	Nonlinear Sframe	Nonlinear Ratio
1	0.002554	0.002553	1.0004	0.002767	0.002763	1.0015
2	0.002473	0.002472	1.0004	0.002678	0.002675	1.0013
3	0.002175	0.002174	1.0006	0.002353	0.002350	1.0011
4	0.001672	0.001671	1.0005	0.001803	0.001801	1.0008
5	0.000930	0.000929	1.0007	0.000997	0.000996	1.0005

max linear error = 0.07% max nonlinear error = 0.15%

Table 5-4: Configuration #1 - vertical megacolumn translation minus vertical core translation

Top of Interval	Megacolumn A			Megacolumn B		
	SSAM	Sframe	Ratio	SSAM	Sframe	Ratio
1	0.0000	0.0000	1.000	0.0000	0.0000	1.000
2	0.0000	0.0000	1.000	0.0000	0.0000	1.000
3	0.0000	0.0000	1.000	0.0000	0.0000	1.000
4	0.0000	0.0000	1.000	0.0000	0.0000	1.000
5	0.0000	0.0000	1.000	0.0000	0.0000	1.000

Top of Interval	Megacolumn C			Megacolumn D		
	SSAM	Sframe	Ratio	SSAM	Sframe	Ratio
1	0.0000	0.0000	1.000	0.0000	0.0000	1.000
2	0.0000	0.0000	1.000	0.0000	0.0000	1.000
3	0.0000	0.0000	1.000	0.0000	0.0000	1.000
4	0.0000	0.0000	1.000	0.0000	0.0000	1.000
5	0.0000	0.0000	1.000	0.0000	0.0000	1.000

max error = 0.00%

Table 5-5: Configuration #1 - core stress (KPa)

Bottom of Interval	SSAM	Sframe	Ratio
1	7128.8693	7127.8425	1.0001
2	10325.5788	10321.9861	1.0003
3	12330.3395	12324.8866	1.0004
4	15100.3036	15091.9960	1.0006
5	16965.2776	16961.2986	1.0002

max error = 0.06%

Table 5-6: Configuration #1 - megacolumn stress (KPa)

Bottom of Interval	Megacolumn A			Megacolumn B		
	SSAM	Sframe	Ratio	SSAM	Sframe	Ratio
1	5622.3807	5642.2829	0.9965	5654.9521	5680.3098	0.9955
2	7184.8934	7229.1492	0.9939	7278.0048	7337.1414	0.9919
3	8010.7539	8062.0372	0.9936	8173.9692	8242.4494	0.9917
4	9375.9937	9452.1382	0.9919	9624.9249	9726.8335	0.9895
5	10301.7301	10301.6533	1.0000	10634.8049	10634.4231	1.0000

Bottom of Interval	Megacolumn C			Megacolumn D		
	SSAM	Sframe	Ratio	SSAM	Sframe	Ratio
1	5654.9521	5681.6678	0.9953	5654.9521	5681.6678	0.9953
2	7278.0048	7337.4124	0.9919	7278.0048	7337.4124	0.9919
3	8173.9692	8242.8105	0.9916	8173.9692	8242.8105	0.9916
4	9624.9249	9727.1394	0.9895	9624.9249	9727.1394	0.9895
5	10634.8049	10634.7010	1.0000	10634.8049	10634.7010	1.0000

max error = 1.05%

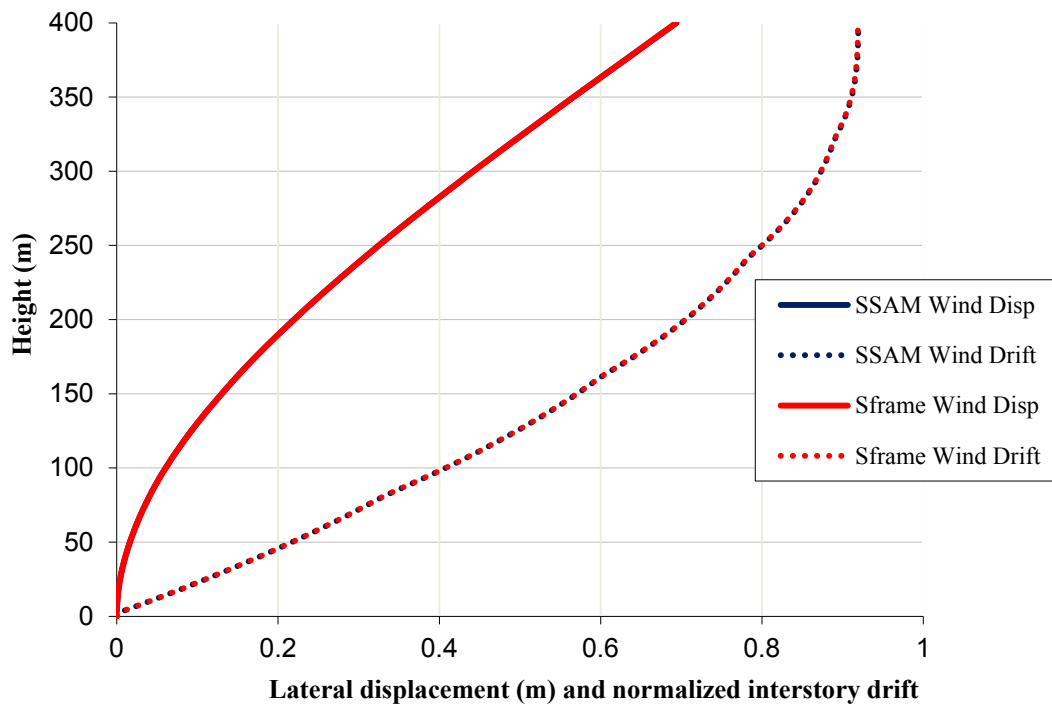


Figure 5-1: Configuration #1 - lateral displacement and interstory drift

5.2 Configuration #2 – core+megacolumns+outriggers

Table 5-7: Configuration #2 - design variables and calculated megacolumn areas

Interval	Core t (m)	Outrig V (m ³)	Belt V (m ³)	Diag V (m ³)	Megaolumn A Area (m ²)	Megaolumns B/D Area (m ²)	Megaolumns C/E Area (m ²)
1	0.2	0	0	0	0.6927	1.2483	1.2483
2	0.3	39	0	0	1.0353	1.8792	1.8656
3	0.5	65	0	0	1.7208	3.1406	3.1008
4	0.7	78	0	0	2.4045	4.4051	4.3329
5	1	58	0	0	3.4332	6.2962	6.1866

Table 5-8: Configuration #2 - lateral core translation (m)

Top of Interval	SSAM	Sframe	Ratio
1	0.693383	0.692891	1.0007
2	0.491356	0.491007	1.0007
3	0.306254	0.306038	1.0007
4	0.152420	0.152315	1.0007
5	0.043712	0.043683	1.0007

max error = 0.07%

Table 5-9: Configuration #2 - core rotation (rad)

Top of Interval	SSAM	Sframe	Ratio
1	0.002577	0.002576	1.0005
2	0.002375	0.002373	1.0007
3	0.002066	0.002065	1.0006
4	0.001599	0.001598	1.0009
5	0.000945	0.000944	1.0011

max error = 0.11%

Table 5-10: Configuration #2 - vertical megacolumn translation minus vertical core translation

Top of Interval	Megaolumn A			Megaolumn B		
	SSAM	Sframe	Ratio	SSAM	Sframe	Ratio
1	0.0000	0.0000	1.0000	0.0532	0.0531	1.0007
2	0.0000	0.0000	1.0000	0.0532	0.0531	1.0007
3	0.0000	0.0000	1.0000	0.0454	0.0453	1.0007
4	0.0000	0.0000	1.0000	0.0328	0.0327	1.0007
5	0.0000	0.0000	1.0000	0.0160	0.0160	1.0007

Top of Interval	Megaolumn C			Megaolumn D		
	SSAM	Sframe	Ratio	SSAM	Sframe	Ratio
1	0.0000	0.0000	1.0000	0.0266	0.0266	1.0007
2	0.0000	0.0000	1.0000	0.0266	0.0266	1.0007
3	0.0000	0.0000	1.0000	0.0227	0.0227	1.0007
4	0.0000	0.0000	1.0000	0.0164	0.0164	1.0007
5	0.0000	0.0000	1.0000	0.0080	0.0080	1.0007

max error = 0.07%

Table 5-11: Configuration #2 - core stress (KPa)

Bottom of Interval	SSAM	Sframe	Ratio
1	15222.8996	15222.3633	1.0000
2	21864.9112	21865.3745	1.0000
3	21975.7891	21977.1556	0.9999
4	23249.1280	23247.5511	1.0001
5	23745.7850	23742.1704	1.0002

max error = 0.02%

Table 5-12: Configuration #2 - megacolumn stress (KPa)

Bottom of Interval	Megaolumn A			Megaolumn B		
	SSAM	Sframe	Ratio	SSAM	Sframe	Ratio
1	11364.7174	11291.8259	1.0065	11416.2780	11343.5559	1.0064
2	15869.4783	15784.6825	1.0054	20208.4572	20113.5529	1.0047
3	15343.2403	15258.0034	1.0056	22324.7656	22227.5752	1.0044
4	15715.2110	15691.9781	1.0015	25008.8354	24964.6820	1.0018
5	15051.2138	15050.8507	1.0000	24011.6734	24000.1864	1.0005

Bottom of Interval	Megaolumn C			Megaolumn D		
	SSAM	Sframe	Ratio	SSAM	Sframe	Ratio
1	11416.2780	11348.1467	1.0060	11416.2780	11348.0227	1.0060
2	15968.2890	15883.1312	1.0054	18089.0756	17996.3230	1.0052
3	15486.1556	15401.4515	1.0055	18907.2497	18812.9495	1.0050
4	15909.3327	15878.1430	1.0020	20462.2415	20421.4768	1.0020
5	15322.8929	15322.4036	1.0000	19671.9816	19663.6635	1.0004

max error = 0.65%

Table 5-13: Configuration #2 - outrigger stress under lateral load only (KPa)

Top of Interval	B			D		
	SSAM	Sframe	Ratio	SSAM	Sframe	Ratio
2	44984.3482	44953.9263	1.0007	22492.1741	22477.7412	1.0006
3	45745.6419	45710.9210	1.0008	22872.8209	22855.8147	1.0007
4	52494.2377	52457.3896	1.0007	26247.1189	26229.1351	1.0007
5	55408.6325	55373.9057	1.0006	27704.3162	27687.3060	1.0006

max error = 0.08%

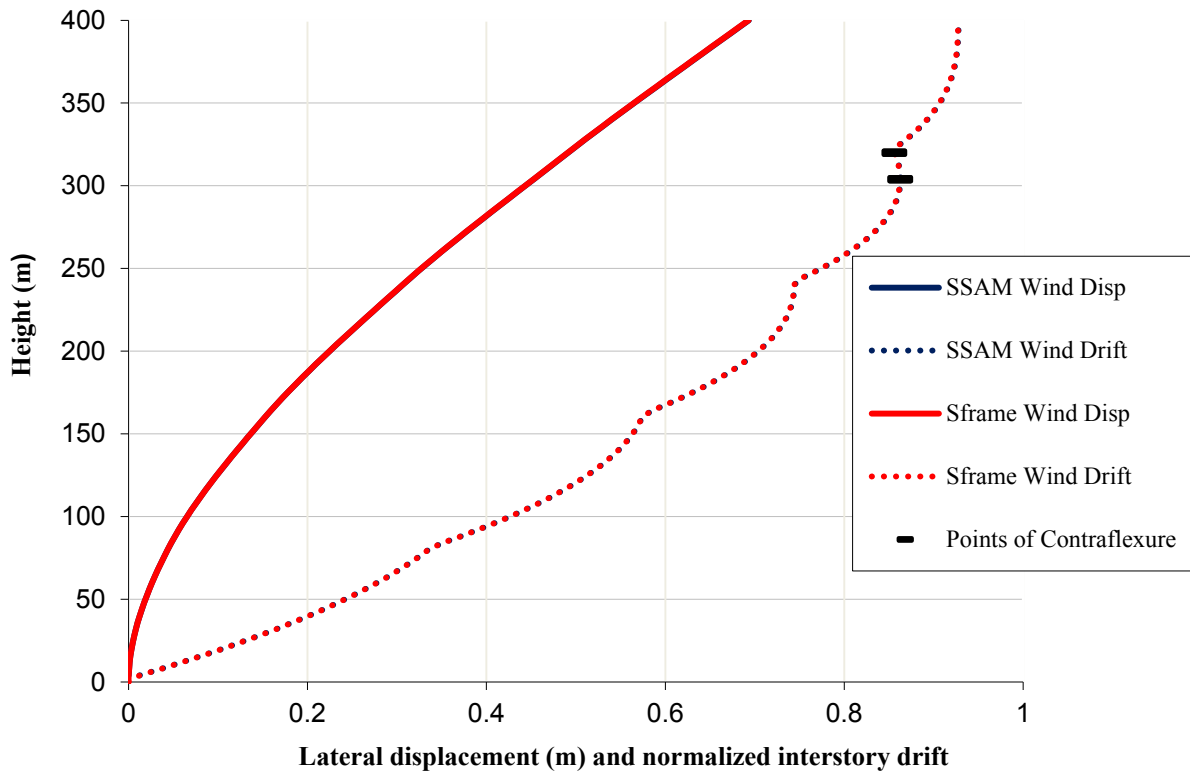


Figure 5-2: Configuration #2 - lateral displacement and interstory drift

5.3 Configuration #3 – core+megacolumns+belts

Table 5-14: Configuration #3 – design variables and calculated megacolumn areas

Interval	Core t (m)	Outrig V (m ³)	Belt V (m ³)	Diag V (m ³)	Megacolumn A Area (m ²)	Megacolumns B/D Area (m ²)	Megacolumns C/E Area (m ²)
1	0.2	0	0	0	0.6927	1.2483	1.2483
2	0.3	0	102	0	1.0747	1.9080	1.9080
3	0.4	0	143	0	1.4611	2.5723	2.5723
4	0.6	0	171	0	2.2222	3.8888	3.8888
5	0.8	0	34	0	2.9436	5.1658	5.1658

Table 5-15: Configuration #3 - lateral core translation (m)

Top of Interval	SSAM	Sframe	Ratio
1	0.704044	0.699316	1.0068
2	0.517826	0.514667	1.0061
3	0.341883	0.34002	1.0055
4	0.182970	0.182244	1.0040
5	0.056885	0.056722	1.0029

max error = 0.68%

Table 5-16: Configuration #3 - core rotation (rad)

Top of Interval	SSAM	Sframe	Ratio
1	0.002380	0.002360	1.0084
2	0.002177	0.002171	1.0028
3	0.002035	0.002032	1.0014
4	0.001713	0.001713	0.9998
5	0.001237	0.001235	1.0019

max error = 0.84%

Table 5-17: Configuration #3 - vertical megacolumn translation minus vertical core translation

Top of Interval	Megacolumn A			Megacolumn B		
	SSAM	Sframe	Ratio	SSAM	Sframe	Ratio
1	0.0411	0.0413	0.9960	0.0367	0.0369	0.9948
2	0.0411	0.0411	1.0006	0.0367	0.0367	1.0003
3	0.0360	0.0360	1.0015	0.0313	0.0313	1.0020
4	0.0260	0.0259	1.0034	0.0212	0.0211	1.0045
5	0.0124	0.0124	1.0015	0.0094	0.0094	1.0002

Top of Interval	Megacolumn C			Megacolumn D		
	SSAM	Sframe	Ratio	SSAM	Sframe	Ratio
1	0.0353	0.0354	0.9944	0.0198	0.0199	0.9953
2	0.0353	0.0352	1.0003	0.0198	0.0198	1.0004
3	0.0298	0.0297	1.0022	0.0172	0.0171	1.0017
4	0.0197	0.0196	1.0046	0.0120	0.0119	1.0044
5	0.0087	0.0087	1.0001	0.0054	0.0054	1.0001

max error = 0.56%

Table 5-18: Configuration #3 - core stress (KPa)

Bottom of Interval	SSAM	Sframe	Ratio
1	15222.8996	14755.1687	1.0317
2	20687.4577	20126.3594	1.0279
3	25164.8733	24542.8792	1.0253
4	24475.7970	23895.0744	1.0243
5	29080.7494	29051.5824	1.0010

max error = 3.17%

Table 5-19: Configuration #3 - megacolumn stress (KPa)

Bottom of Interval	Megacolumn A			Megacolumn B		
	SSAM	Sframe	Ratio	SSAM	Sframe	Ratio
1	11364.7174	11192.4457	1.0154	11416.2780	10839.4043	1.0532
2	18530.1441	18352.4852	1.0097	18786.8899	18355.1234	1.0235
3	23964.7985	23781.4997	1.0077	24128.3034	23770.5900	1.0150
4	24842.0815	24586.8684	1.0104	24041.3592	23755.9853	1.0120
5	24518.0750	24515.2250	1.0001	23192.4124	23200.8980	0.9959

Bottom of Interval	Megacolumn C			Megacolumn D		
	SSAM	Sframe	Ratio	SSAM	Sframe	Ratio
1	11416.2780	10842.9054	1.0529	11416.2780	10842.9045	1.0529
2	18825.0708	18396.9926	1.0233	17297.8410	16867.5663	1.0255
3	24076.7192	23722.7410	1.0149	21464.9875	21106.5570	1.0170
4	23649.9418	23357.7009	1.0125	21225.5716	20940.8840	1.0136
5	22796.1558	22801.6575	0.9998	21000.2127	21008.4266	0.9996

max error = 5.32%

Table 5-20: Configuration #3 - belt truss stress under lateral load only (KPa)

Top of Interval	AB			BC		
	SSAM	Sframe	Ratio	SSAM	Sframe	Ratio
2	34091.8555	34100.2843	0.9998	11462.0951	11464.4492	0.9998
3	36617.7339	36862.7669	0.9934	12008.4000	12039.1857	0.9974
4	37160.7101	37498.0444	0.9910	11270.3162	11456.9165	0.9837
5	23372.9232	24320.5346	0.9610	5669.7787	6002.3570	0.9446

Top of Interval	AD			DE		
	SSAM	Sframe	Ratio	SSAM	Sframe	Ratio
2	46071.0865	46434.0904	0.9922	57218.1212	57581.8362	0.9937
3	51061.3895	52528.7085	0.9721	64111.4385	65809.9134	0.9742
4	57366.3489	60005.8780	0.9560	73373.8281	76281.9196	0.9619
5	65316.2096	67916.3240	0.9617	78480.1129	80588.9503	0.9738

max error = 5.54%

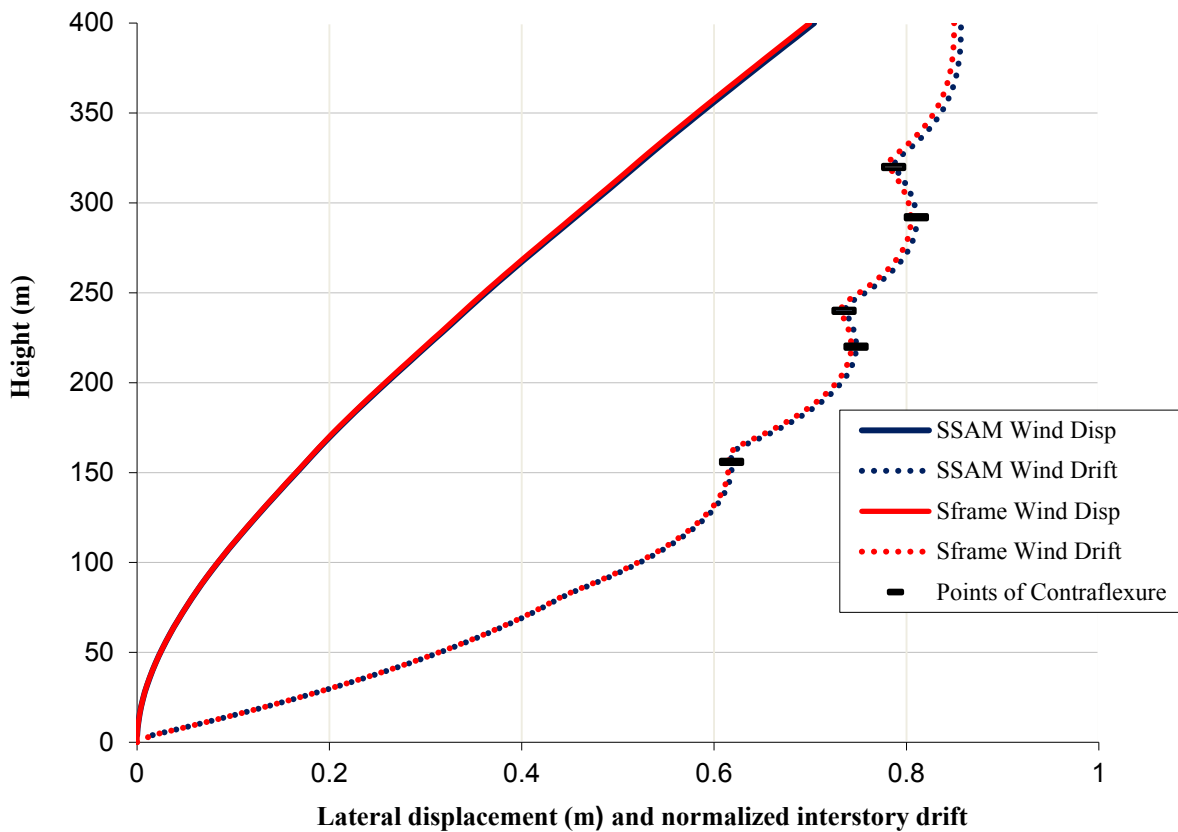


Figure 5-3: Configuration #3 - lateral displacement and interstory drift

5.4 Configuration #4 – core+megacolumns+diagonals

Table 5-21: Configuration #4 – design variables and calculated megacolumn areas

Interval	Core t (m)	Outrig V (m ³)	Belt V (m ³)	Diag V (m ³)	Megacolumn A Area (m ²)	Megacolumns B/D Area (m ²)	Megacolumns C/E Area (m ²)
1	0.1	0	0	43	0.3021	0.5369	0.5369
2	0.2	0	0	214	0.4718	0.8184	0.8184
3	0.4	0	0	255	1.1710	2.0082	2.0082
4	0.5	0	0	301	1.5033	2.5575	2.5575
5	0.7	0	0	35	2.5503	4.3708	4.3708

Table 5-22: Configuration #4 - lateral core translation (m)

Top of Interval	SSAM	Sframe	Ratio
1	0.700961	0.701863	0.9987
2	0.504953	0.506065	0.9978
3	0.326486	0.32738	0.9973
4	0.172002	0.172012	0.9999
5	0.054124	0.053793	1.0061

max error = 0.61%

Table 5-23: Configuration #4 - core rotation (rad)

Top of Interval	SSAM	Sframe	Ratio
1	0.002450	0.002448	1.0010
2	0.002356	0.002367	0.9954
3	0.002076	0.002092	0.9924
4	0.001734	0.001751	0.9904
5	0.001152	0.001144	1.0070

max error = 0.96%

Table 5-24: Configuration #4 - vertical megacolumn translation minus core vertical translation

Top of Interval	Megacolumn A			Megacolumn B		
	SSAM	Sframe	Ratio	SSAM	Sframe	Ratio
1	0.0524	0.0513	1.0224	0.0497	0.0479	1.0380
2	0.0498	0.0489	1.0194	0.0475	0.0457	1.0390
3	0.0420	0.0419	1.0041	0.0389	0.0376	1.0357
4	0.0316	0.0318	0.9958	0.0283	0.0276	1.0249
5	0.0166	0.0179	0.9265	0.0126	0.0123	1.0212

Top of Interval	Megacolumn C			Megacolumn D		
	SSAM	Sframe	Ratio	SSAM	Sframe	Ratio
1	0.0488	0.0463	1.0535	0.0257	0.0251	1.0234
2	0.0467	0.0440	1.0622	0.0246	0.0239	1.0260
3	0.0379	0.0354	1.0713	0.0205	0.0200	1.0247
4	0.0272	0.0255	1.0634	0.0152	0.0150	1.0125
5	0.0115	0.0109	1.0588	0.0072	0.0068	1.0634

max error = 7.35%

Table 5-25: Configuration #4 - core stress (KPa)

Bottom of Interval	SSAM	Sframe	Ratio
1	24491.3087	24076.1019	1.0172
2	24652.5844	23783.7907	1.0365
3	20901.6996	20278.8252	1.0307
4	24710.9186	24565.4534	1.0059
5	30260.4110	30190.1385	1.0023

max error = 3.65%

Table 5-26: Configuration #4 - megacolumn stress (KPa)

Bottom of Interval	Megaolumn A			Megaolumn B		
	SSAM	Sframe	Ratio	SSAM	Sframe	Ratio
1	22188.1356	24343.4592	0.9115	22004.7379	21960.3607	1.0020
2	25884.2484	25718.5434	1.0064	26334.6572	31532.2974	0.8352
3	23073.5915	23758.6810	0.9712	23276.7999	25267.4646	0.9212
4	27781.5777	25460.0655	1.0912	28229.3729	34199.6648	0.8254
5	28129.5845	31497.4134	0.8931	26213.8365	25813.6650	1.0155

Bottom of Interval	Megaolumn C			Megaolumn D		
	SSAM	Sframe	Ratio	SSAM	Sframe	Ratio
1	21957.6201	21857.8058	1.0046	21446.7176	20791.3225	1.0315
2	26462.4989	31584.0125	0.8378	23891.2614	26418.0173	0.9044
3	23320.0463	25376.9671	0.9189	20350.6673	20866.5435	0.9753
4	28195.7336	32223.3218	0.8750	24067.8469	28997.8631	0.8300
5	25645.7292	24450.5625	1.0489	23294.9342	22886.4234	1.0178

max error = 17%

Table 5-27: Configuration #4 - diagonal stress (KPa)

Bottom of Interval	AB			BC		
	SSAM	Sframe	Ratio	SSAM	Sframe	Ratio
1	81313.2121	97191.2950	0.8366	53515.7579	53745.4289	0.9957
2	78286.8973	64893.0101	1.2064	70972.4314	66846.3767	1.0617
3	62204.8291	57484.1797	1.0821	63507.8966	58387.9340	1.0877
4	64801.9911	36811.8336	1.7604	79792.3507	72844.7126	1.0954
5	83113.2553	80962.9631	1.0266	75733.4648	68248.1244	1.1097

Bottom of Interval	AD			DE		
	SSAM	Sframe	Ratio	SSAM	Sframe	Ratio
1	105912.1905	123399.1864	0.8583	94579.5296	96004.8275	0.9852
2	115143.6822	103985.5454	1.1073	105799.9883	102856.8695	1.0286
3	110160.4497	105055.9993	1.0486	103968.4388	100529.9374	1.0342
4	122931.4833	83483.3273	1.4725	120278.9758	112236.7924	1.0717
5	92421.3678	89841.3784	1.0287	95533.6065	89181.8488	1.0712

max error = 76%

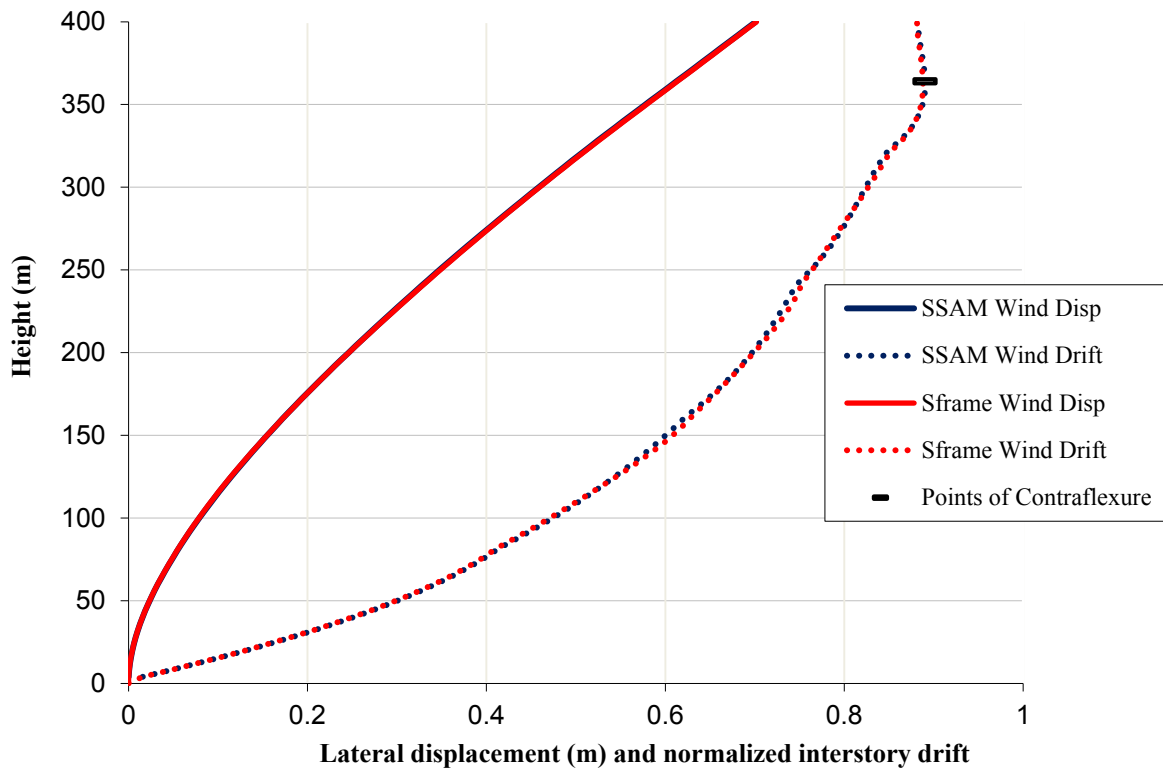


Figure 5-4: Configuration #4 - lateral displacement and interstory drift

5.5 Configuration #5 – core+megacolumns+outriggers+belts

Table 5-28: Configuration #5 – design variables and calculated megacolumn areas

Interval	Core t (m)	Outrig V (m ³)	Belt V (m ³)	Diag V (m ³)	Megacolumn A Area (m ²)	Megacolumns B/D Area (m ²)	Megacolumns C/E Area (m ²)
1	0.2	0	0	0	0.6927	1.2483	1.2483
2	0.3	41	43	0	1.0501	1.8945	1.8802
3	0.4	58	33	0	1.4008	2.5355	2.5051
4	0.6	74	20	0	2.0962	3.8090	3.7497
5	0.7	59	14	0	2.4416	4.4440	4.3695

Table 5-29 Configuration #5: - lateral core translation (m)

Top of Interval	SSAM	Sframe	Ratio
1	0.637650	0.637058	1.0009
2	0.465645	0.465354	1.0006
3	0.303810	0.303700	1.0004
4	0.159402	0.159369	1.0002
5	0.049382	0.049371	1.0002

max error = 0.09%

Table 5-30: Configuration #5 - core rotation (rad)

Top of Interval	SSAM	Sframe	Ratio
1	0.002202	0.002198	1.0019
2	0.001999	0.001999	1.0002
3	0.001860	0.001860	0.9999
4	0.001525	0.001526	0.9994
5	0.001023	0.001024	0.9993

max error = 0.19%

Table 5-31: Configuration #5 - vertical megacolumn translation minus core vertical translation

Top of Interval	Megacolumn A			Megacolumn B		
	SSAM	Sframe	Ratio	SSAM	Sframe	Ratio
1	0.0434	0.0435	0.9970	0.0438	0.0437	1.0019
2	0.0434	0.0433	1.0022	0.0438	0.0438	0.9989
3	0.0371	0.0369	1.0035	0.0393	0.0394	0.9984
4	0.0254	0.0253	1.0046	0.0301	0.0302	0.9983
5	0.0131	0.0130	1.0051	0.0170	0.0170	0.9985

Top of Interval	Megacolumn C			Megacolumn D		
	SSAM	Sframe	Ratio	SSAM	Sframe	Ratio
1	0.0395	0.0395	0.9990	0.0224	0.0224	1.0005
2	0.0395	0.0393	1.0054	0.0224	0.0224	0.9988
3	0.0326	0.0324	1.0069	0.0201	0.0201	0.9984
4	0.0214	0.0212	1.0077	0.0153	0.0153	0.9983
5	0.0106	0.0106	1.0079	0.0086	0.0086	0.9984

Max error = 0.79%

Table 5-32: Configuration #5 - core stress (KPa)

Bottom of Interval	SSAM	Sframe	Ratio
1	15222.8996	14754.8100	1.0317
2	20722.3915	20143.2498	1.0288
3	25345.5702	24983.7534	1.0145
4	24767.1003	24608.8396	1.0064
5	30466.8330	30469.8923	0.9999

max error = 3.17%

Table 5-33: Configuration #5 - megacolumn stress (KPa)

Bottom of Interval	Megacolumn A			Megacolumn B		
	SSAM	Sframe	Ratio	SSAM	Sframe	Ratio
1	11364.7174	10819.1557	1.0504	11416.2780	10871.5529	1.0501
2	19235.2364	18822.7648	1.0219	18310.6594	17917.6110	1.0219
3	24935.0696	24612.5733	1.0131	23727.1676	23390.6889	1.0144
4	24286.7997	24033.8655	1.0105	24880.0275	24615.4035	1.0108
5	27004.3520	26998.3974	1.0002	29436.5226	29421.2024	1.0005

Bottom of Interval	Megacolumn C			Megacolumn D		
	SSAM	Sframe	Ratio	SSAM	Sframe	Ratio
1	11416.2780	10875.9508	1.0497	11416.2780	10875.8908	1.0497
2	19607.8206	19217.9597	1.0203	17160.4669	16762.9066	1.0237
3	24831.5393	24507.1229	1.0132	21318.4127	20985.2979	1.0159
4	23592.7490	23325.9078	1.0114	21385.8312	21124.1238	1.0124
5	25968.9250	25946.5362	1.0009	24881.8330	24868.6022	1.0005

max error = 5.04%

Table 5-34: Configuration #5 - outrigger stress under lateral load only (KPa)

Top of Interval	B			D		
	SSAM	Sframe	Ratio	SSAM	Sframe	Ratio
2	45035.2256	44577.5789	1.0103	18919.8601	18665.0165	1.0137
3	51945.4870	51564.8600	1.0074	23095.2281	22900.8217	1.0085
4	58063.3030	57824.4431	1.0041	27352.3210	27226.2807	1.0046
5	62190.0087	62060.0618	1.0021	30264.2007	30193.9614	1.0023

max error = 1.37%

Table 5-35: Configuration #5 - belt truss stress under lateral load only (KPa)

Top of Interval	AB			BC		
	SSAM	Sframe	Ratio	SSAM	Sframe	Ratio
2	3232.7632	3017.2696	1.0714	33405.4233	34238.7440	0.9757
3	17629.0634	17844.8855	0.9879	51982.8703	52978.4759	0.9812
4	36793.7220	36402.7207	1.0107	67828.6849	67465.0595	1.0054
5	30804.0766	31010.3883	0.9933	49485.4582	50678.8492	0.9765

Top of Interval	AD			DE		
	SSAM	Sframe	Ratio	SSAM	Sframe	Ratio
2	31137.7201	33000.5671	0.9436	20216.3696	22017.0424	0.9182
3	48456.3261	51825.2521	0.9350	24677.8604	27699.4054	0.8909
4	69609.2164	73130.1273	0.9519	29226.6765	33110.0471	0.8827
5	64917.6447	67511.1317	0.9616	32338.0968	36489.2712	0.8862

max error = 11.7%

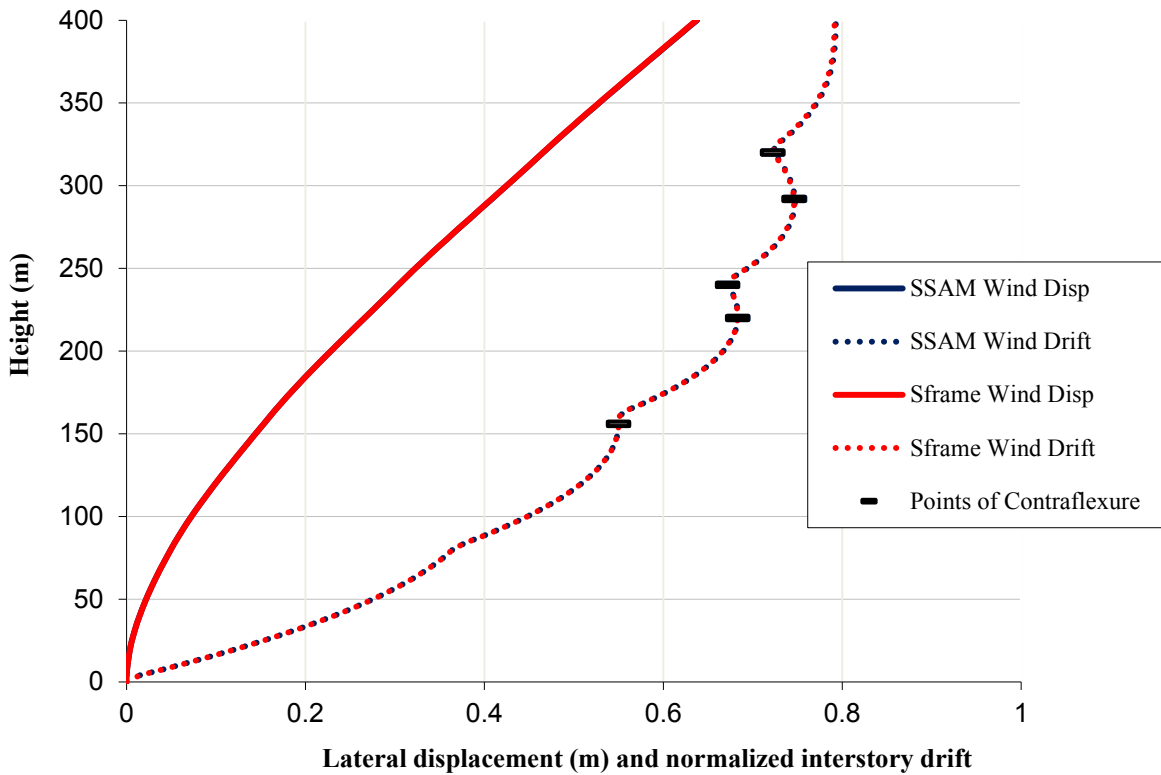


Figure 5-5: Configuration #5 - lateral displacement and interstory drift

5.6 Configuration #6 – core+megacolumns+outriggers+belts+diagonals

Table 5-36: Configuration #6 – design variables and calculated megacolumn areas

Interval	Core t (m)	Outrig V (m ³)	Belt V (m ³)	Diag V (m ³)	Megacolumn A Area (m ²)	Megacolumns B/D Area (m ²)	Megacolumns C/E Area (m ²)
1	0.1	0	0	12	0.3341	0.5998	0.5998
2	0.2	37	37	0	0.7010	1.2625	1.2535
3	0.4	56	33	0	1.4023	2.5350	2.5054
4	0.5	67	17	0	1.7479	3.1721	3.1249
5	0.7	57	7	0	2.4408	4.4394	4.3676

Table 5-37: Configuration #6 - lateral core translation (m)

Top of Interval	SSAM	Sframe	Ratio
1	0.695754	0.695147	1.0009
2	0.500956	0.500729	1.0005
3	0.322717	0.322649	1.0002
4	0.168275	0.168239	1.0002
5	0.050341	0.050327	1.0003

max error = 0.09%

Table 5-38: Configuration #6 - core rotation (rad)

Top of Interval	SSAM	Sframe	Ratio
1	0.002507	0.002501	1.0022
2	0.002199	0.002199	0.9998
3	0.001977	0.001979	0.9991
4	0.001659	0.001659	0.9997
5	0.001047	0.001047	1.0002

max error = 0.22%

Table 5-39: Configuration #6 - vertical megacolumn translation minus vertical core translation

Top of Interval	Megacolumn A			Megacolumn B		
	SSAM	Sframe	Ratio	SSAM	Sframe	Ratio
1	0.0503	0.0506	0.9946	0.0484	0.0483	1.0021
2	0.0486	0.0485	1.0033	0.0486	0.0487	0.9974
3	0.0394	0.0392	1.0050	0.0419	0.0420	0.9976
4	0.0273	0.0271	1.0050	0.0328	0.0329	0.9982
5	0.0122	0.0122	1.0038	0.0173	0.0173	0.9992

Top of Interval	Megacolumn C			Megacolumn D		
	SSAM	Sframe	Ratio	SSAM	Sframe	Ratio
1	0.0460	0.0460	1.0017	0.0250	0.0250	0.9985
2	0.0446	0.0441	1.0107	0.0249	0.0249	0.9967
3	0.0347	0.0343	1.0103	0.0214	0.0214	0.9975
4	0.0231	0.0229	1.0095	0.0166	0.0167	0.9981
5	0.0101	0.0100	1.0080	0.0087	0.0088	0.9989

max error = 1.07%

Table 5-40: Configuration #6 - core stress (KPa)

Bottom of Interval	SSAM	Sframe	Ratio
1	27387.9184	26620.0518	1.0288
2	29424.0492	28598.3007	1.0289
3	24363.6381	24021.8767	1.0142
4	28732.2483	28628.6999	1.0036
5	29877.1437	29878.9769	0.9999

max error = 2.89%

Table 5-41: Configuration #6 - megacolumn stress (KPa)

Bottom of Interval	Megacolumn A			Megacolumn B		
	SSAM	Sframe	Ratio	SSAM	Sframe	Ratio
1	21791.9345	20759.1685	1.0497	20844.1869	20402.7193	1.0216
2	26938.6898	26633.5447	1.0115	25664.4886	25126.2786	1.0214
3	24301.7041	24016.8300	1.0119	22770.2188	22454.1357	1.0141
4	28161.3801	27880.5510	1.0101	28609.3859	28295.8382	1.0111
5	25815.4518	25816.0029	1.0000	28861.1466	28846.3621	1.0005

Bottom of Interval	Megacolumn C			Megacolumn D		
	SSAM	Sframe	Ratio	SSAM	Sframe	Ratio
1	21700.8457	21626.6607	1.0034	20989.5741	20134.0916	1.0425
2	27428.7821	26662.3160	1.0287	23918.2093	23353.7580	1.0242
3	24135.6608	23774.5607	1.0152	20410.8066	20095.4986	1.0157
4	27235.3554	26896.6907	1.0126	24485.4249	24176.4379	1.0128
5	24930.3514	24896.2452	1.0014	24210.6468	24198.4173	1.0005

max error = 4.97%

Table 5-42: Configuration #6 - outrigger stress under lateral load only (KPa)

Top of Interval	B			D		
	SSAM	Sframe	Ratio	SSAM	Sframe	Ratio
2	46261.5351	45510.2512	1.0165	19093.0546	18564.0411	1.0285
3	54787.1379	54326.4558	1.0085	24328.4516	24070.2618	1.0107
4	62792.5224	62541.1241	1.0040	29685.5489	29536.8798	1.0050
5	64374.0247	64284.4537	1.0014	31554.6433	31492.5186	1.0020

max error = 2.85%

Table 5-43: Configuration #6 - belt truss stress under lateral load only (KPa)

Top of Interval	AB			BC		
	SSAM	Sframe	Ratio	SSAM	Sframe	Ratio
2	242.9812	2937.2585	0.0827	30852.7526	34012.3290	0.9071
3	19429.7002	20427.1005	0.9512	56116.9603	58352.3398	0.9617
4	43192.0741	42899.3472	1.0068	75696.5409	75563.9430	1.0018
5	39531.7217	39606.8331	0.9981	56116.1896	57445.9654	0.9769

Top of Interval	AD			DE		
	SSAM	Sframe	Ratio	SSAM	Sframe	Ratio
2	28787.2568	32665.9935	0.8813	20401.4326	22984.5134	0.8876
3	51975.6100	56562.4222	0.9189	25995.5923	29401.6620	0.8842
4	78567.7486	82673.7412	0.9503	31719.7921	36072.7633	0.8793
5	74600.0965	77105.0059	0.9675	33716.9688	38158.8394	0.8836

max error = 91.7%

Table 5-44: Configuration #6 - diagonal stress (KPa)

Bottom of Interval	AB			BC		
	SSAM	Sframe	Ratio	SSAM	Sframe	Ratio
1	69067.7863	55893.0411	1.2357	74604.5230	59454.8293	1.2548

Bottom of Interval	AD			DE		
	SSAM	Sframe	Ratio	SSAM	Sframe	Ratio
1	105123.4311	92455.7701	1.1370	91890.2709	81635.0762	1.1256

max error = 25.5%

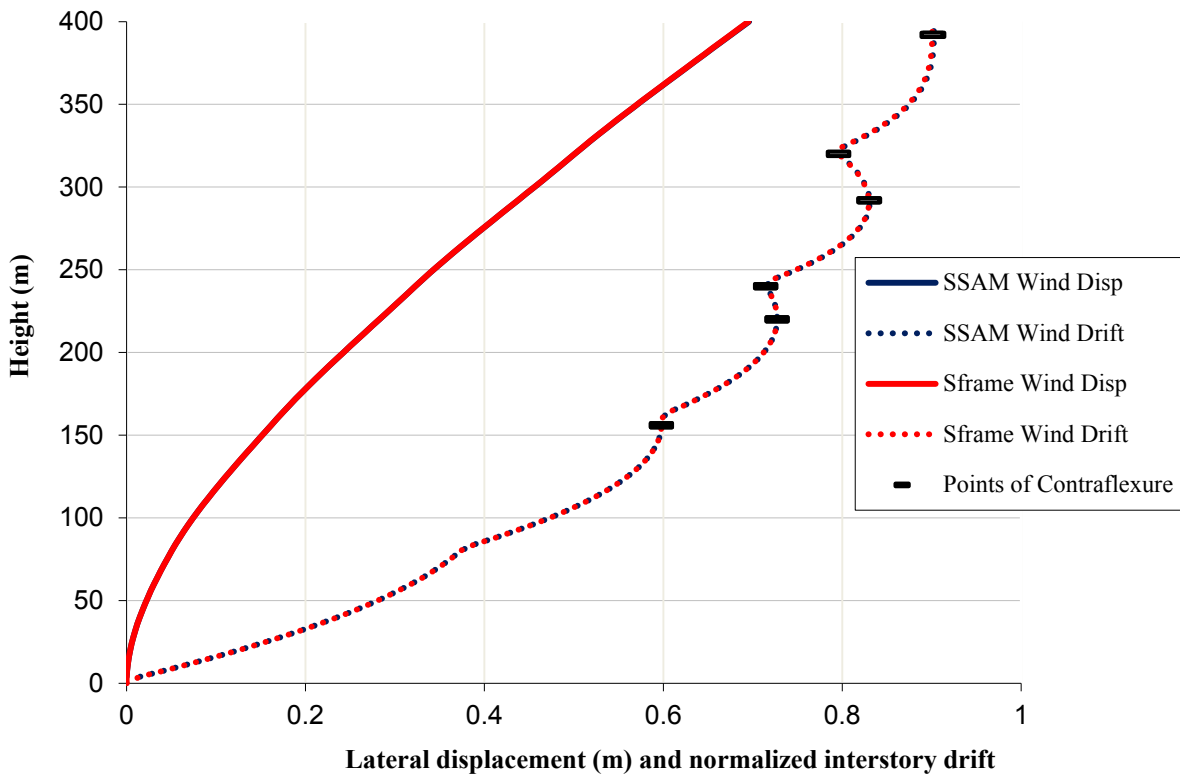


Figure 5-6: Configuration #6 - lateral displacement and interstory drift

5.7 Configuration #7 – core+megacolumns+outrigger at one level only

Table 5-45: Configuration #7 - design variables and calculated megacolumn areas

Interval	Core t (m)	Outrig V (m ³)	Belt V (m ³)	Diag V (m ³)	Megacolumn A Area (m ²)	Megacolumns B/D Area (m ²)	Megacolumns C/E Area (m ²)
1	0.2	0	0	0	0.6927	1.2483	1.2483
2	0.3	100	0	0	1.0295	1.8897	1.8551
3	0.5	0	0	0	1.7204	3.1412	3.1002
4	0.7	0	0	0	2.4118	4.3919	4.3461
5	1	0	0	0	3.4482	6.2691	6.2136

Table 5-46: Configuration #7 - lateral core translation (m)

Top of Interval	SSAM	Sframe	Ratio
1	0.940770	0.939826	1.0010
2	0.737032	0.736291	1.0010
3	0.505269	0.504765	1.0010
4	0.256719	0.256467	1.0010
5	0.071406	0.071338	1.0010

max error = 0.10%

Table 5-47: Configuration #7 - core rotation (rad)

Top of Interval	SSAM	Sframe	Ratio
1	0.002599	0.002596	1.0011
2	0.002396	0.002394	1.0008
3	0.003211	0.003208	1.0011
4	0.002822	0.002819	1.0011
5	0.001637	0.001636	1.0009

max error = 0.11%

Table 5-48: Configuration #7 - vertical megacolumn translation minus vertical core translation

Top of Interval	Megacolumn A			Megacolumn B		
	SSAM	Sframe	Ratio	SSAM	Sframe	Ratio
1	0.0000	0.0000	1.0000	0.0529	0.0528	1.0010
2	0.0000	0.0000	1.0000	0.0529	0.0528	1.0010
3	0.0000	0.0000	1.0000	0.0302	0.0302	1.0010
4	0.0000	0.0000	1.0000	0.0166	0.0166	1.0010
5	0.0000	0.0000	1.0000	0.0068	0.0068	1.0011

Top of Interval	Megacolumn C			Megacolumn D		
	SSAM	Sframe	Ratio	SSAM	Sframe	Ratio
1	0.0000	0.0000	1.0000	0.0264	0.0264	1.0010
2	0.0000	0.0000	1.0000	0.0264	0.0264	1.0010
3	0.0000	0.0000	1.0000	0.0151	0.0151	1.0010
4	0.0000	0.0000	1.0000	0.0083	0.0083	1.0010
5	0.0000	0.0000	1.0000	0.0034	0.0034	1.0011

max error = 0.11%

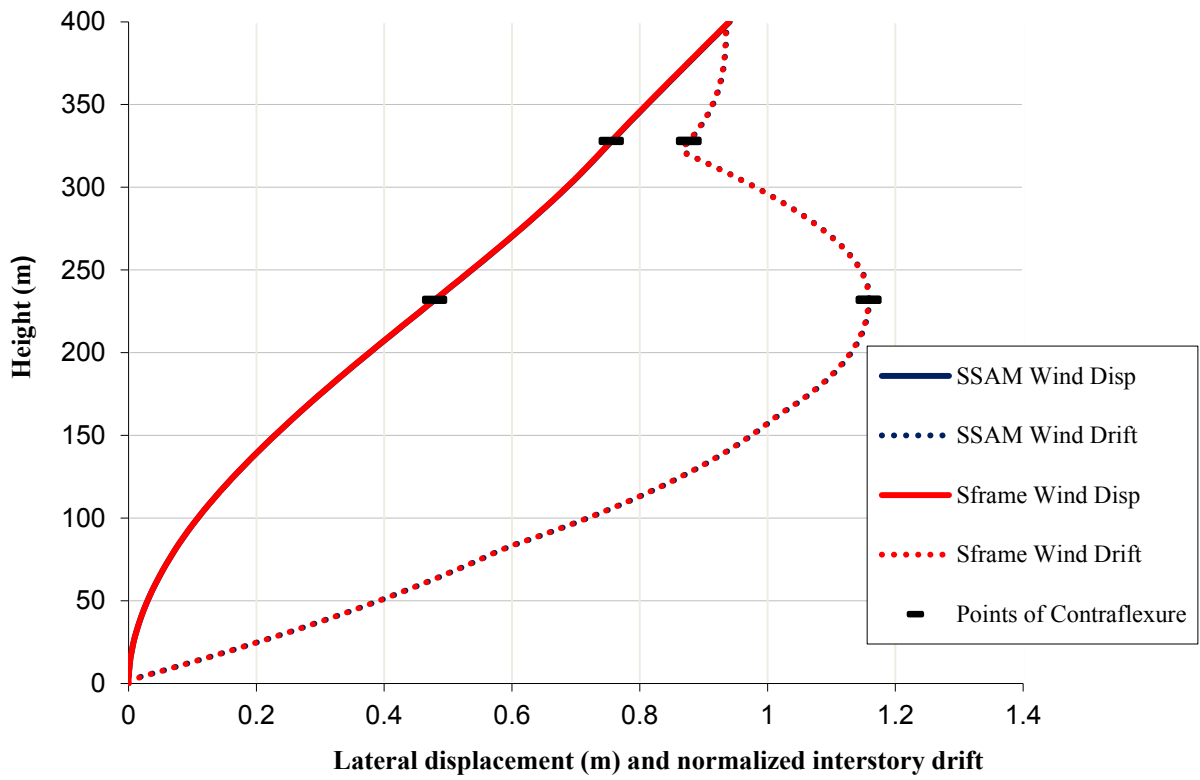


Figure 5-7: Configuration #7 - lateral displacement and interstory drift

6 CONCLUSIONS

The SSAM was developed, implemented, and tested. The SSAM was able to predict the existence of points of contraflexure in the deflected shape of configurations involving outriggers, belts, and diagonals, as verified by the space frame model. Such points of contraflexure cannot be predicted with continuum models.

The accuracy of the SSAM was compared against the space frame model. For all configurations that exclude diagonals, the maximum error was 1% for linear and nonlinear lateral translations, 1% for linear and nonlinear rotations, and 1% for vertical translations. Furthermore, the maximum error in stress was 3% for the core, 3% for the megacolumns, 1% for outriggers, and 12% for belts. For configurations that included diagonals, the maximum error was 1% for linear lateral translations, 1% for linear rotations, and 7% for vertical translations. Additionally, the maximum error in stress was 4% for the core, 17% for the megacolumns, 3% for the outriggers, 92% for the belts, and 76% for the diagonals. Thus, the accuracy of the SSAM is very good for translations and rotations, and reasonably good for stress in configurations that exclude diagonals. Stress formulas for configurations that include diagonals need further development.

The speed of execution, data preparation, data extraction, and optimization is much faster with the SSAM than with general space frame programs, both that of Balling (1991) and ADINA. Execution of the SSAM is instantaneous since it only involves 30 DOF's for the generic skyscraper. Execution of the space frame model of the generic skyscraper with 10,776

DOF's on the space frame program from Balling (1991) required about 25 minutes on a computer. Preparation of data for the SSAM spreadsheet on a new skyscraper will take some time. But preparation/extraction of data for general space frame and finite element programs for a skyscraper involving 5668 members and 1877 nodes will take more time. Rapid trial-and-error optimization is possible with the SSAM spreadsheet, but not possible with general space frame and finite element programs. The SSAM appears to be ideal for preliminary skyscraper design and educational purposes for students learning about the behavior and design of modern skyscrapers.

REFERENCES

- Abergel, D. P., and Smith, B. S. (1983). "Approximate analysis of high-rise structures comprising coupled walls and shear walls." *Building and Environment*, 18(1), 91-96.
- American Society of Civil Engineers (ASCE). (2006). "Minimum design loads for buildings and other structures." ASCE 7-05, New York.
- Bakker, M. C. M., Hoenderkamp, J. C. D., and Snijder, H. H. (2003). "Preliminary design of high-rise outrigger braced shear wall structures on flexible foundations." *HERON*, 48(2), 81-98.
- Balling, R. J. (1991). *Computer Structural Analysis*, BYU Academic Publishing, Provo, UT.
- Bozdogan, K. B. (2009). "An approximate method for static and dynamic analyses of symmetric wall-frame buildings." *The Structural Design of Tall and Special Buildings*, 18(3), 279-290.
- Bozdogan, K. B., and Ozturk, D. (2009). "An approximate method for lateral stability analysis of wall-frame buildings including shear deformations of walls." *Indian Academy of Sciences*, 35(3), 241-253.
- Choi, H. S., Ho, G., Joseph, L., and Mathias, N. (2012). "Outrigger Design for High-Rise Buildings: An output of the CTBUH Outrigger Working Group."
- De Llera, J. C. L., and Chopra, A. K. (1995). "A simplified model for analysis and design of asymmetric-plan buildings." *Earthquake engineering & structural dynamics*, 24, 21.
- Heidebrecht, A. C., and Smith, B. S. (1973). "Approximate analysis of tall wall-frame structures." *Journal of the Structural Division*, 99(2), 199-220.

- Hoenderkamp, J. C. D. (2004). "Shear wall with outrigger trusses on wall and column foundations." *The Structural Design of Tall and Special Buildings*, 13(1), 73-87.
- Hoenderkamp, J. C. D. (2008). "Second outrigger at optimum location on high-rise shear wall." *The Structural Design of Tall and Special Buildings*, 17(3), 619-634.
- Hoenderkamp, J. C. D., and Bakker, M. C. M. (2003). "Analysis of high-rise braced frames with outriggers." *The Structural Design of Tall and Special Buildings*, 12(4), 335-350.
- Hoenderkamp, J. C. D., Kuster, M., and Smith, B. S. (1984). "Generalized method for estimating drift in high-rise structures." *Journal of Structural Engineering*, 110(7), 1549-1562.
- Inc., K. K. E. "Structural Design for High-rise Building."
<http://www4.kke.co.jp/stde/en/consulting/highrise_bldg.html>.
- Katz, P., Robertson, L. E., and See, S. (2008). "Case Study: Shanghai World Financial Center." *CTBUH Journal*, 1(2), 10-14.
- Kaviani, P., Rahgozar, R., and Saffari, H. (2008). "Approximate analysis of tall buildings using sandwich beam models with variable cross-section." *The Structural Design of Tall and Special Buildings*, 17(2), 401-418.
- Kian, P. S., and Siahhaan, F. T. (2001). "The Use of Outrigger and Belt Truss System for High-Rise Concrete Buildings." *Dimensions of Civil Engineering*, 3(1), 6.
- Kobayashi, M., Takabatake, H., and Takesako, R. (1995). "A simplified analysis of doubly symmetric tube structures." *The Structural Design of Tall Buildings*, 4, 137-153.
- Kwan, A. K. H. (1994). "Simple method for approximate analysis of framed tube structures." *Journal of Structural Engineering*, 120(4), 1221-1239.
- Lin, L., Pekau, O. A., and Zielinski, Z. A. (1994). "Displacement and natural frequencies of tall building structures by finite story method." *Computers & Structures*, 54(1), 1-13.
- Mass, D. C., Poon, D., and Xia, J. (2010). "Case Study: Shanghai Tower." *CTBUH Journal*, 1(2), 12-18.

- Nollet, M.-J., and Smith, B. S. (1997). "Stiffened-story wall-frame tall building structure." *Computers & Structures*, 66(2-3), 225-240.
- Potzta, G., and Kollar, L. P. (2003). "Analysis of building structures by replacement sandwich beams." *International Journal of Solids and Structures*, 40, 535-553.
- Rahgozar, R., and Sharifi, Y. (2009). "An approximate analysis of combined system of framed tube, shear core and belt truss in high-rise buildings." *The Structural Design of Tall and Special Buildings*, 18(6), 607-624.
- Rahgozar, R., Ahmadi, A. R., and Sharifi, Y. (2010). "A simple mathematical model for approximate analysis of tall buildings." *Applied Mathematical Modelling*, 34(9), 2437-2451.
- Rutenberg, A. (1987). "Lateral load response of belted tall building structures." *Engineering Structures*, 9(1), 53-67.
- Rutenberg, A., and Heidebrecht, A. C. (1975). "Approximate analysis of asymmetric wall-frame structures." *Building Science*, 10(1), 27-35.
- Stafford Smith, B., and Coull, A. (1991). *Tall building structures: analysis and design*, John Wiley & Sons, Inc., New York.
- Smith, B. S., and Salim, I. (1981). "Parameter Study of Outrigger-Braced Tall Building Structures." *Journal of the Structural Division*, 107(ST10), 2001-2013.
- Takabatake, H. (2012). "A Simplified Analytical Method for High-Rise Buildings."
- Taranath, B. S. (2005). *Wind and earthquake resistant buildings: structural analysis and design*, Marcel Dekker, New York.
- Toutanji, H. A. (1997). "The effect of foundation flexibility on the interaction between shear walls and frames." *Engineering Structures*, 19(12), 1036-1042.
- Wong, V. (June 2002). "Concrete core detail."
<<http://www.emporis.com/images/list/building/two-international-finance-centre-hong-kong-china/8>>.

Wu, J. R., and Li, Q. S. (2003). "Structural performance of multi-outrigger-braced tall buildings." *The Structural Design of Tall and Special Buildings*, 12(2), 155-176.

APPENDIX A. SSAM EXCEL SPREADSHEET (CONFIGURATION #6)

The SSAM was executed on an Excel spreadsheet. A typical spreadsheet has five sheets:
1) Properties sheet, 2) Design sheet, 3) Matrices sheet, 4) Lateral sheet, and 6) Stress sheet. An example will follow with Configuration #6.

Properties Sheet

Concrete		
allowable stress (KPa)		48000
modulus (KPa)		43400000
density (KN/m ³)		21.7
cost (\$/m ³)		157
Steel		
allowable stress (KPa)		207000
modulus (KPa)		200000000
density (KN/m ³)		77
cost (\$/KN)		70
Weight Data		
floor dead load (KPa)		4.34
floor live load (KPa)		2.4
cladding weight (KPa)		1.3
Wind Data		
speed (mph)		123
reference height (m)		274
exponent alpha		9.5
drift allowable		360
Seismic Data		
spectral acceleration (g)		0.2
ductility factor		3
exponent k		2
drift allowable		50

	hor 100	rot 100	ver A 100	ver B 100	ver C 100	ver D 100	hor 80	rot 80	ver A 80	ver B 80	ver C 80	ver D 80
hor 100	274457.47	-10599559	-15149.602	0	0	0	-274457.47	-10599559	-15149.602	0	0	0
rot 100	-10599559	565309799	0	0	0	0	10599558.7	282654899	0	0	0	0
ver A 100	-15149.602	0	375178.266	-96957.455	0	-96957.455	15149.6023	0	-181263.36	0	0	0
ver B 100	0	0	-96957.455	519283.781	-96957.455	0	0	0	0	-325368.87	0	0
ver C 100	0	0	0	-96957.455	259641.89	0	0	0	0	0	-162684.44	0
ver D 100	0	0	-96957.455	0	0	519283.781	0	0	0	0	0	-325368.87
hor 80	-274457.47	10599558.7	15149.6023	0	0	0	804667.637	-10608848	15149.6023	0	0	0
rot 80	-10599559	282654899	0	0	0	0	-10608848	2867546273	-8708440.5	-30509134	0	-15254567
ver A 80	-15149.602	0	-181263.36	0	0	0	15149.6023	-8708440.5	2148831.53	-793632.69	0	-793632.69
ver B 80	0	0	0	-325368.87	0	0	0	-30509134	-793632.69	3817892.73	-793632.69	0
ver C 80	0	0	0	0	-162684.44	0	0	0	0	-793632.69	1296336.02	0
ver D 80	0	0	0	0	0	-325368.87	0	-15254567	-793632.69	0	0	3817892.73
hor 60	0	0	0	0	0	0	-530210.17	21208406.7	0	0	0	0
rot 60	0	0	0	0	0	0	-21208407	565557512	0	0	0	0
ver A 60	0	0	0	0	0	0	0	0	-380302.79	0	0	0
ver B 60	0	0	0	0	0	0	0	0	0	-684893.11	0	0
ver C 60	0	0	0	0	0	0	0	0	0	0	-340018.9	0
ver D 60	0	0	0	0	0	0	0	0	0	0	0	-684893.11
hor 40	0	0	0	0	0	0	0	0	0	0	0	0
rot 40	0	0	0	0	0	0	0	0	0	0	0	0
ver A 40	0	0	0	0	0	0	0	0	0	0	0	0
ver B 40	0	0	0	0	0	0	0	0	0	0	0	0
ver C 40	0	0	0	0	0	0	0	0	0	0	0	0
ver D 40	0	0	0	0	0	0	0	0	0	0	0	0
hor 20	0	0	0	0	0	0	0	0	0	0	0	0
rot 20	0	0	0	0	0	0	0	0	0	0	0	0
ver A 20	0	0	0	0	0	0	0	0	0	0	0	0
ver B 20	0	0	0	0	0	0	0	0	0	0	0	0
ver C 20	0	0	0	0	0	0	0	0	0	0	0	0
ver D 20	0	0	0	0	0	0	0	0	0	0	0	0

	hor 60	rot 60	ver A 60	ver B 60	ver C 60	ver D 60	hor 40	rot 40	ver A 40	ver B 40	ver C 40	ver D 40
hor 100	0	0	0	0	0	0	0	0	0	0	0	0
rot 100	0	0	0	0	0	0	0	0	0	0	0	0
ver A 100	0	0	0	0	0	0	0	0	0	0	0	0
ver B 100	0	0	0	0	0	0	0	0	0	0	0	0
ver C 100	0	0	0	0	0	0	0	0	0	0	0	0
ver D 100	0	0	0	0	0	0	0	0	0	0	0	0
hor 80	-530210	-2.1E+07	0	0	0	0	0	0	0	0	0	0
rot 80	21208407	5.66E+08	0	0	0	0	0	0	0	0	0	0
ver A 80	0	0	-380303	0	0	0	0	0	0	0	0	0
ver B 80	0	0	0	-684893	0	0	0	0	0	0	0	0
ver C 80	0	0	0	0	-340019	0	0	0	0	0	0	0
ver D 80	0	0	0	0	0	-684893	0	0	0	0	0	0
hor 60	1591488	-2.1E+07	0	0	0	0	-1061278	-4.2E+07	0	0	0	0
rot 60	-2.1E+07	5.03E+09	-7766987	-4.6E+07	0	-2.3E+07	42451120	1.13E+09	0	0	0	0
ver A 60	0	-7766987	2383784	-621359	0	-621359	0	0	-760763	0	0	0
ver B 60	0	-4.6E+07	-621359	5149913	-621359	0	0	0	0	-1375263	0	0
ver C 60	0	0	0	-621359	1640961	0	0	0	0	0	-679583	0
ver D 60	0	-2.3E+07	-621359	0	0	5149913	0	0	0	0	0	-1375263
hor 40	-1061278	42451120	0	0	0	0	2388408	-1.1E+07	0	0	0	0
rot 40	-4.2E+07	1.13E+09	0	0	0	0	-1.1E+07	6.92E+09	-4001175	-5.5E+07	0	-2.8E+07
ver A 40	0	0	-760763	0	0	0	0	-4001175	2349188	-320094	0	-320094
ver B 40	0	0	0	-1375263	0	0	0	-5.5E+07	-320094	5946164	-320094	0
ver C 40	0	0	0	0	-679583	0	0	0	0	-320094	1847295	0
ver D 40	0	0	0	0	0	-1375263	0	-2.8E+07	-320094	0	0	5946164
hor 20	0	0	0	0	0	0	-1327130	53085186	0	0	0	0
rot 20	0	0	0	0	0	0	-5.3E+07	1.42E+09	0	0	0	0
ver A 20	0	0	0	0	0	0	0	0	-948237	0	0	0
ver B 20	0	0	0	0	0	0	0	0	0	-1720863	0	0
ver C 20	0	0	0	0	0	0	0	0	0	0	-847617	0
ver D 20	0	0	0	0	0	0	0	0	0	0	0	-1720863

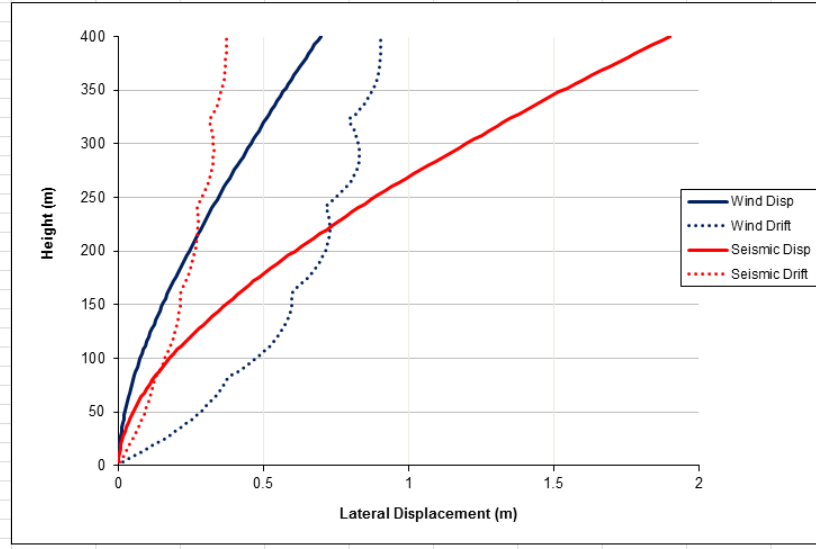
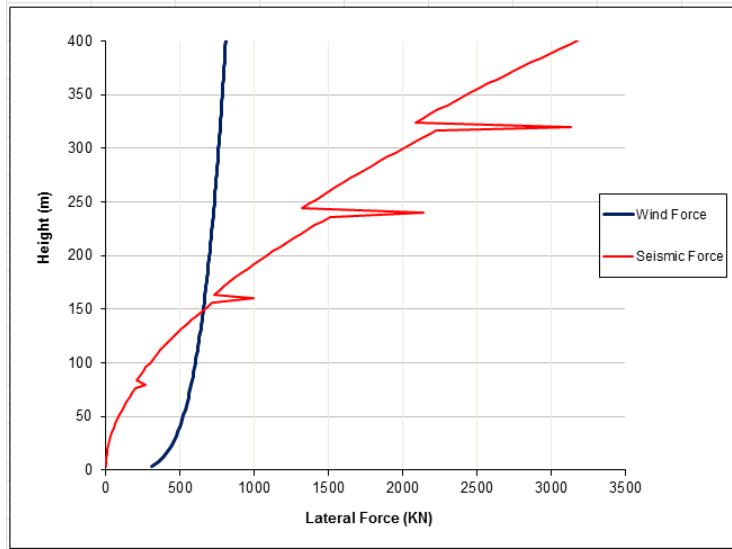
	hor 20	rot 20	ver A 20	ver B 20	ver C 20	ver D 20	wind force	wind disp	wind non	wind non'	seis force	seis disp	seis non	seis non'
hor 100	0	0	0	0	0	0	2092.591	0.695754	0	129.7124	7424.802	1.898224	0	379.4906
rot 100	0	0	0	0	0	0	-26368.3	0.002507	0	-1502.72	-89473.4	0.007413	0	-4358.6
ver A 100	0	0	0	0	0	0	0	0.050332	0	0	0	0.142633	0	0
ver B 100	0	0	0	0	0	0	0	0.048445	0	0	0	0.136335	0	0
ver C 100	0	0	0	0	0	0	0	0.046049	0	0	0	0.129058	0	0
ver D 100	0	0	0	0	0	0	0	0.02497	0	0	0	0.07048	0	0
hor 80	0	0	0	0	0	0	3848.283	0.500956	0	222.4013	11014.87	1.327065	0	611.3454
rot 80	0	0	0	0	0	0	1085.577	0.002199	0	-55.49	20463.01	0.006277	0	52.4423
ver A 80	0	0	0	0	0	0	0	0.048627	0	0	0	0.13686	0	0
ver B 80	0	0	0	0	0	0	0	0.048596	0	0	0	0.136627	0	0
ver C 80	0	0	0	0	0	0	0	0.044621	0	0	0	0.12472	0	0
ver D 80	0	0	0	0	0	0	0	0.024854	0	0	0	0.069981	0	0
hor 60	0	0	0	0	0	0	3620.132	0.322717	0	177.6061	7246.049	0.824929	0	421.0079
rot 60	0	0	0	0	0	0	1366.988	0.001977	0	-51.97	15787.59	0.005407	0	81.68344
ver A 60	0	0	0	0	0	0	0	0.039387	0	0	0	0.10768	0	0
ver B 60	0	0	0	0	0	0	0	0.04189	0	0	0	0.114147	0	0
ver C 60	0	0	0	0	0	0	0	0.034661	0	0	0	0.094854	0	0
ver D 60	0	0	0	0	0	0	0	0.021367	0	0	0	0.058235	0	0
hor 40	-1327130	-5.3E+07	0	0	0	0	3318.545	0.168275	0	61.78149	3761.977	0.41234	0	61.79209
rot 40	53085186	1.42E+09	0	0	0	0	1901.708	0.001659	0	708.1185	17147.72	0.004302	0	2077.548
ver A 40	0	0	-948237	0	0	0	0	0.027255	0	0	0	0.07299	0	0
ver B 40	0	0	0	-1720863	0	0	0	0.032819	0	0	0	0.086336	0	0
ver C 40	0	0	0	0	-847617	0	0	0.023067	0	0	0	0.06227	0	0
ver D 40	0	0	0	0	0	-1720863	0	0.016645	0	0	0	0.043791	0	0
hor 20	3186595	-2.1E+07	0	0	0	0	2838.055	0.050341	0	-260.939	1125.717	0.117251	0	-709.855
rot 20	-2.1E+07	8.31E+09	-1647543	-4.7E+07	0	-2.4E+07	3525.94	0.001047	0	1774.957	9654.054	0.00252	0	3762.77
ver A 20	0	-1647543	2535980	-131803	0	-131803	0	0.012226	0	0	0	0.032357	0	0
ver B 20	0	-4.7E+07	-131803	6272845	-131803	0	0	0.017319	0	0	0	0.043817	0	0
ver C 20	0	0	0	-131803	2164139	0	0	0.010089	0	0	0	0.027058	0	0
ver D 20	0	-2.4E+07	-131803	0	0	6272845	0	0.008746	0	0	0	0.022135	0	0

story	story height	height	int position	int height	wind P	wind width	wind F	wind F bot	wind F top	wind M bot	wind M top	wind disp	wind drift
	m	m	m	m	KPa	m	KN	KN	KN	KNm	KNm	m	
0		0	0									0	
1	4	4	4	80	1.53080519	50	306.161038	303.94137	2.21966753	1105.24135	58.1705972	0.00016742	0.0150675
2	4	8	8	80	1.77131036	50	354.262071	344.342733	9.919338	2295.61822	255.068691	0.00066067	0.04439289
3	4	12	12	80	1.92915226	50	385.830452	362.391252	23.4391999	3345.15002	590.320591	0.00146632	0.07250821
4	4	16	16	80	2.04960135	50	409.920269	367.288561	42.631708	4197.58356	1049.39589	0.00257098	0.09941984
5	4	20	20	80	2.14818414	50	429.636828	362.506074	67.1307544	4833.41431	1611.1381	0.00396137	0.12513474
6	4	24	24	80	2.23224183	50	446.448366	350.015519	96.432847	5250.23278	2250.09976	0.00562426	0.14966036
7	4	28	28	80	2.30587257	50	461.174514	331.238594	129.935919	5455.6945	2937.68165	0.00754653	0.17300447
8	4	32	32	80	2.3716147	50	474.32294	307.361265	166.961675	5464.20027	3642.80018	0.00971515	0.19517519
9	4	36	36	80	2.43115745	50	486.23149	279.461549	206.769941	5295.06092	4332.32257	0.01211716	0.21618086
10	4	40	40	80	2.48568586	50	497.137172	248.568586	248.568586	4971.37172	4971.37172	0.01473971	0.23603011
11	4	44	44	80	2.53606565	50	507.213129	215.692383	291.520746	4519.26898	5523.55098	0.01757007	0.25473174
12	4	48	48	80	2.58294987	50	516.589974	181.839671	334.750303	3967.411	5951.1165	0.02059556	0.27229478
13	4	52	52	80	2.6268442	50	525.368841	148.022671	377.34617	3346.59952	6215.11339	0.02380366	0.28872844
14	4	56	56	80	2.66814875	50	533.629751	115.264026	418.365725	2689.49394	6275.48587	0.0271819	0.30404209
15	4	60	60	80	2.70718594	50	541.437188	84.5995606	456.837627	2030.38945	6091.16836	0.03071796	0.31824526
16	4	64	64	80	2.74421965	50	548.84393	57.0797687	491.764161	1405.04046	5620.16184	0.0343996	0.33134763
17	4	68	68	80	2.7794688	50	555.893761	33.770546	522.123215	850.517454	4819.59891	0.0382147	0.34335904
18	4	72	72	80	2.81311717	50	562.623434	15.7534562	546.869978	405.088873	3645.79985	0.04215125	0.35428945
19	4	76	76	80	2.84532061	50	569.064123	4.12571489	564.938408	108.122183	2054.32148	0.04619735	0.36414894
20	4	80	80	80	2.87621255	50	575.242511	0	575.242511	0	0	0.05034121	0.37294772
21	4	84	4	80	2.90590815	50	581.18163	576.968063	4.21356681	2098.06568	110.42451	0.05466417	0.38906646
22	4	88	8	80	2.93450752	50	586.901504	570.468262	16.4332421	3803.12175	422.569083	0.0592446	0.4122382
23	4	92	12	80	2.96209832	50	592.419665	556.43017	35.9894946	5136.27849	906.402087	0.06406646	0.43396765
24	4	96	16	80	2.98875774	50	597.751548	535.585387	62.166161	6120.97585	1530.24396	0.0691139	0.45426973
25	4	100	20	80	3.01455412	50	602.910825	508.706008	94.2048164	6782.74678	2260.91559	0.07437123	0.47315195
26	4	104	24	80	3.03954832	50	607.909664	476.601177	131.308487	7149.01765	3063.86471	0.07982292	0.49065216
27	4	108	28	80	3.06379474	50	612.758947	440.114114	172.644833	7248.93835	3903.27449	0.08545362	0.50676305
28	4	112	32	80	3.08734224	50	617.468448	400.119554	217.348894	7113.23652	4742.15768	0.09124815	0.52150762
29	4	116	36	80	3.11023489	50	622.046978	357.5215	264.525477	6774.09159	5542.43857	0.0971915	0.53490146
30	4	120	40	80	3.13251256	50	626.502513	313.251256	313.251256	6265.02513	6265.02513	0.10326884	0.54696027
31	4	124	44	80	3.15421149	50	630.842297	268.265687	362.57661	5620.80487	6869.87262	0.1094655	0.55769986
32	4	128	48	80	3.17536465	50	635.07293	223.545671	411.527259	4877.3601	7316.04015	0.11576702	0.56713618
33	4	132	52	80	3.19600221	50	639.200442	180.094725	459.105718	4071.70682	7561.74123	0.12215907	0.57528525
34	4	136	56	80	3.21615181	50	643.230362	138.937758	504.292603	3241.88102	7564.38905	0.12862755	0.58216324
35	4	140	60	80	3.23583883	50	647.167767	101.119964	546.047803	2426.87912	7280.63737	0.13515851	0.58778639
36	4	144	64	80	3.25508668	50	651.017336	67.7058029	583.311533	1666.60438	6666.41752	0.14173819	0.59217107
37	4	148	68	80	3.27391694	50	654.783388	39.7780908	615.005297	1001.81858	5676.97198	0.14835301	0.59533372
38	4	152	72	80	3.29234961	50	658.469922	18.4371578	640.032764	474.098344	4266.8851	0.15498958	0.59729092
39	4	156	76	80	3.31040322	50	662.080644	4.80008467	657.280559	125.795322	2390.11113	0.16163468	0.5980593
40	4	160	80	80	3.32809499	50	665.618998	0	665.618998	0	0	0.1682753	0.59765562

Lateral Sheet (Only 35 of 100 stories)

story	story height m	height m	floor area m ²	perimeter m	concrete V m ³	steel V m ³	seis W KN	seis W*H ^A KN*m ²	seis F KN	seis F bot KN	seis F top KN	seis M bot KNm	seis M top KNm	seis disp m	seis drift
0		0												0	
1	4	4	2500	200	530.9944	0	23412.58	374601.3	0.548749	0.544771	0.003978	1.980984	0.104262	0.000371	0.004642
2	4	8	2500	200	530.9944	0	23412.58	1498405	2.194997	2.133537	0.06146	14.22358	1.580398	0.001469	0.01372
3	4	12	2500	200	530.9944	0	23412.58	3371411	4.938742	4.638714	0.300029	42.8189	7.556276	0.003268	0.022489
4	4	16	2500	200	530.9944	0	23412.58	5993620	8.779986	7.866868	0.913119	89.90706	22.47676	0.005744	0.030949
5	4	20	2500	200	530.9944	0	23412.58	9365032	13.71873	11.57518	2.143551	154.3357	51.44523	0.008872	0.0391
6	4	24	2500	200	530.9944	0	23412.58	13485646	19.75497	15.4879	4.267073	232.3184	99.56504	0.012627	0.046942
7	4	28	2500	200	530.9944	0	23412.58	18355462	26.88871	19.31281	7.575894	318.0934	171.2811	0.016985	0.054475
8	4	32	2500	200	530.9944	0	23412.58	23974481	35.11995	22.75772	12.36222	404.5818	269.7212	0.021921	0.0617
9	4	36	2500	200	530.9944	0	23412.58	30342703	44.44868	25.54688	18.9018	484.0461	396.0377	0.027411	0.068615
10	4	40	2500	200	530.9944	0	23412.58	37460127	54.87491	27.43746	27.43746	548.7491	548.7491	0.033428	0.075222
11	4	44	2500	200	530.9944	0	23412.58	45326754	66.39865	28.23602	38.16262	591.6119	723.0813	0.03995	0.08152
12	4	48	2500	200	530.9944	0	23412.58	53942583	79.01988	27.815	51.20488	606.8727	910.309	0.046951	0.087509
13	4	52	2500	200	530.9944	0	23412.58	63307615	92.73861	26.1291	66.6095	590.7449	1097.098	0.054406	0.09319
14	4	56	2500	200	530.9944	0	23412.58	73421849	107.5548	23.23184	84.32299	542.0764	1264.845	0.062291	0.098563
15	4	60	2500	200	530.9944	0	23412.58	84285286	123.4686	19.29196	104.1766	463.0071	1389.021	0.070581	0.103629
16	4	64	2500	200	530.9944	0	23412.58	95897925	140.4798	14.6099	125.8699	359.6282	1438.513	0.079252	0.108386
17	4	68	2500	200	530.9944	0	23412.58	1.08E+08	158.5885	9.634252	148.9543	242.6404	1374.962	0.088279	0.112836
18	4	72	2500	200	530.9944	0	23412.58	1.21E+08	177.7947	4.978252	172.8165	128.0122	1152.11	0.097637	0.11698
19	4	76	2500	200	530.9944	0	23412.58	1.35E+08	198.0984	1.436214	196.6622	37.6387	715.1354	0.107303	0.120817
20	4	80	2500	200	530.9944	64	28340.58	1.81E+08	265.7011	0	265.7011	0	0	0.117251	0.124347
21	4	84	2500	200	379.4712	0	20124.53	1.42E+08	208.0122	206.5041	1.508089	750.9241	39.52232	0.127672	0.130269
22	4	88	2500	200	379.4712	0	20124.53	1.56E+08	228.2946	221.9023	6.392248	1479.349	164.3721	0.138752	0.138502
23	4	92	2500	200	379.4712	0	20124.53	1.7E+08	249.5203	234.362	15.15836	2163.341	381.7661	0.150457	0.146309
24	4	96	2500	200	379.4712	0	20124.53	1.85E+08	271.6894	243.4337	28.2557	2782.1	695.5249	0.162752	0.153689
25	4	100	2500	200	379.4712	0	20124.53	2.01E+08	294.8019	248.7391	46.0628	3316.521	1105.507	0.175604	0.160645
26	4	104	2500	200	379.4712	0	20124.53	2.18E+08	318.8577	249.9845	68.87327	3749.767	1607.043	0.188978	0.167177
27	4	108	2500	200	379.4712	0	20124.53	2.35E+08	343.8569	246.9752	96.88169	4067.827	2190.369	0.202841	0.173286
28	4	112	2500	200	379.4712	0	20124.53	2.52E+08	369.7995	239.6301	130.1694	4260.09	2840.06	0.217159	0.178974
29	4	116	2500	200	379.4712	0	20124.53	2.71E+08	396.6854	227.995	168.6905	4319.904	3534.467	0.231898	0.184241
30	4	120	2500	200	379.4712	0	20124.53	2.9E+08	424.5147	212.2574	212.2574	4245.147	4245.147	0.247025	0.189089
31	4	124	2500	200	379.4712	0	20124.53	3.09E+08	453.2874	192.7605	260.5269	4038.791	4936.3	0.262507	0.193519
32	4	128	2500	200	379.4712	0	20124.53	3.3E+08	483.0034	170.0172	312.9862	3709.466	5564.199	0.278309	0.197532
33	4	132	2500	200	379.4712	0	20124.53	3.51E+08	513.6628	144.7245	368.9383	3272.032	6076.631	0.2944	0.201132
34	4	136	2500	200	379.4712	0	20124.53	3.72E+08	545.2656	117.7774	427.4882	2748.139	6412.323	0.310745	0.204318
35	4	140	2500	200	379.4712	0	20124.53	3.94E+08	577.8117	90.28308	487.5286	2166.794	6500.382	0.327312	0.207093
36	4	144	2500	200	379.4712	0	20124.53	4.17E+08	611.3012	63.57533	547.7259	1564.931	6259.724	0.344069	0.209458
37	4	148	2500	200	379.4712	0	20124.53	4.41E+08	645.7341	39.22834	606.5057	987.9731	5598.514	0.360983	0.211417
38	4	152	2500	200	379.4712	0	20124.53	4.65E+08	681.1103	19.07109	662.0392	490.3994	4413.595	0.37802	0.212971
39	4	156	2500	200	379.4712	0	20124.53	4.9E+08	717.4299	5.201367	712.2285	136.3117	2589.922	0.39515	0.214122
40	4	160	2500	200	379.4712	84	26592.53	6.81E+08	997.2503	0	997.2503	0	0	0.41234	0.214872

story	story height	height	total W	axial force	wind PD	wPD F bot	wPD F top	wPD M bot	wPD M top	seis PD	sPD F bot	sPD F top	sPD M bot	sPD M top
	m	m	KN	KN	KNm	KN	KN	KNm	KNm	KNm	KN	KN	KNm	KNm
0		0												
1	4	4	29412.58	2438795	408.2948	-1.45455	1.45455	329.698	37.76727	905.6801	-3.22649	3.226485	731.3367	83.77541
2	4	8	29412.58	2409382	1188.438	-8.02196	8.021959	748.7161	202.0345	2644.562	-17.8508	17.85079	1666.074	449.5756
3	4	12	29412.58	2379970	1917.415	-18.3353	18.33528	896.3915	445.799	4281.885	-40.9455	40.94553	2001.781	995.5383
4	4	16	29412.58	2350557	2596.578	-31.1589	31.15893	830.9049	727.0418	5819.832	-69.838	69.83798	1862.346	1629.553
5	4	20	29412.58	2321145	3227.287	-45.3837	45.38372	605.1163	1008.527	7260.586	-102.102	102.102	1361.36	2268.933
6	4	24	29412.58	2291732	3810.905	-60.0218	60.02175	266.7633	1257.599	8606.332	-135.55	135.5497	602.4433	2840.09
7	4	28	29412.58	2262319	4348.793	-74.2013	74.20128	-141.336	1445.974	9859.259	-168.224	168.2236	-320.426	3278.204
8	4	32	29412.58	2232907	4842.311	-87.1616	87.1616	-581.077	1549.54	11021.56	-198.388	198.388	-1322.59	3526.898
9	4	36	29412.58	2203494	5292.814	-98.2479	98.24787	-1018.87	1548.148	12095.42	-224.521	224.5211	-2328.37	3537.909
10	4	40	29412.58	2174082	5701.653	-106.906	106.906	-1425.41	1425.413	13083.03	-245.307	245.3069	-3270.76	3270.758
11	4	44	29412.58	2144669	6070.17	-112.678	112.6775	-1775.52	1168.508	13986.61	-259.626	259.6264	-4091.08	2692.422
12	4	48	29412.58	2115257	6399.703	-115.195	115.1947	-2047.91	767.9644	14808.34	-266.55	266.5501	-4738.67	1777.001
13	4	52	29412.58	2085844	6691.583	-114.175	114.1751	-2224.95	217.4764	15550.44	-265.329	265.3293	-5170.52	505.3892
14	4	56	29412.58	2056431	6947.13	-109.417	109.4173	-2292.55	-486.299	16215.11	-255.388	255.388	-5350.99	-1135.06
15	4	60	29412.58	2027019	7167.657	-100.795	100.7952	-2239.89	-1343.94	16804.57	-236.314	236.3142	-5251.43	-3150.86
16	4	64	29412.58	1997606	7354.468	-88.2536	88.25361	-2059.25	-2353.43	17321.03	-207.852	207.8523	-4849.89	-5542.73
17	4	68	29412.58	1968194	7508.856	-71.8034	71.80344	-1745.81	-3510.39	17766.72	-169.894	169.8942	-4130.76	-8305.94
18	4	72	29412.58	1938781	7632.107	-51.5167	51.51672	-1297.46	-4808.23	18143.85	-122.471	122.471	-3084.45	-11430.6
19	4	76	29412.58	1909368	7725.494	-27.5221	27.52207	-714.608	-6238.34	18454.66	-65.7447	65.74473	-1707.06	-14902.1
20	4	80	34340.58	1879956	7790.281	0	0	0	-7790.28	18701.38	0	0	0	-18701.4
21	4	84	26124.53	1845615	7978.522	-28.4235	28.42349	6442.657	738.0133	19234.18	-68.5218	68.52176	15531.6	1779.161
22	4	88	26124.53	1819491	8334.04	-56.2548	56.25477	5250.445	1416.787	20160.29	-136.082	136.082	12700.98	3427.249
23	4	92	26124.53	1793366	8647.366	-82.6904	82.69044	4042.644	2010.513	20990.8	-200.725	200.7245	9813.198	4880.361
24	4	96	26124.53	1767242	8920.049	-107.041	107.0406	2854.416	2497.614	21728.49	-260.742	260.7419	6953.117	6083.978
25	4	100	26124.53	1741117	9153.624	-128.723	128.7228	1716.304	2860.507	22376.16	-314.665	314.6648	4195.53	6992.55
26	4	104	26124.53	1714993	9349.61	-147.256	147.2564	654.4727	3085.371	22936.6	-361.251	361.2515	1605.562	7569.079
27	4	108	26124.53	1688868	9509.511	-162.256	162.256	-309.059	3161.912	23412.61	-399.478	399.4777	-760.91	7784.694
28	4	112	26124.53	1662744	9634.816	-173.427	173.4267	-1156.18	3083.141	23807	-428.526	428.5259	-2856.84	7618.239
29	4	116	26124.53	1636619	9726.999	-180.557	180.5574	-1872.45	2845.147	24122.55	-447.775	447.7749	-4643.59	7055.846
30	4	120	26124.53	1610495	9787.517	-183.516	183.5159	-2446.88	2446.879	24362.09	-456.789	456.7891	-6090.52	6090.522
31	4	124	26124.53	1584370	9817.811	-182.243	182.2431	-2871.71	1889.929	24528.41	-455.309	455.3085	-7174.56	4721.718
32	4	128	26124.53	1558246	9819.304	-176.747	176.7475	-3142.18	1178.317	24624.32	-443.238	443.2377	-7879.78	2954.918
33	4	132	26124.53	1532121	9793.407	-167.1	167.1	-3256.31	318.2857	24652.62	-420.635	420.6354	-8197	801.2103
34	4	136	26124.53	1505996	9741.509	-153.429	153.4288	-3214.7	-681.906	24616.13	-387.704	387.7041	-8123.32	-1723.13
35	4	140	26124.53	1479872	9664.984	-135.914	135.9138	-3020.31	-1812.18	24517.65	-344.779	344.7795	-7661.77	-4597.06
36	4	144	26124.53	1453747	9565.191	-114.782	114.7823	-2678.25	-3060.86	24359.98	-292.32	292.3197	-6820.79	-7795.19
37	4	148	26124.53	1427623	9443.467	-90.3032	90.30316	-2195.61	-4414.82	24145.91	-230.895	230.8952	-5613.92	-11288.2
38	4	152	26124.53	1401498	9301.136	-62.7827	62.78267	-1581.19	-5859.72	23878.24	-161.178	161.1781	-4059.3	-15043.3
39	4	156	26124.53	1375374	9139.501	-32.5595	32.55947	-845.404	-7380.15	23559.77	-83.9317	83.93168	-2179.28	-19024.5
40	4	160	32592.53	1349249	8959.849	0	0	0	-8959.85	23193.28	0	0	0	-23193.3



Stress Sheet

Wind Lateral Displacement			Wind Vertical Displacement				Distance Times Wind Rotation or Drift				
story	translation	rotation	column A	column B	column C	column D	column A	column B	column C	diag AD	diag DE
100	0.69575429	0.00250655	0.05033243	0.04844472	0.04604911	0.0249705	0.06266364	0.06266364	0.03133182	0.02882749	0.0305098
80	0.50095565	0.00219857	0.04862737	0.04859607	0.04462136	0.02485385	0.05496426	0.05496426	0.02748213	0.02629823	0.02827789
60	0.32271658	0.00197729	0.03938731	0.0418904	0.03466096	0.02136713	0.04943219	0.04943219	0.0247161	0.02219324	0.02423365
40	0.1682753	0.00165852	0.02725487	0.03281922	0.02306738	0.0166451	0.04146301	0.04146301	0.0207315	0.01506832	0.0181079
20	0.05034121	0.00104721	0.012226	0.0173188	0.01008946	0.00874645	0.02618029	0.02618029	0.01309014	0.00251765	0.00677692
base	0	0	0	0	0	0	0	0	0	0	0
Wind Displacement Coefficients											
stories	height	cubic	quadratic	linear	constant						
81 to 100	80	-2.576E-08	5.0158E-06	0.00219857	0.50095565						
61 to 80	80	-4.377E-08	6.6352E-06	0.00197729	0.32271658						
41 to 60	80	-3.519E-08	6.2152E-06	0.00165852	0.1682753						
21 to 40	80	-3.791E-08	8.3698E-06	0.00104721	0.05034121						
1 to 20	80	-3.302E-08	1.0507E-05	0	0						
Gravity Core Stress			Wind Core Stress				Gravity Plus Wind Core Stress				
stories											
81 to 100	20692.25		6695.66843				27387.9184				
61 to 80	21631.475		7792.57417				29424.0492				
41 to 60	17344.7		7018.93814				24363.6381				
21 to 40	19454.6		9277.64829				28732.2483				
1 to 20	18371.5286		11505.6151				29877.1437				
max/allow	0						0.62244049				
Gravity Column Stress			Wind Column Stress				Gravity Plus Wind Column Stress				
stories	height		column A	column B	column C	column D	column A	column B	column C	column D	
81 to 100	20692.25		1099.68453	151.93691	1008.59566	297.324052	21791.9345	20844.1869	21700.8457	20989.5741	
61 to 80	21631.475		5307.21482	4033.0136	5797.30705	2286.73427	26938.6898	25664.4886	27428.7821	23918.2093	
41 to 60	17344.7		6957.00405	5425.51884	6790.96082	3066.1066	24301.7041	22770.2188	24135.6608	20410.8066	
21 to 40	19454.6		8706.78008	9154.78592	7780.75536	5030.82486	28161.3801	28609.3859	27235.3554	24485.4249	
1 to 20	18371.5286		7443.92323	10489.6181	6558.82282	5839.11821	25815.4518	28861.1466	24930.3514	24210.6468	
max/allow							0.58669542	0.60127389	0.57143296	0.51011302	0.60127389
Gravity Outrigger Stress			Wind Outrigger Stress				Gravity Plus Wind Outrigger Stress				
stories			outrig B	outrig D			outrig B	outrig D			
81 to 100	0		0	0			0	0			
61 to 80	0		46261.5351	19093.0546			46261.5351	19093.0546			
41 to 60	0		54787.1379	24328.4516			54787.1379	24328.4516			
21 to 40	0		62792.5224	29685.5489			62792.5224	29685.5489			
1 to 20	0		64374.0247	31554.6433			64374.0247	31554.6433			
max/allow							0.31098563	0.15243789	0.31098563		
Gravity Belt Stress			Wind Belt Stress				Gravity Plus Wind Belt Stress				
stories			belt AB	belt BC	belt AD	belt DE	belt AB	belt BC	belt AD	belt DE	
81 to 100	0		0	0	0	0	0	0	0	0	
61 to 80	0		242.981202	30852.7526	28787.2568	20401.4326	242.981202	30852.7526	28787.2568	20401.4326	
41 to 60	0		19429.7002	56116.9603	51975.61	25995.5923	19429.7002	56116.9603	51975.61	25995.5923	
21 to 40	0		43192.0741	75696.5409	78567.7486	31719.7921	43192.0741	75696.5409	78567.7486	31719.7921	
1 to 20	0		39531.7217	56116.1896	74600.0965	33716.9688	39531.7217	56116.1896	74600.0965	33716.9688	
max/allow			0.20865736	0.36568377	0.37955434	0.16288391	0.20865736	0.36568377	0.37955434	0.16288391	0.37955434
Gravity Diagonal Stress			Wind Diagonal Stress				Gravity Plus Wind Diagonal Stress				
stories	diag AB/AD	diag BC/DE	diag AB	diag BC	diag AD	diag DE	diag AB	diag BC	diag AD	diag DE	
81 to 90	68570.6001	51427.9501	497.186211	23176.5729	36552.831	40462.3209	69067.7863	74604.523	105123.431	91890.2709	
61 to 70	0	0	0	0	0	0	0	0	0	0	
41 to 50	0	0	0	0	0	0	0	0	0	0	
21 to 30	0	0	0	0	0	0	0	0	0	0	
1 to 10	0	0	0	0	0	0	0	0	0	0	
max/allow							0.3336608	0.36040832	0.50784266	0.44391435	0.50784266

Seismic Lateral Displacement			Seismic Vertical Displacement				Distance Times Seismic Rotation or Drift				
story	translation	rotation	column A	column B	column C	column D	column A	column B	column D	diag AD	diag DE
100	1.89822385	0.00741268	0.14263269	0.13633526	0.12905774	0.07047952	0.18531706	0.18531706	0.09265853	0.08324945	0.08941832
80	1.32706469	0.00627656	0.13685952	0.13662731	0.12472045	0.06998079	0.15691393	0.15691393	0.07845696	0.07271268	0.07945773
60	0.82492911	0.00540738	0.10768041	0.11414692	0.09485362	0.0582353	0.13518453	0.13518453	0.06759226	0.05804461	0.06432131
40	0.41233964	0.00430229	0.07299047	0.08633561	0.06226991	0.04379064	0.10755725	0.10755725	0.05377862	0.03657716	0.04474344
20	0.11725054	0.00252021	0.03235713	0.0438165	0.02705751	0.02213479	0.06300531	0.06300531	0.03150265	0.00562229	0.0154249
base	0	0	0	0	0	0	0	0	0	0	0
Seismic Displacement Coefficients											
stories	height	cubic	quadratic	linear	constant						
81 to 100	80	-9.215E-08	1.8158E-05	0.00627656	1.32706469						
61 to 80	80	-1.359E-07	2.1735E-05	0.00540738	0.82492911						
41 to 60	80	-9.454E-08	1.8252E-05	0.00430229	0.41233964						
21 to 40	80	-8.668E-08	2.1539E-05	0.00252021	0.11725054						
1 to 20	80	-6.423E-08	2.3459E-05	0	0						
Gravity Core Stress			Seismic Core Stress				Gravity Plus Seismic Core Stress				
stories											
81 to 100	20692.25		23633.9878				44326.2378				
61 to 80	21631.475		24899.1868				46530.6618				
41 to 60	17344.7		20203.8002				37548.5002				
21 to 40	19454.6		23490.2648				42944.8648				
1 to 20	18371.5286		25462.5188				43834.0474				
max/allow							0.96938879				
Gravity Column Stress			Seismic Column Stress				Gravity Plus Seismic Column Stress				
stories			column A	column B	column C	column D	column A	column B	column C	column D	
81 to 100	20692.25		3748.54899	667.671953	3179.09287	1096.67572	24440.799	21359.922	23871.3429	21788.9257	
61 to 80	21631.475		16770.6098	13458.344	17461.0023	7634.65812	38402.0848	35089.819	39092.4773	29266.1331	
41 to 60	17344.7		19899.1671	16539.5514	19120.0546	9288.14383	37243.8671	33884.2514	36464.7546	26632.8438	
21 to 40	19454.6		23445.3042	24954.9343	20976.9348	13636.616	42899.9042	44409.5343	40431.5348	33091.216	
1 to 20	18371.5286		19349.2314	26191.9068	17080.5084	14429.5798	37720.76	44563.4354	35452.037	32801.1083	
max/allow							0.893748	0.9284049	0.84232364	0.68940033	0.9284049
Gravity Outrigger Stress			Seismic Outrigger Stress				Gravity Plus Seismic Outrigger Stress				
stories			outrig B	outrig D			outrig B	outrig D			
81 to 100	0		0	0			0	0			
61 to 80	27708.4377		168004.933	71891.6207			195713.37	99600.0584			
41 to 60	28966.1288		168612.36	75866.0026			197578.489	104832.131			
21 to 40	23225.8232		174233.776	82592.3174			197459.599	105818.141			
1 to 20	26051.1338		171761.164	84234.8676			197812.298	110286.001			
max/allow							0.95561496	0.53278262	0.95561496		
Gravity Belt Stress			Seismic Belt Stress				Gravity Plus Seismic Belt Stress				
stories			belt AB	belt BC	belt AD	belt DE	belt AB	belt BC	belt AD	belt DE	
81 to 100	0		0	0	0	0	0	0	0	0	
61 to 80	803.988281		1802.42771	92424.4117	89873.5282	65794.4397	2606.41599	93228.4	90677.5165	66598.428	
41 to 60	803.988281		50194.8654	149760.005	140863.31	72631.3401	50998.8537	150563.994	141667.298	73435.3283	
21 to 40	803.988281		103588.713	186804.676	190787.494	77529.5355	104392.701	187608.664	191591.483	78333.5238	
1 to 20	803.988281		88950.8522	130088.01	165183.777	72715.9458	89754.8405	130891.998	165987.765	73519.9341	
max/allow							0.50431256	0.90632205	0.92556272	0.37842282	0.92556272
Gravity Diagonal Stress			Seismic Diagonal Stress				Gravity Plus Seismic Diagonal Stress				
stories	diag AB/AD	diag BC/DE	diag AB	diag BC	diag AD	diag DE	diag AB	diag BC	diag AD	diag DE	
81 to 90	68570.6001	51427.9501	2194.82523	69502.5942	118618.62	138878.896	70765.4253	120930.544	187189.22	190306.846	
61 to 70	0	0	0	0	0	0	0	0	0	0	
41 to 50	0	0	0	0	0	0	0	0	0	0	
21 to 30	0	0	0	0	0	0	0	0	0	0	
1 to 10	0	0	0	0	0	0	0	0	0	0	
max/allow							0.34186196	0.58420553	0.90429575	0.91935675	0.91935675